Institut d'Histologie et d'Embryologie générale
Université de Fribourg (Suisse)

THESE

# Tenascin-R and perineuronal nets of extracellular matrix

Présentée à la Faculté des Sciences de l'Université de Fribourg (Suisse) pour l'obtention du grade de *Doctor rerum naturalium*

**Anders Kristian Haunsø**
de
Odense (Danemark)

Thèse n°
1307

Imprimerie Saint-Paul, Fribourg
2000

Acceptée par la Faculté des Sciences de l'Université de Fribourg (Suisse) sur la proposition de messieurs Dr. Pierre-Alain Menoud, directeur de thèse, Institut d'Histologie, Université de Fribourg; Prof. Marco Celio, directeur de l'Institut d'Histologie, Université de Fribourg; PD Dr.sc.nat. Matthias Chiquet, Maurice E. Müller-Institut für Biomechanik. Université de Berne et Dr. Zhicheng Xiao, Institut für Biosynthese Neuraler Structuren, Universität Hamburg.

Fribourg, le 24 juin 2000.

Président du jury

Prof. Jean-Pierre Montani

Le Doyen

Prof. Beat Hirsbrunner

# Table of contents

**Page**

**Page**

## List of Tables

## List of Figures

**Page**

# Disclaimer

All the work presented in this PhD thesis was performed by Anders Haunsø, except the genotyping of the animals used for the article "Morphology of Perineuronal Nets in Tenascin-R and Parvalbumin Single and Double Knockout Mice", published in **Brain Research**, **864 (1)**; 142-145; (2000). I am grateful to Mmes. Pythoud and Gioria for determining the genotype of the parvalbumin knockout mice and to Dr. Bartsch for genotyping of the tenascin-R knockout mice. The preparation of first dimension Immobiline DryStrip gels, for the 2D electrophoresis, was performed in collaboration with Dr. Racay.

# 1. Summary

Tenascin-R (TN-R) is a glycosylated brain extracellular matrix protein (BECM; Zamze et al., 1999) restricted to the central nervous system (Pesheva et al., 1989; Rathjen et al., 1991; Weber et al., 1999). A special feature of TN-R, and some of its known ligands, is their accumulation around certain sub-populations of neurones, forming perineuronal nets of extracellular matrix (PNEMs; Wintergerst et al., 1996; Matsui et al., 1998; Hagihara et al., 1999; Haunso et al., 1999).

In these studies, bacterial expression of the C-terminal domain of TN-R, the FG-knob, led to the formation of inclusion bodies concurring those of previous studies (Norenberg et al., 1995; Elefteriou et al., 1999). Heterologous expression of the FG-knob, as a secreted protein, in the yeast *P. pastoris* gave rise to different glycosylated proteins. The majority of these expressed proteins remained within the yeast cells, with only extremely low amounts being secreted. Expression of recombinant FG-knob, as a secreted protein, in a mammalian cell line (Cos-1/M6) produced two different glycosylated forms with a size difference of 40 kDa. However, these forms were not detected in conditioned medium as the FG-knob precipitated around the host cells upon secretion leading to the formation of large cell aggregates. Despite the general insolubility of the FG-knob, an affinity column was generated and potential ligands purified from pig cortex. These ligands contained neither sites to common matrix components such as elastin, collagen type II and IV or hyaluronic acid nor did they contain the carbohydrate N-acetyl-D-galactosamine (GalNAc), a common constituent of proteoglycans such as chondroitin sulphates and keratan sulphates, found extensively in extracellular matrices (Lodish et al., 1995).

PNEMs are lattice-like accumulations of BECM components, consisting mainly of chondroitin sulphate proteoglycans (CSPGs; Margolis and Margolis, 1993; Ruoslahti, 1996), around GABAergic interneurones expressing the calcium binding protein parvalbumin (PV). Here, it is shown that phosphacan, a specific member of the CSPG family (Matsui et al., 1998; Hagihara et al., 1999), preferentially associates with both cortical and non-cortical PNEMs. In this study, the identification of phosphacan in PNEMs *in vivo* provides functional and biological importance to previously described interactions with other defined PNEM components *in vitro* (Milev et al., 1997, 1998; Xiao et al., 1997). Recently, it has been shown *in vitro* that

all lecticans, a family of CSPGs which form large aggregates with hyaluronic acid, interact with TN-R (Aspberg et al., 1997). Examination of PV and TN-R single and double knockout (KO) mice revealed that PNEMs appear normal in mice lacking PV whereas TN-R deficient mice show morphological alterations in these entities. These alterations have been shown to occur because defined lecticans such as phosphacan and neurocan were no longer present in PNEMs. Neither the membrane-related cytoskeleton in PV-expressing GABAergic interneurones, nor the density or distribution of cortical GABAergic interneurones were altered in any of the examined KO mice. Thus, the principal role for TN-R in PNEMs may be to attract and/or retain other matrix components. TN-R is however not envisaged to be involved in determining which neurones form PNEMs or the GABAergic properties of these neurones. The intimate involvement of TN-R in the formation of the lattice-like structure of PNEMs is probably effectuated via the multimerisation of TN-R molecules leading to the formation of a scaffold onto which other PNEM components assemble.

# 2. Résumé

La tenascine-R (TN-R) est une glycoprotéine de la matrice extracellulaire du cerveau (Zamze et al., 1999) dont la distribution est restreinte au système nerveux central. (Pesheva et al., 1989; Rathjen et al., 1991; Weber et al., 1999) Une des caractéristiques de la TN-R et de quelques-uns de ses ligands connus, est son accumulation autour de certaines sous-population de neurones, formant ainsi les réseaux périneuraux de la matrice extracellulaire (PNEMs; Hagihara et al., 1999; Haunso et al., 1999; Matsui et al., 1998; Wintergerst et al., 1996).

Dans ces études, l'expression bactérienne du domaine COOH-terminal de la TN-R, le bouton Fibrinogène (FG), conduit à la formation de corps d'inclusion en accord avec la littérature. (Norenberg et al., 1995; Elefteriou et al., 1999). L'expression hétérologue du bouton FG sous forme de protéine sécrétée par la souche de levure *P. Pastoris*, a donné différentes protéines glycosylées. La majorité de ces protéines recombinantes se trouvent à l'intérieure des levures et seule une infime quantité est sécrétée. L'expression du bouton FG dans une lignée de cellules de mammifère (Cos-1/M6) sous forme de protéine sécrétée a produit deux formes de protéines glycosylées avec une différence de 40 kDa entre elles. Cependant ces deux formes n'ont pas pu être détectées dans le milieu conditionné car le polypeptide recombinant précipitait autour des cellules hôtes lors de la sécrétion conduisant à la formation de larges agrégats cellulaires. Malgré l'insolubilité générale du bouton FG, une colonne d'affinité a été faite pour tenter de purifier des ligands à partir du cortex cérébral de cerveaux de porcs. Ces ligands ne contiennent pas de sites communs aux composants de la matrice extracellulaire tels que l'élastine, le collagène type II et IV ou l'acide hyaluronique. Ils ne contiennent pas non plus d'hydrates de carbone tel que du N-acétyl-D-galactosamine (GalNAc), un constituant commun aux protéoglycans comme la chodroïtine sulfate et les kératanes sulfate que l'on trouve en grande quantité dans les matrices extracellulaires. (Lodish et al., 1995).

Les PNEMs sont des accumulations en forme de treillis de composants de la matrice extracellulaire du cerveau. Ils sont constitués principalement de protéoglycans-chondroïtine sulfate (CSPGs; Margolis et Margolis et al., 1993; Ruoslahti, 1996). Ils sont localisés autour des interneurones GABAergiques exprimant une protéine liant le calcium: la parvalbumine. Dans ce travail, nous montrons que le

phosphacan, un membre spécifique de la famille des CSPG (Hagihara et al., 1999; Matsui et al., 1998), s'associe de préférence avec les PNEMs corticaux et non-corticaux. Par l'identification des phosphacans dans les PNEMs *in vivo*, nous montrons qu'ils ont une importance fonctionnelle et biologique dans les interactions précédemment décrite in vitro avec d'autres composants du PNEM (Milev et al., 1997; Xiao et al., 1997). Il a été récemment montré in vitro que tous les lecticans, une famille de CSPGs formant de larges agrégats avec l'acide hyaluronique, agissent avec la TN-R. L'étude des souris déficientes pour les gènes de la PV et/ou de la TN-R a révélé que les PNEMs apparaissaient normaux dans le cerveau des souris déficientes pour le gène de la PV alors que dans le cerveau de celles dont le gène de la TN-R avait été supprimé, les PNEMs montraient des altérations morphologiques. Ces désordres des PNEMs survenaient parce que certains lecticans tels que le phosphacan et le neurocan n'étaient plus présents dans les PNEMs. Ni le cytosquelette lié à la membrane cellulaire des interneurones GABAergiques exprimant la parvalbumine ni la densité ou la distribution corticale de ces cellules n'étaient altérées dans les cerveaux des souris déficientes pour les gènes suscités.

Ainsi le rôle principal de la TN-R dans les PNEMs pourrait être d'attirer et/ou de retenir d'autres composants de la matrice. Cependant, la TN-R ne semble pas être impliquée dans la détermination du type de neurones susceptible de former des PNEMs ou d'avoir des propriétés GABAergiques. L'implication intime de la TN-R dans la formation d'une structure en forme de treillis des PNEMs est probablement possible via une multimérisation des molécules de TN-R. Cette dernière conduit à la formation d'un échafaudage sur lequel viennent s'assembler les composants du PNEM..

# 3. General introduction

## 3.1 Extracellular matrices

### *3.1.1 Extracellular matrix*

The extracellular matrix (ECM) is a macromolecular ground substance of connective material secreted by fibroblasts and other connective tissue cells into the surrounding medium. The ECM comprises the non-cellular portions of animal tissues and consists of proteins, polysaccharides and proteoglycans (Lawrence, 1995). Recently, the ECM has been shown to be intimately involved in regulating the behaviour of the cells it surround (Blackshaw et al., 1995).

### *3.1.2 Brain extracellular matrix*

Until recently, the amount and even the existence of a brain extracellular matrix (BECM) has been much disputed (for a historic overview and original references see Celio, 1999). With the introduction of improved tissue preparation techniques for electron microscopy the existence of a substantial matrix-filled interstitial space, comprising up to 20% of the brain volume, has recently been established (Carlson and Hockfield, 1996). Yet, in contrast to extracellular matrices (ECMs) in other organs the BECM shows a relative low content of fibrous matrix components such as collagens, fibronectin and vitronectin (Rucklidge et al., 1989; Gladson and Cheresh, 1991). The BECM is however composed of a complex network of glycosaminoglycans, proteoglycans and glycoproteins (for review see Celio and Blümcke, 1994; Ruoslahti, 1996; Celio, 1999). Using less specific staining methods such as the colloidal-iron or the periodic-acid Schiff methods (for review see Celio and Blümcke, 1994), it has been shown that all neurones throughout the central nervous system (CNS) are surrounded by a ‘glycocalyx’ or ECM. This matrix has been shown to be involved in cell migration, maturation (Rutka et al., 1988) and tumour cell invasion (Ruoslahti and Giancotti, 1989). Moreover, it is also involved in regulation of cell adhesion, neurite outgrowth and can serve both as co-factors and as regulators of growth factors (Ruoslahti and Yamaguchi, 1991). Through this multitude of effects, the BECM is intimately involved in the normal development and maintenance of nervous system functions (Schachner, 1994).

## 3.2 Perineuronal nets of extracellular matrix

### *3.2.1 Historic perspectives*

Perineuronal nets of extracellular matrix (PNEMs; reviewed in Celio and Blümcke, 1994) were first described by Camillo Golgi at the end of the 19th century (for a historic overview and original references see Celio et al., 1998). Golgi observed "a delicate covering, mainly reticular in structure, but also in the form of tiny tiled scales or an interrupted envelope which surrounds the cell body of all nerve cells and continues along their protoplasmic extensions...."[a] in the grey matter of the CNS. These nets were further characterised by Donaggio[a] who showed that the nets were continuous with both the intracellular neurofibrillar network and the extracellular environment. He also proposed that the observed holes in the lattice-like structure were places where axon terminals interacted with the surface of nerve cells. In 1931, while examining animals belonging to the Phylum Chordata, Rondinini showed that PNEMs also existed in the CNS of such diverse classes as amphibians, reptiles and birds.

### *3.2.2 Composition of PNEMs and their distribution*

It is generally believed that PNEMs are pericellular condensations of ECM components forming a fine meshwork within the local neuropil (Celio, 1999). With the introduction of immunohistochemical, biochemical and molecular biological methods, it has become possible to further characterise PNEMs and identify their individual constituents. PNEMs are composed of classical BECM molecules, which are present in higher concentration within these PNEMs (Celio and Blümcke, 1994). At the ultrastructural level, it has been confirmed that PNEM components are found between synaptic boutons impinging upon the cell body and major dendritic arborisations (Bruckner et al., 1993; Celio and Blümcke, 1994).

PNEMs are exclusively detected during postnatal (P) development with the first nets observed around P7 and fully developed nets around P28 (Schweizer et al., 1993). PNEMs have been described in a variety of locations such as spinal cord, deep cerebellar nuclei, hippocampus and cerebral cortex (Brauer et al., 1982, 1984;

[a] From Celio *et al*. 1998

Hockfield and McKay, 1983; Lafarga et al., 1984; Naegele et al., 1988) and are mainly found surrounding nerve cells, which have a considerable proportion of their cell bodies devoted to synaptic contacts (Celio and Blümcke, 1994). In spite of a complex pattern of distribution in the cerebral cortex and hippocampal formation, nets are mainly observed surrounding a subpopulation of non-pyramidal GABAergic neurones (Celio, 1986, 1993) expressing the calcium-binding protein parvalbumin (PV; Kosaka and Heizmann, 1989; Kosaka et al., 1989, 1990, 1992; Naegele and Barnstable, 1989).

Using immunohistochemistry, several distinct molecules belonging to different classes of BECM components have been identified in PNEMs. Chondroitin sulphate proteoglycans (CSPGs) are the main constituents of PNEMs (Margolis and Margolis, 1993; Ruoslahti, 1996) with individual members such as brevican (Hagihara et al., 1999), neurocan (Matsui et al., 1998; Haunso et al., 2000) and phosphacan (Lodish et al., 1995; Haunso et al., 1999, 2000) have been identified in PNEMs. Certain glycoproteins such as tenascin-C (Celio and Chiquet-Ehrismann, 1993) and –R (Celio and Rathjen, 1993; Wintergerst et al., 1996) are also present in high amounts in PNEMs. Moreover, hyaluronic acid has also been shown to be accumulated in PNEMs (Delpech et al., 1982; Bignami et al., 1992). This heterogeneity in composition is reflected by the fact that PNEM components are not secreted by the neurones surrounded by the nets, but by neighbouring neurone and glia populations (Maleski and Hockfield, 1997; Lander et al., 1998). A biologically significant role for the presence of these components in PNEMs *in vivo* has been further validated as several of them also interact *in vitro* (Aspberg et al., 1995, 1997; Xiao et al., 1997).

*3.2.3 Putative functions for PNEMs*

The exact functions of PNEMs have yet to be elucidated, but many have been proposed. A direct function of these matrix components could be to prevent the occlusion of the extracellular space (Celio and Blümcke, 1994). PNEMs may also function in synapse stabilisation (Bertolotto et al., 1990; Zaremba et al., 1990) or as a barrier for the formation of new synaptic contacts (Celio and Blümcke, 1994) and influencing the maintenance of cellular relationships in adult CNS (Hockfield and McKay, 1983). Other putative functions could be the generation of an ion-buffering microenvironment or the attraction and concentration of growth factors, proteases and

protease-inhibitors in the vicinity of the neurones, thereby modulating their microenvironment (Celio and Blümcke, 1994). An overall role in neuroprotection has also been suggested (Okamoto et al., 1994). Härtig *et al.* (1999) hypothesised that physico-chemical properties of PNEMs provide the basis for neurones to sustain fast-spiking activity. Finally, a membrane related cytoskeleton (MRC), partly composed of ankyrin$_R$, has been identified in parvalbumin expressing cortical interneurones with a proposal that the PNEMs may be interacting with this intracellular scaffold via transmembrane receptors (Celio and Rathjen, 1993; Celio and Blümcke, 1994; Wintergerst et al., 1996) thus influencing the morphology of the neurone and its intracellular signalling.

*3.2.4 PNEMs and pathology*

PNEMs were first described at the end of the 19$^{th}$ century and although their existence at that time was much disputed, the first description of morphological changes in pathological conditions occurred already in 1911. Here, Bethe[b] observed that PNEMs remained intact although neurones and the converging synapses were severely affected by lesions. It was observed that modifications of PNEMs occurred independently of those observed in neurones. In recent years it has been reported that alterations and destruction of PNEMs occurs in a number of diseases such as patients infected with human immunodeficiency virus (HIV; Belichenko et al., 1997b), suffering from Rett syndrome (Belichenko et al., 1997a) and transmissible spongiform encephalopathies (TSEs) including Creutzfeldt-Jacob disease (CJD; Guentchev et al., 1998; Belichenko et al., 1999). Loss of ECM components may therefore be involved in the observed decline of cognitive, motor and behavioural functions in some patients belonging to these groups. Furthermore, PNEMs have been thought to be effected in Alzheimer's disease (AD; Kobayashi et al., 1989) but this notion still remains controversial (Celio et al., 1998). However, recent observations have shown that PNEM components are not directly involved in the pathogenic processes in AD but lowers the neurones susceptibility to neurofibrillary changes (Bruckner et al., 1999).

[b] For original references see Celio et al., 1998.

### 3.3 The tenascin multi-gene family

Glycoproteins are major constituents of extracellular matrices in organs of higher order animals (Johansson, 1996). One such group of matrix molecules is the tenascin multi-gene family (tenascins) comprising members of structurally related modular glycoproteins (Chiquet-Ehrismann, 1995). These members are believed to be important in regulating numerous developmental processes such as organogenesis and morphogenetic cell migration (Chiquet-Ehrismann et al., 1994). In the literature, five individual tenascins, including tenascin-C, -R, -X, -Y and -W, have been described in diverse species such as zebrafish (Weber et al., 1998), chicken (Jones et al., 1988; Norenberg et al., 1992; Hagios et al., 1999), rodents (Saga et al., 1991; Fuss et al., 1993) and man (Gulcher et al., 1989; Matsumoto et al., 1992; Bristow et al., 1993; Carnemolla et al., 1996). All members of the tenascin family are modular glycoproteins with repeating sequence motifs folding into small globular domains (Bork and Koonin, 1996). Each member is very homologous to tenascins in other species and show relatively high similarity to other family members (Chiquet-Ehrismann et al., 1994). Tenascins share four distinctive domains (Erickson, 1993) and vary in calculated molecular size from 132 kDa for TN-W to >400 kDa for TN-X (Johansson, 1996). The amino-terminal of the tenascins contains a cysteine-rich segment that is unique to members of this family (Norenberg et al., 1995). This segment contains oligomerisation sites involved in the assembly of monomers into dimers, trimers or hexamers (Pesheva et al., 1989; Spring et al., 1989; Erickson, 1993; Pesheva et al., 1993; Norenberg et al., 1995). The cysteine-rich segment is followed by a variable number (3.5 to 18.5) of epidermal growth factor (EGF) like repeats (Erickson, 1993) and a series of fibronectin (FN) type III like domains (5 to 33) depending upon the species and type of tenascin molecule (Chiquet-Ehrismann et al., 1994). The carboxyl-terminal segment of the tenascins is similar to the carboxyl-terminal domain of β- and γ-fibrinogen (FG; Erickson, 1993; Chiquet-Ehrismann et al., 1994).

#### *3.3.1 Tenascin-C*

Tenascin-C (TN-C) was the first discovered, and remains by far the most extensively studied member of the tenascin family (tenascins; for review see Erickson

and Bourdon, 1989; Weber et al., 1999). TN-C, formerly termed J1-200/220 (Kruse et al., 1985; Faissner and Kruse, 1990; Lochter et al., 1991 Bartsch et al., 1992), hexabrachion (Erickson and Inglesias, 1984) or cytotactin (Grumet et al., 1985; Jones et al., 1988, 1989) has been found in both the central (Grumet et al., 1985; Kruse et al., 1985; Prieto et al., 1990) and peripheral nervous system (Daniloff et al., 1989; Martini et al., 1990) and in various non-neuronal structures (Erickson and Inglesias, 1984; Chiquet-Ehrismann et al., 1986). In the CNS, TN-C has been implicated in a range of different morphogenetic processes during development such as promotion of neurite outgrowth, neuronal migration, repulsion of neuronal cell bodies and growth cones, polarisation of neuronal morphology and inhibition of axonal regeneration in adults (Husmann et al., 1992; Prieto et al., 1992; Lochter and Schachner, 1993; Taylor et al., 1993)

Surprisingly, mice deficient for TN-C (Saga et al., 1992) develop normally and show no major neurological alterations or gross changes in behaviour, indicating that the TN-C either has no essential function that the loss can be compensated for by other proteins (Chiquet-Ehrismann et al., 1994).

*3.3.2 Tenascin-X, -Y and –W*

The three tenascins, TN-X, TN-Y and TN-W, have yet to be well characterised with a function only proposed for TN-X. The mRNA of TN-X has been detected in foetal muscle, testis, adrenal gland, kidney and lung and it has been suggested that TN-X may exert a role in connective-tissue structure and function (Bristow et al., 1993; Johansson, 1996). More recently, an association between TN-X deficiencies and a group of connective tissue disorders, the Ehlers-Danlos syndrome, has been proposed (Burch et al., 1997).

TN-Y has been identified in chicken and is highly expressed in developing lung, kidney, skin (Hagios et al., 1999), and in the connective tissue of adult skeletal muscle of this species (Hagios et al., 1996) but has also been detected in the avian nervous system (Tucker et al., 1999).

TN-W has been identified in zebrafish, with a distribution partly overlapping that of TN-C, and has been proposed to be involved in the migration of neural crest and sclerotome cells (Weber et al., 1998).

## 3.4 Tenascin-R

### *3.4.1 Structure of tenascin-R*

Tenascin-R (TN-R; for review see Schachner et al., 1994), formerly termed janusin (Fawcett et al., 1992; Bartsch et al., 1993; Wintergerst et al., 1993), restrictin (Rathjen et al., 1991; Norenberg et al., 1992) and J1-160/180 (Fuss et al., 1993), is an extracellular matrix glycoprotein (Zamze et al., 1999) detected in the CNS (Pesheva et al., 1989; Rathjen et al., 1991; Weber et al., 1999). The gene for TN-R gives rise to two alternative splice variants with molecular sizes of either 160 or 180 kDa and has recently been mapped to the region q23-q24 on chromosome 1 in humans (Carnemolla et al., 1996). Both TN-R splice variants are composed of a cysteine-rich amino-terminal, which is followed by 4.5 EGF-like repeats, eight or nine FN type III like domains (depending upon the isoform) and a FG-knob at the carboxyl-terminal (Norenberg et al., 1992; Fuss et al., 1993; Johansson, 1996; see figure 3.4.1). TN-R, as the other tenascins, is a glycoprotein and carbohydrates comprise 10 – 20% (w/w) of the observed molecular size (Zamze et al., 1999). Electron microscopic investigations of the multimerisation of TN-R have revealed that the 180 kDa isoform assemble into dimeric or trimeric structures whereas the 160 kDa isoform mainly exists as a monomer (Pesheva et al., 1989; Norenberg et al., 1992).

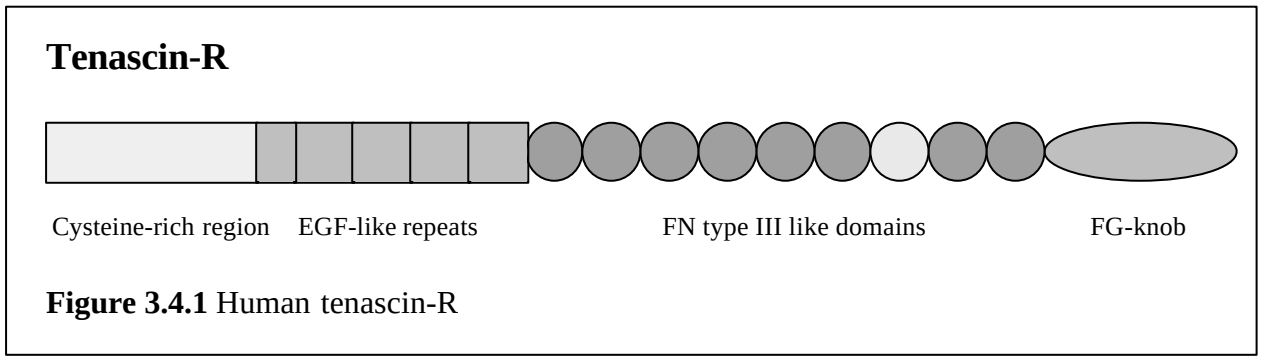


**Figure 3.4.1** Human tenascin-R

### *3.4.2 Expression pattern of tenascin-R*

Expression of TN-R mainly occurs late during development (Pesheva et al., 1989), with the larger isoform predominating in humans (Carnemolla et al., 1996). TN-R is mainly synthesised by oligodendrocytes during the onset and early phase of myelination (Bartsch et al., 1993; Wintergerst et al., 1993) but TN-R has also been detected *in vitro* in type-2 astrocytes (Ffrench-Constant and Raff, 1986; Wintergerst et al., 1993). TN-R is also expressed *in vivo* in subsets of neurones such as stellate cells

and basket cells in the cerebellar cortex, motor neurones in the spinal cord and neurones in the hippocampus and olfactory bulb (Fuss et al., 1993; Wintergerst et al., 1993). In the CNS, the protein appears mainly to be associated with the surface of oligodendrocytes, myelinated axons in the white matter (Norenberg et al., 1992; Bartsch et al., 1993), and with PNEMs around certain groups of interneurones and motor neurones throughout the nervous system (Celio and Rathjen, 1993; Wintergerst et al., 1996). During postnatal development the expression of TN-R by oligodendrocytes decreases significantly whereas labelling intensity of neurones remains constant (Bartsch et al., 1993; Wintergerst et al., 1993). This pattern of expression suggests a role in the process of myelination, stabilisation and maintenance of nerve fibre tracts and axosomatic synaptic contacts in the CNS.

### *3.4.3 Properties of tenascin-R domains*

Tenascin-R has been shown to be involved in promotion of neurite outgrowth and morphological polarisation of different neurones when presented as a uniform substrate *in vitro* (Lochter and Schachner, 1993; Lochter et al., 1994). TN-R is also a repellent for growth cone advance when presented as a sharp substrate boundary (Pesheva et al., 1993; Taylor et al., 1993), promotes adhesion and differentiation of oligodendrocytes and astrocytes (Pesheva et al., 1989, 1997; Morganti et al., 1990) and has also been suggested as a modulator of fasciculation (Xiao et al., 1998). Different properties accounting for various functions observed for TN-R have been localised to different structural domains of the protein core *in vitro* (Xiao et al., 1996; see table 3.4.1). Nonetheless, additional functions may be observed for native TN-R as the type of attached carbohydrates may also play a role.

| **Table 3.4.1** Properties of Rat TN-R domains | *Cys & EGF* | *FN 1-3* | *FN 3-5* | *FN 6-8* | *FG-knob* | *Native TN-R* |
|---|---|---|---|---|---|---|
| Short term neuronal adhesion | ± | + | ± | ++ | ++ | ++ |
| Repulsion of neuronal cell bodies | ± | + | + | + | ++ | ++ |
| Repulsion of growth cones | ++ | + | + | + | ++ | ++ |
| Polarisation of neuronal morphology | - | - | - | - | ++ | ++ |

Compiled from Xiao et al., 1996. *Abbreviations*: Cys & EGF; cysteine rich and EGF-like domains, FN; fibronectin type III-like repeats, FG; fibrinogen like. Arbitrary scale of activity ranging from no observed activity, - to high activity, ++.

Therefore, the cellular responses to TN-R are complex and probably mediated by several neuronal receptors interacting with distinct domains of the TN-R molecule (Xiao et al., 1996; Weber et al., 1999).

As was observed for mice deficient for TN-C, mice lacking TN-R also develop normally and show no major neurological alterations or gross changes in behaviour, indicating that the functions of individual tenascins can be compensated for by other members of the family (Weber et al., 1999).

*3.4.4 Receptors for tenascin-R*

TN-R, like most other ECM molecules, is a modular protein containing many potential sites for interaction with other ligands (Xiao et al., 1996). As TN-R is a secreted extracellular matrix glycoprotein, these ligands are either cell receptors or other ECM molecules. So far three receptors, F3/F11/contactin (Pesheva et al., 1993) and myelin-associated glycoprotein (MAG; Yang et al., 1999), both belonging to the immunoglobulin (Ig) superfamily, and chicken acidic leucine-rich EGF-like domain containing brain protein (CALEB) have been shown to interact with TN-R *in vitro* (Schumacher et al., 1997).

F3/F11/contactin is a 135 kDa glycosyl-phosphatidyl-inositol (GPI)-anchored cell surface glycoprotein, predominantly expressed by neurones and presumably involved in promoting axon outgrowth (Brummendorf et al., 1989; Gennarini et al., 1989) and neurone-glial interactions (Revest et al., 1999). Interaction between F3/F11/contactin and TN-R has been shown to occur through the Ig-like domains on F3/F11/contactin (Brummendorf et al., 1993; Norenberg et al., 1995; Xiao et al., 1996, 1998) and the FN repeats of TN-R (Xiao et al., 1996, 1999). This interaction mediates the antagonistic TN-R–elicited effects on neurites and growth cones and axonal defasciculation, when presented as uniform or sharp substrate boundaries (as described above; Pesheva et al., 1993; Xiao et al., 1996, 1998). In addition, because of a high sequence homology between F3/F11/contactin and the β2-subunit of the voltage-gated sodium channel (Isom et al., 1995), TN-R was thought to function as a regulator of sodium channel localisation and play a role at nodes of Ranvier. This notion has now been substantiated by the recently shown interaction between TN-R and the β2-subunit of the voltage-gated sodium channel (Srinivasan et al., 1998; Xiao et al., 1999).

The second receptor, so far shown to bind to TN-R, is myelin-associated glycoprotein (MAG) now also designated siglec-4 (for review see Schachner and Bartsch, 2000). MAG is a minor constituent of myelin and is implicated in formation and maintenance of myelin and in interactions between nerve cells and myelin-forming glial cells (Poltorak et al., 1987). Two isoforms of MAG are expressed (67 or 72 kDa) with the larger isoform being functionally important in the CNS and the smaller in the PNS (Inuzuka et al., 1991). Expression of MAG and TN-R has been shown to overlap both in time and space (Yang et al., 1999). Both molecules accumulate at nodes of Ranvier (Weber et al., 1999) indicating their involvement in regulating voltage dependent $Na^+$ channel properties (Srinivasan et al., 1998; Xiao et al., 1999). Furthermore, it has been shown that MAG is involved in the signalling pathway of TN-R repulsion and that this action is mediated via its interaction with both the amino-terminal region and the FG-knob of TN-R (Yang et al., 1999).

CALEB, the third receptor for TN-R identified so far, is also the least described. It is a transmembrane glycoprotein, restricted to the developing and adult chick nervous system and associated with neuronal and glial surfaces (Schumacher et al., 1997). It has been immunohistochemically shown to overlap with TN-R in the retina and implicated in neurite formation *in vitro* (Schumacher et al., 1997).

*3.4.5 ECM ligands for tenascin-R*

TN-R has also been shown *in vitro* to interact with several ECM components such as a group of chondroitin sulphate proteoglycans (CSPGs) comprising aggrecan, brevican, neurocan, versican (Aspberg et al., 1995, 1997) and phosphacan (Xiao et al., 1997; Milev et al., 1998). These interactions are mediated either by carbohydrate-protein (Aspberg et al., 1995) or by protein-protein interactions (Aspberg et al., 1997). Using immunohistochemistry, co-localisation between TN-R and different CSPGs has been shown in many areas of the CNS (Aspberg et al., 1995; Xiao et al., 1997; Matsui et al., 1998; Hagihara et al., 1999; Haunso et al., 1999), indicating that their interactions observed *in vitro* also plays a biologically significant role *in vivo.* It has been proposed that these interactions between ECM molecules may influence the properties of the intercellular space (Weber et al., 1999) or may be involved in attracting different ECM components to their correct location in the CNS, leading to the correct assembly of matrix components between and around cell bodies. This notion is supported by the observation that PNEMs have an altered appearance in

TN-R deficient mice, resulting from an impaired attraction of certain CSPGs when TN-R is lacking (Weber et al., 1999; Haunso et al., 2000). Finally, these ligands not only interact with TN-R but also with each other, different receptors and ECM molecules, all depending upon the developmental stage and region of the CNS, further increasing the complexity of these interactions and their functions.

*3.4.6 Tenascin-R and pathological conditions*

The involvement of TN-R in human pathological conditions has yet to be extensively studied. As TN-R is a major component of PNEMs (Celio and Rathjen, 1993; Wintergerst et al., 1996) and it can be envisaged that the alteration or destruction of PNEMs in diseases such as HIV, Rett syndrome and CJD also influences the distribution of TN-R in these entities. Recently, a loss of TN-C and -R in acute plaques in multiple sclerosis (MS) has been reported (Gutowski et al., 1999). This remodelling of ECM components increase during development of MS, indicating an increase in enzyme-mediated breakdown of ECM components. This was followed by an increase in TN-C and -R production by astrocytes resulting in glial scar formation hindering re-myelination and axonal repair in MS lesions (Gutowski et al., 1999).

**3.5 Aims**

In these studies, the aim was to further identify and characterise the role of TN-R in PNEMs and its involvement with the membrane-related cytoskeleton found in GABAergic PV-expressing cortical interneurones. For this purpose a number of biochemical and molecular biological techniques were applied to identify ligands/receptors for TN-R *e.g.* expression of recombinant proteins in bacteria, yeast and mammalian cell lines, generation of TN-R affinity column and analysis of TN-R associating proteins. As the FG fragment is the most conserved domain in the tenascins (Erickson, 1993) the research focused mainly on this C-terminal fragment. Furthermore, using combined immunofluorescence and confocal microscopic techniques, immunohistochemical characterisation of PNEMs and the membrane-related cytoskeleton was performed to help elucidate the role of TN-R in these entities.

# Part A

# 4. Bacterial expression of recombinant proteins

## 4.1 Introduction

From a comparison between the protein sequences of different tenascins it has become evident that the FG domain is the most conserved module in the tenascins (Erickson, 1993). The FG-knob of rat TN-R strongly mediates short-term neuronal adhesion, repulsion of neuronal cell bodies, repulsion of growth cones and polarisation of neuronal morphology (Xiao et al., 1996). Although the FG region is relatively conserved between TN-C and -R, similar effects are not observed for FG-knob of TN-C (Xiao et al., 1996). This, together with the fact that ligands mainly binding to the amino-terminal region or the FN repeats of TN-R have been discovered, lead us to postulate that putative receptors/ligands existed for the FG region of TN-R.

Recently, by affinity chromatography using a recombinant fragment of rat TN-R comprising the amino-terminal cysteine-rich stretch and all EGF repeats, Xiao *et al*. isolated a phosphacan-related molecule from mouse brain (Xiao et al., 1997). Interactions between recombinant produced chimera of members of the CSPG family and native full length rat TN-R or recombinant rat TN-R fragments have also been shown *in vitro,* with these interactions being mediated by the protein core and not by carbohydrate-protein interactions (Aspberg et al., 1997). Despite the fact that the obtained recombinant material does not contain carbohydrates and is potentially incorrectly folded, these two reports indicate that recombinant technology is a powerful tool that may be used to identify natural ligands interacting in a non-carbohydrate mediated manner with TN-R.

## 4.2 Materials and methods

### *4.2.1 Recombinant DNA technology*

#### *4.2.1.1 Polymerase chain reaction*

To amplify tenascin-R cDNA fragments required for construction of expression vectors, polymerase chain reaction (PCR; Saiki et al., 1988) was performed on plasmids containing human tenascin-R cDNA fragments (kindly provided by Dr. Zardi; Carnemolla et al., 1996). All primers were produced by Microsynth (Switzerland) and used at a concentration of 0.4 pmol/µL. To run the PCR, 1 unit of Pfu DNA polymerase (Promega), forward and reverse primers, 200 ng of template plasmid and 0.2 nmol/µL of dNTPs (GibcoBRL) were mixed in 1 x Pfu-buffer (Promega). The PCR was performed as shown in figure 4.2.1 with a schematic overview of the PCR process shown in figure 4.2.2.

94°C for 2 min.

**10 cycles at:**
94°C for 30 sec.
55°C for 15 sec.
ΔT=0.1°C/sec. until 45°C
72°C for 3 min.

**30 cycles at:**
94°C for 30 sec.
50°C for 15 sec.
ΔT=0.5°C/sec. until 72°C
72°C for 3 min.

72°C for 5 min.

**Figure 4.2.1** PCR program

All PCRs were run using a Peltier Thermal Cycler PTC-200 DNA engine (MJ Research). The produced R1 cDNAs spanned bases 2831-4158, whereas the FG cDNAs spanned bases 3561-4158 of human tenascin-R.

The amplification products were separated on 1% agarose gels in 0.5 x TBE, cast using a Mini-Gel electrophoresis unit (Cosmo Bio Co) and purified from there using the QIAEX II gel extraction kit, according to the protocol supplied by the manufacturer (Qiagen).

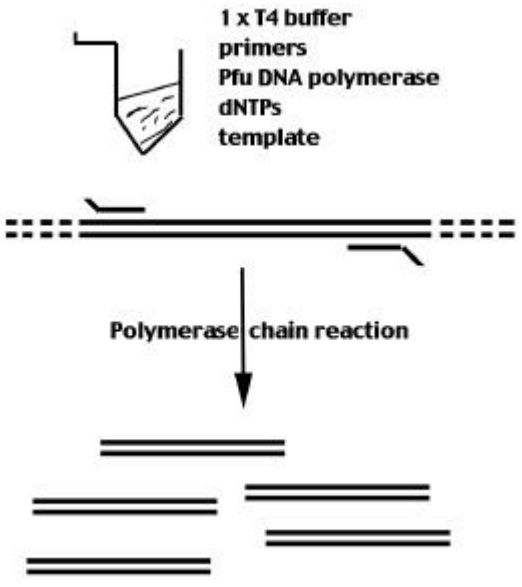


**Figure 4.2.2** PCR procedure

The sequences for the primers for cloning R1 into pRSET-B were:

hTNR-F-R1 : $^{5'}$G<u>GGATCC</u>G **GAA** TTC ACC ATC ACC AGA C$^{3'}$

R-R1-pRSET : $^{5'}$ <u>TCTAGA</u> **TCA** GAA CTG TAA GGA CTG$^{3'}$

The sequences for the primers for cloning R1 into pGEX-1 were:

hTNR-F-R1 : $^{5'}$G<u>GGATCC</u>C **GAA** TTC ACC ATC ACC AGA C$^{3'}$

R-R1-pGEX : $^{5'}$ <u>GGATCC</u> **TCA** GAA CTG TAA GGA CTG C$^{3'}$

The sequences for the primers for cloning FG into both pRSET-B and pGEX-1 were:

hTNR-F-FG : $^{5'}$G<u>GGATCC</u>C GAG **CTG** AGC CAG AAA TTA C$^{3'}$

R-PRIMER : $^{5'}$ <u>GAAT **TC**A</u> GAA CTG TAA GGA CTG C$^{3'}$

The position of the restriction sites for the endonucleases, included in the primer sequences, are underlined above. The primers hTNR-F-R1, hTNR-F-FG and R-R1-pGEX contained restriction sites for BamH1, R-PRIMER for EcoR1 and R-R1-pRSET for BglII. The first and stop codon in the tenascin-R fragments are indicated in bold above.

*<u>4.2.1.2 cDNA cloning and construction of expression vectors</u>*

Expression of cDNAs, cloned into the pRSET-B vector (Invitrogen) resulted in the production of recombinant proteins with nine additional residues (RGSHHHHHH, subsequently termed the hexahistidine tag) at the amino-terminus. Expression of cDNA cloned into the pGEX-1 (Pharmacia biotech) vector resulted in proteins fused with glutathione-S-transferase (GST) at the amino-terminus.

*<u>4.2.1.3 Enzymatic digestion, ligation and transformation into E. coli</u>*

Purified R1 cDNA for ligation into pGEX-1 was digested with BamH1 (GibcoBRL), whereas R1 cDNA for ligation into pRSET-B was digested with BamH1 and BglII (Boeringer Mannheim). FG cDNAs for ligation into pGEX-1 and pRSET-B were digested with BamH1 and EcoR1 (Boeringer Mannheim). The appropriate vectors (pBluescript II KS +/-, pRSET-B and pGEX-1) were digested using the same enzymes. All digestions were performed for 1 hr at 37°C in the optimal buffers. All

digested vectors and cDNAs were purified from 1% agarose gels using the QIAEX II gel extraction kit.

Unless otherwise stated, all the following centrifugations were performed for 1 min. at 13,000 rpm in a Micro Centaur table centrifuge and all media contained 50 mM ampicillin (Sigma). Approximately 50 ng of the appropriately digested cDNA and 20 ng of pBluescript II KS +/- vector, together with 2 units T4 DNA ligase (Fermentas) in 1 x T4 DNA ligase buffer (GibcoBRL) were incubated at room temp. for 3 hrs. Subsequently, tubes were placed for 5 min. at 56°C, transferred on ice, 100 µL chemical competent XL-1 Blue bacteria (Promega, for production of chemical competent bacteria see the appendix) were added and the mixture placed on ice for 20 min. The mixtures were then heated to 42°C for 45 sec. in a Techne Dri-block DB-20 heating block (Witec AG) and placed on ice for 5 min. One mL Lennox L broth base (LB-medium GibcoBRL), without ampicillin, was added and the solutions were placed for 1 hr at 37°C, followed by centrifugation. Centrifuged pellets were re-suspended in 50 µL LB-medium and plated on LB-agar (GibcoBRL) plates together with 10 µL 0.1 M IPTG (Saxon Biochemicals GMBA) and 80 µL 20 mg/mL X-Gal (Axonlab AG) per 9 cm petri-dish (Milan). This makes it possible to distinguish clones containing inserts as white and clones without insert as blue. Plates were subsequently placed overnight in an incubator (Köttermann) at 37°C. The following day ten white clones were randomly chosen, placed individually in 14 mL polystyrene tubes containing 3 mL LB-medium and left to grow overnight at 37°C in an orbital shaking incubator (Gallenkamp). Plasmids were extracted from the transfected bacteria by centrifuging 1 mL of the cultures, grown overnight, in 1.5 mL Eppendorf tubes. Supernatants were removed and mini-preparations carried out according to a procedure described by Feliciello and Chinali (1993). Supernatants were centrifuged and 200 µL of solution I was added after which the pellets were re-suspended by vortexing. Subsequently, 200 µL of solution II was added to each of the tubes, the contents were mixed by inverting the tubes 5-6 times and then 200 µL of solution III was added, and the contents mixed by inverting (see the appendix for solutions I, II & III used in the mini-preparation of plasmid cDNAs from bacteria). All tubes were subsequently centrifuged, supernatant transferred to new tubes, 600 µL of absolute ethanol added and briefly mixed by vortexing. The contents of the tubes were centrifuged for 10 min. at 13,000 rpm followed by aspiration of the supernatant

after which 500 µL of 70% ethanol was added and the pellets partly re-suspended by vortexing. The tubes were centrifuged for 5 min. at 13,000 rpm, the supernatant removed and pellets left to dry in a table excicator (Kartell). Pellets were then re-suspended in 10 mM Tris-HCl, (pH8.0) and stored at -20°C.

Mini-preparations of the plasmids were checked by digesting the plasmids with restriction enzymes, as described previously, and the results were evaluated on 1% agarose gels. Plasmids containing inserts of the appropriate sizes were sequenced as described in section **5.2.2**. Plasmids containing the appropriate inserts were digested as described above and the inserts purified from the agarose gels using the QIAEX II kit and ligated into their appropriately digested expression vectors (pRSET-B or pGEX-1). The ligation products were introduced into BL21(DE3) pLysS bacteria (Promega) as previously described. After 1 hr at 37°C in LB-medium, without ampicillin, tubes were spun, pellets re-suspended in 50 µL LB-medium, plated on LB-agar plates and placed at 37°C overnight. Clones were then picked for expression of recombinant material (for a schematic overview of the ligation of FG or R1 into pRSET-B or pGEX-1 see Fig. 4.2.3).

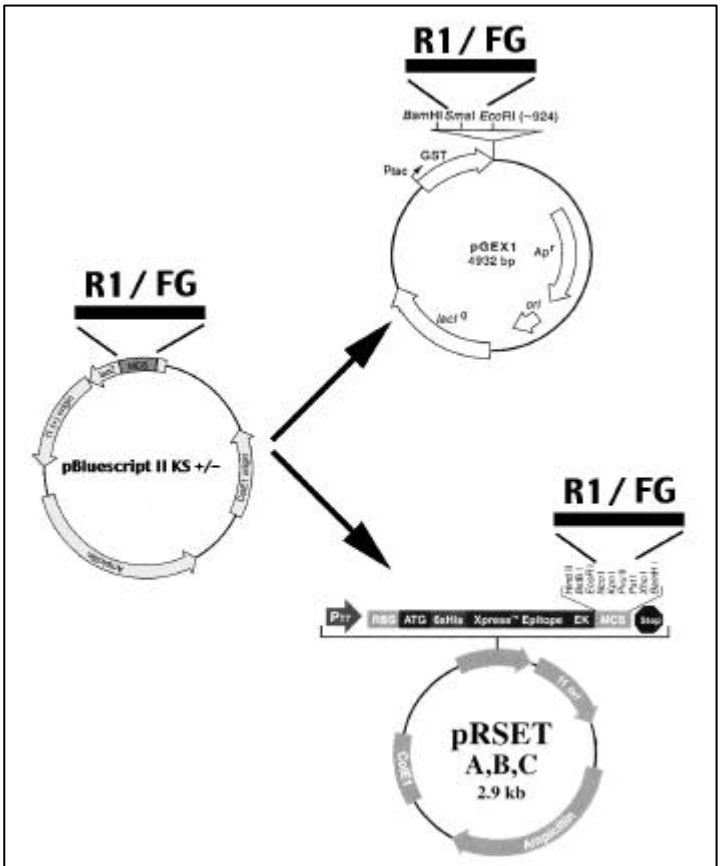


**Figure 4.2.3** Ligation of cDNA for R1 and the FG-knob into pGEX1 and pRSET-B

### *4.2.2 Expression and purification of recombinant material*[c]

#### *4.2.2.1 Pilot expression of recombinant material*

For bacteria transformed with pRSET-B-R1, pRSET-B-FG or pGEX-1-FG, five clones were picked from the LB-agar plates and transferred to 14 mL polystyrene tubes containing 3 mL LB-medium with ampicillin. Ten clones were chosen from bacteria transformed with pGEX-1-R1 and placed in 14 mL tubes with 3 mL LB-medium containing ampicillin. Tubes were agitated for 1 hr at 37°C in an orbital shaking incubator and the content subsequently divided into two. Expression of recombinant proteins were achieved by adding IPTG to a final concentration of 0.5 mM to one half of the tubes whereas the other half were left un-induced. Tubes were then agitated for 3 hrs at 37°C after which 1 mL bacteria containing LB-medium was removed and centrifuged for 1 min. at 13,000 rpm. Pellets were subsequently re-suspended in 1 x Laemmli loading buffer, sonicated for 2 times 20 sec. using a Micro Ultrasonic Cell Disrupter (Kontes) and heated for 2 min. at 94°C on a heating block before applying onto small SDS-PAGE gels to evaluate the expression.

### *4.2.3 Gel electrophoresis*[d]

#### *4.2.3.1 Preparation, staining and drying of small SDS-PAGE gels*

Small (8 x 6.5 cm) discontinuous SDS-containing (Sigma) polyacrylamide gel electrophoresis slab gels (subsequently termed small SDS-PAGE gels) were prepared using a Mighty Small SE245 Dual Gel Caster System (Hoefer). The concentration of acrylamide varied in the separation gels depending upon the experiment (6 - 12%) whereas stacking gels contained 5% acrylamide. Samples were prepared by dissolving in Laemmli loading buffer and heated to 94°C on a heating block for 2 min. then applied to wells made in the stacking gels. The small SDS-PAGE gels were subsequently run at 20 mA per gel in a Mighty Small II SE250/260 running chamber (Hoefer) until the tracking dye was 5 mm from the bottom of the gel. Subsequently, gels were placed in Coomassie Brilliant Blue R-250 solution (Serva) and left to stain for 3 hrs under agitation. The staining solution was removed and destaining solution

[c] See Guan and Dixon, 1991

[d] See Laemmli, 1970 and Hames and Rickwood, 1990

added to the gels, which were then left to destain overnight. The following day, the gels were placed for 1 hr in drying solution (10% ethanol, 4% glycerol) and subsequently placed on wet 3M chromatography paper (Whatman) in a GD 5040 gel dryer (Witec AG) and dried at 60°C for 1 hr under vacuum.

*4.2.3.2 Preparation of large SDS-PAGE gels*

Large polyacrylamide gels were prepared using a large gel caster (Hoefer). Separation gels were prepared from acrylamide solutions of two different concentrations (4% and 16%), which were mixed together using a Hoefer SG50 linear gradient mixer, and poured in between electrophoretic glass plates (15 x 13 cm), sealed by spacers and electrophoretic vaseline. Acrylamide solutions were immersed with water, saturated with butanol, and allowed to polymerise for approximately 1 hr at room temperature. Subsequently, the water was removed and a 3% stacking gel comprising of acrylamide was poured in between the electrophoretic glass plates. Wells were made by placing a comb into the acrylamide solution, which was left to polymerise for 1 hr. Samples were prepared as described above. Electrophoresis of the large SDS-PAGE gels were performed at 40 mA per gel in a vertical gel electrophoresis system (Life Technologies Inc) until the tracking dye was 5 mm from the bottom of the gels. Following the electrophoresis, the polyacrylamide gels were removed from the glass plates and either stained by the silver staining method or by Coomassie Brilliant Blue R-250 where after they were placed overnight in drying solution. Gels were then placed between two (22 x 22 cm) cellophane sheets wetted in drying solution, placed on wet 3M paper and dried at 60°C for 4 hrs in a gel dryer under vacuum.

*4.2.3.3 2D electrophoresis, first dimension*

Two-dimensional gel electrophoresis was used in order to analyse homogenate and eluates from the tenascin-R FG affinity column. Proteins were first separated by isoelectric focusing on 18 cm long Immobiline Drystrips (Pharmacia) with immobilised linear pH gradient ranging from pH3 to 10. The next step comprised the separation on linear gradient of 4% to 16% polyacrylamide gels (see section **4.2.3.4**).

To perform the first dimension of the isoelectric focusing, Immobiline DryStrip gels (IPG) were re-hydrated in re-hydration buffer (8 M urea, 2% (w/v)

CHAPS, 10 mM DTE, 2% (v/v) resolyte 3.5-10, 0.02 (w/v) bromphenol blue) overnight at room temperature. After re-hydration, strips were briefly washed with de-ionised water and transferred to adjacent grooves of the aligner in the Immobiline DryStrip tray. Strips were placed with the angular end (acidic) at the top of the tray near the red electrode (anode). The moistened electrode strips were placed across the cathode and anode ends of the aligned IPG. Both electrodes were aligned over an electrode strip and pressed down to contact the electrode strips. Sample cups were placed on the sample cup bars, high enough to avoid touching the gel surface. The sample cup bars were positioned and pushed towards the electrodes until the spacers (on the side of sample cup bars) touched the electrodes. The sample cups were pressed against the IPG strips to ensure good contact with each IPG strip and 230 ml of silicone oil was poured to completely cover the IPG strips. Samples were applied to the sample cups by pipetting under the surface of the silicone oil. Samples for 2D electrophoresis (100 µL) were lyophilised in a speed vak (SC1000, Savant) and subsequently dissolved in 100 µl of sample buffer (7 M urea, 2 M thiourea, 4% (w/v) CHAPS, 1% (w/v) DTE, 20 mM Tris, 0.02 (w/v) bromphenol blue, 1 mM EDTA, 1 mini EDTA-free protease inhibitor cocktail tablet (Boehringer & Mannheim)) per 10 ml of sample buffer just prior to use. After placing the safety lid and setting the cooler to 14°C, the Multiphor unit was connected to the power supply. For the first 15-20 minutes, voltage was set at 250 V where after the voltage was increased to 500 V for 1-2 hrs. Finally, the voltage was increased by 250 V each 15 minutes up to 3500 V. In total the samples were exposed to approximately 100 kV-hrs of isoelectric focusing (1.5 day).

*4.2.3.4 2D electrophoresis, second dimension*

Polyacrylamide gels were prepared from acrylamide solutions of two different concentrations (4% and 16%; see the appendix), which were mixed together using a gradient maker and poured in between electrophoretic glass plates (20 x 20 cm) sealed by spacers and electrophoretic vaseline. Acrylamide solution in between the electrophoretic glasses was immersed by water, saturated with butanol, and allowed to polymerise for approximately 1 hr at room temperature. After isoelectric focusing, strips were picked from strip tray and placed individually in labelled 9 cm petri-dishes with the plastic side from the strip touching the wall of the petri dish. Strips were first

pre-incubated for 15 min. at room temp. in equilibrium buffer (0.05 M Tris-HCl (pH6.8), 6 M urea, 30% (v/v) glycerol, 2% (w/v) SDS, 0.02 (w/v) bromphenol blue) containing 1% (w/v) DTE. The strips were further incubated for 15 min. at room temp. in equilibrium buffer containing 2.5 % (w/v) of iodoacetamide. After incubation with equilibrium buffers, the anode and cathode ends of the strips were removed and the strips placed on top of the polymerised polyacrylamide gels. Strips were fixed to the top of the gels by adding melted agarose sealing solution (0.5 % (w/v) agarose and 0.02 % (w/v) bromphenol blue in running buffer) with the aid of a Pasteur pipette, and allowed to solidify. After filling the electrophoretic chamber with running buffer, electrophoresis was performed at constant current in two steps. During the initial migration, a current of approximately 15 mA per gel was used then increased to 30 mA per gel after 30 min. and electrophoresis continued until the front of the tracking dye was approximately 5 mm from the bottom. After electrophoresis, gels were placed in a plastic tray and proteins were fixed and stained either by the silver staining method or by Coomassie Brilliant Blue R-250. The gels were dried as described in section **4.2.3**.

*4.2.3.5 Rapid silver staining method*

Polyacrylamide gels were silver stained according to the procedure described in "Short Protocols in Molecular Biology" (Ausubel et al., 1995). The gels were fixed for 20 min. in 150 mL formaldehyde fixing solution (40% methanol, 0.5 mL/L 37% formaldehyde), after which they were washed twice for 10 min. with double distilled water ($ddH_2O$). Subsequently gels were soaked in 150 mL 0.2g/L sodium thiosulfate ($Na_2S_2O_3$, Fluka) for 2 min., washed 3 times for 1 min. with $ddH_2O$ and placed in 0.1% $AgNO_3$ in $ddH_2O$ for 10 min. After incubating in silver-containing solution, gels were briefly rinsed in $ddH_2O$ followed by thiosulfate developing solution (TDS) comprised of 3% $Na_2CO_3$, 0.0004% $Na_2S_2O_3$, 0.5 mL/L 37% formaldehyde, and placed in TDS until adequate spot intensities were achieved (between 1 to 10 min.). Silver precipitation was stopped by adding 5 mL 2.3 M citric acid per 100 mL TDS and gels left to agitate for 20 min. Subsequently, the gels were washed for 20 min. in $ddH_2O$ and placed overnight in drying solution. The following day, the gels were placed on wet 3M chromatography paper and dried at 60°C for 4 to 5 hrs in a gel dryer under vacuum (GD 5040, Witec AG).

### *4.2.4 Production and affinity purification of recombinant material*[e]

#### *4.2.4.1 Large-scale production of recombinant material*

Three litres of ampicillin containing LB-medium in Erlenmeyer flasks was inoculated with 3 mL overnight culture of the appropriately transfected BL21 bacteria. The medium was agitated at 37ºC in an orbital shaking incubator until an $OD_{600}$ of 0.2 was reached, where after the expression of recombinant protein was induced by adding IPTG to a final concentration of 0.5 mM. After 5 hrs of incubation at 30ºC, the bacteria were pelleted by centrifugation at 5,000 rpm for 15 min. in a Sorval RCSC centrifuge (GSA rotor). For recombinant material expressed from the pGEX-1 vector, pellets were re-suspended in 10 mL GST-lysis buffer containing 1 mini EDTA-free protease inhibitor cocktail tablet (Boehringer and Mannheim). Recombinant material produced from the pRSET-B vector was either re-suspended under native (50 mM Tris-HCl, 500 mM NaCl, 1 mini EDTA-free protease inhibitor cocktail tablet, pH7.8) or denaturing conditions (50 mM Tris-HCl, 500 mM NaCl, 8 M urea, pH7.8). Re-suspended pellets were subsequently frozen in liquid $N_2$, then thawed at 37ºC in a heating block and sonicated on ice for 3 times 30 sec. with 30 sec. pauses. This procedure was performed twice for each pellets and homogenates were cleared by centrifugation at 10,000 rpm for 10 min. in a Sorval centrifuge (SS-34 rotor). The supernatant was subsequently loaded on appropriate pre-calibrated affinity columns (see below).

#### *4.2.4.2 Purification of hexahistidine-fusion proteins*

Purification of hexahistidine containing fusion proteins (his-tag) was performed under both native and denaturing conditions. Buffers for the native and denaturing affinity-purification were similar except, for denaturing conditions the solutions in addition contained 6 M urea. All the following manipulations of the column were performed with the aid of a peristaltic pump (Perplex). In 5" P.P. chromatography columns (Evergreen Scientific; dimensions, l:d:$V_T$ ; 11 cm:1 cm: 7 mL) was packed 1.5 mL of Ni-NTA (nickel-nitrotriacetic acid) agarose (Qiagen) gel, re-suspended in either 10 mL native or denaturing buffer. Subsequently 10 mL native

[e] See Pharmacia, 1993 and Scopes, 1994

or denatured protein lysate was applied to the column and left to run through. After either washing with 2 x 10 mL native or denaturing His washing solution (nHis or dHis), 5 mL of nHis or dHis elution buffer was applied and 1 mL fractions were collected. Ni-NTA agarose columns were regenerated by extensive washes with either nHis or dHis washing buffer, and stored at 4ºC in either nHis or dHis washing buffer (native buffer containing 0.02% sodium azide (Merck)). Analysis of eluted material was performed by SDS-PAGE, using a 1:1 mixture of eluted fraction with 2 x Laemmli loading buffer (samples containing urea were not heated before being applied to the SDS-PAGE gel). The gels were stained with Coomassie Brilliant Blue R-250 and dried in a gel dryer (as previously described).

#### *4.2.4.3 Purification of GST-fused recombinant proteins*

All the following manipulations of the column were performed with the aid of a peristaltic pump. In a 5" P.P. chromatography column was packed 1.5 mL of glutathione sepharose 4B gel (Pharmacia Biotech), re-suspended in 10 mL GST-washing buffer. Subsequently, the 10 mL protein lysate was applied to the column and left to run through. After washing with 2 times 10 mL GST-washing solution, 5 mL of GST-elution buffer was applied and 1 mL fractions collected. Glutathione sepharose columns were regenerated by extensive washing with GST-washing buffer, and stored at 4ºC in GST-washing buffer containing 0.02 % sodium azide. Elution fractions were diluted 1:1 by 2 x Laemmli loading buffer and analysed by SDS-PAGE as previously described.

### *4.2.5 Generation of an affinity column and analysis of eluting proteins*[f]

#### *4.2.5.1 Generation of human tenascin-R column*

Recombinant hexahistidine FG protein (hFG, $V_{total}$ = 20 mL), purified under denaturing conditions as described above, was dialysed 3 times against 1 litre 3 M sodium thiocyanate (NaSCN, Aldrich) in 0.1 M $NaHCO_3$, pH8.3. Subsequently, the solution was centrifuged at 10,000 rpm for 10 min. in a Sorval centrifuge (rotor SS-34). 0.45g of cyanogen bromide (CNBr) activated sepharose 4 fast flow gel (Pharmacia Biotech) was placed in a 15 mL centrifuge tube (Milan) and washed 8

[f] See Pharmacia, 1993 and Scopes, 1994

times in 10 mL ice-cold 1 mM HCl, pH3.0. Dialysed recombinant hFG was added to the washed sepharose gel and the tube was rotated in a multi-purpose rotor (Bender-Hobein) for 17 hrs at 4ºC. Subsequently, the sepharose gel was pelleted by centrifugation for 3 min. at 2,000 rpm in a Rotina 46R table centrifuge (Hettich) and washed for 5 min. in 14 mL 2 M NaSCN. This was followed by 5 min. washes in 1 M NaSCN and 0.5 M NaSCN (all in 0.1 M $NaHCO_3$, 0.25 M NaCl, 2.5% glycerol, pH8.3). Finally, the sepharose gel was washed in coupling buffer (0.1 M $NaHCO_3$, 0.5 M NaCl, pH8.3). All centrifugations were performed at 2,000 rpm for 3 min. Thereafter, remaining active CNBr groups were blocked by incubating the sepharose gel with 0.2 M glycine (pH8.0) for 2 hrs at room temperature. Subsequently, the sepharose gel was washed 3 times with coupling buffer followed by acetate buffer (0.1 M sodium acetate, 0.5 M NaCl, pH4.0). Finally, the tenascin-R-coupled sepharose gel was packed in a 5" P.P. chromatography column and stored at 4ºC.

*4.2.5.2 Preparation of pig cortex homogenate*

Whole pig brains were obtained from the slaughterhouse and placed on ice for the duration of the transportation (approximately 20 min.). The cortex was separated from the white matter by dissection under a light microscope (Zeiss), aliquoted into 2 g portions, frozen in liquid nitrogen and stored at -80ºC until used. Approximately 2 g of pig cortex was placed in 10 mL ice-cold homogenisation buffer A containing 1 mini EDTA-free protease inhibitor cocktail tablet and homogenised using a hand-operated 15 mL glass homogeniser (Braun Melsungen) on ice for 10 min. The homogenate was transferred to a 14 mL polystyrene tube and rotated overnight at 4ºC in a multi-purpose rotor. The following day the solution was centrifuged at 100,000 g in a Sorval Ultra 80 ultracentrifuge (37,000 rpm, rotor T-865-1), and the pellet re-suspended in 2 mL homogenisation buffer B and further rotated overnight at 4ºC. Thereafter, the solution was cleared by centrifugation at 100,000 g, the supernatant diluted 1:10 in homogenisation buffer C and loaded on the prepared human tenascin-R FG affinity column. The column was washed 10 times with 1 mL washing buffer (10 mM Tris-HCl, 1 mM EDTA, 1 mM EGTA, 0.02% sodium azide, pH7.0) containing stepwise increasing NaCl concentrations (0.0 M to 1.0 M NaCl, $\Delta c$=0.1 M) and 10 mL homogenisation buffer D was applied. Proteins still binding to the column were eluted with 3 mL homogenisation buffer E, collected in 0.5 mL fractions into

Eppendorf tubes containing 0.2 mL 1 M Tris-HCl, pH6.8. Before dialysing the eluates against a carbonate buffer (0.1 M $NaHCO_3$, 0.15 M NaCl, 0.1% Tween-20, pH8.8) and storage at -20ºC, 100 µL eluate was removed from each Eppendorf tube and analysed either by SDS-PAGE (large gel) or 2D electrophoresis as described in the respective sections. The column was washed in 1 M Tris-HCl (pH6.8) followed by extensive washing with homogenisation buffer A in which it was also stored at 4°C.

*4.2.5.3 Enzymatic digestion of eluates*

All the following digestions of material eluted from the recombinant FG column were performed for 1 hr at 37ºC with a concentration of enzyme of approximately 0.02 U. Collagenase type II (Koch-Light Laboratories) digestions were carried out at pH7.5 whereas digestions for elastase (Koch-Light Laboratories), hyaluronidase (Sigma) and chondroitinase ABC (Sigma; Yamagata et al., 1968) all were performed at pH8.0. Additionally, digestion of collagenase type II was performed in the presence of 3 mM $CaCl_2$. Eluate (100 µL) was mixed together with 50 µL 1 M sodium phosphate buffer of the appropriate pH, 0.02 U enzyme and $ddH_2O$ up to a total volume of 200 µL. After 1 hr of digestion at 37ºC, 33 µL 6 x Laemmli loading buffer together with 2 µL 0.1 M DTT were added, the samples heated to 95ºC for 5 min. and subsequently loaded on a large 4 to 16% linear gradient SDS-PAGE gel. Proteins were detected by the silver staining method.

*4.2.5.4 FITC-labelling and fluorometric detection of ligand - hexahistidine FG interactions*

To 1.2 mL dialysed eluate was added 6 µL FITC (in absolute ethanol), the tube was wrapped in silver paper, placed in a multi-purpose rotor and mixed by rotation for 40 min. at room temperature. Subsequently, 100 µL saturated glycine in $ddH_2O$ was added, to block the remaining free FITC molecules, and the tube was incubated for an additional 15 min. at room temperature. The solution was applied to a spin column, already pre-packed with P-6 Bio-Gel (BioRad, bead sizes = 90-180 µm) re-hydrated in homogenisation buffer C, and then centrifuged for 3 min. at 3,000 rpm. To four of eight wells in a Ni-NTA HisSorb Strip was added 100 µL purified recombinant hFG (in 50 mM Tris-HCl, 150 mM NaCl, 4 M urea; pH7.8) which was subsequently incubated overnight at 4°C. Then, the content of all eight wells was

washed three times in homogenisation buffer C and 100 µL FITC-labelled eluate was added to seven of the eight wells. To the last remaining well 100 µL homogenisation buffer C was added and the strip subsequently incubated overnight at 4°C. Three consecutive washes in homogenisation buffer C and incubation for 1 min. in 100 µL homogenisation buffer E, to release any proteins binding to the hFG-fragment, preceded mixing with 100 µL 1 M Tris-HCl (pH6.8) and collection in micro-cuvettes (for a schematic overview of the solution added to the NTA-coated wells see Fig. 4.2.4). Solutions were excited at 494 nm and emissions were measured at 520 nm using a luminescence spectrometer (Perkin Elmer LS50B). OD values for wells incubated both with recombinant hFG and FITC-labelled eluate were compared with values obtained from the wells incubated only with FITC-labelled eluate or only with recombinant hFG.

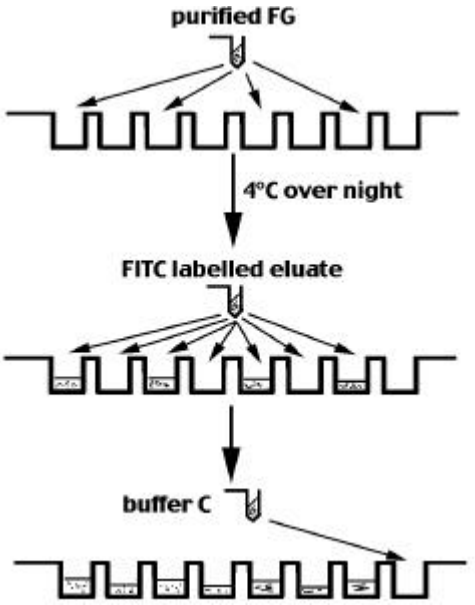


**Figure 4.2.4** Solutions added to NTA-coated wells

## 4.3 Results

### *4.3.1 Expression of recombinant material from pGEX-1 vectors*

Expression of recombinant material, from cDNA ligated into the pGEX-1 vector, resulted in production of proteins fused at the N-terminal to GST. Production of recombinant GST-R1 and GST-FG in BL21(DE3) pLysS bacteria was confirmed

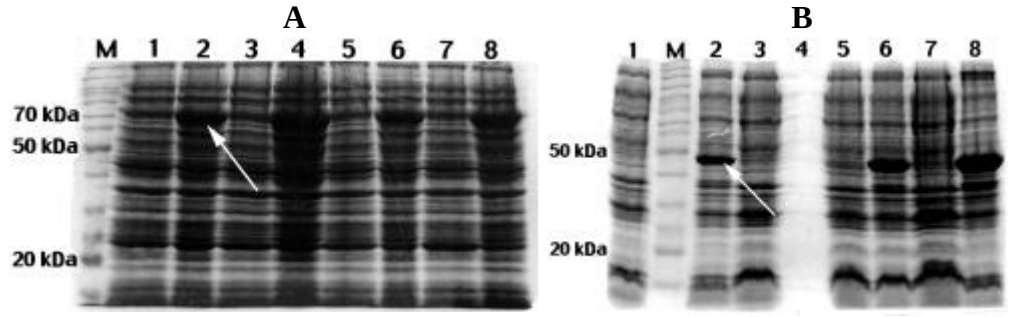


**Figure 4.3.1 Coomassie Blue stained SDS-PAGE gels of bacterial pellets**.
Expression of recombinant GST-R1 (**A**) and GST-FG (**B**) in BL21 bacteria. Lane **M (A & B)**, 10 kDa molecular marker (Pharmacia Biotech). Lanes **1**, **3**, **5** and **7** represent pellets from non-induced bacteria and lanes **2**, **4**, **6** and **8** pellets from IPTG induced bacteria. Arrows in **A** & **B** indicate the expression of recombinant material of 70 and 45 kDa respectively. The lack of material in lane 4 (**B**) occurred due to a problem during the loading of the material.

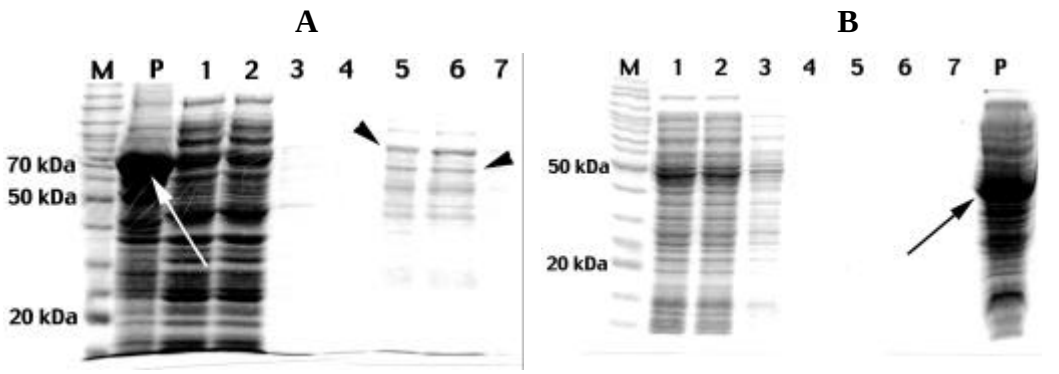


**Figure 4.3.2 Coomassie Blue stained SDS-PAGE gels of eluates from the glutathione gel**.
Detection of recombinant GST-R1 (**A**) and GST-FG (**B**). Lane **M (A & B)**, 10 kDa molecular marker. Lane **P**, pellet from induced bacteria. The numbered lanes represent: **1**; the solution loaded onto column, **2**; the run-through from column, **3**; GST washing buffer and **4** to **7**; eluates from the glutathione gel. Arrows in **A** & **B** give an example of the expression of recombinant material. Arrowheads in **A** indicate elution of proteins associating with the glutathione gel.

by Coomassie Blue staining of bacterial pellets loaded on SDS-PAGE gels. Notably, the production of recombinant material was only observed in bacteria after induction with IPTG (Figs 4.3.1 A & B). From SDS-PAGE gels, the molecular size of GST-R1 was estimated to be 70 kDa (Fig. 4.3.1 A, lanes 2, 4, 6 & 8) and the size of GST-FG

to be 45 kDa (Fig. 4.3.1 B, lanes 2, 6 & 8) both fitting with the calculated sizes. Evaluation on Coomassie Blue stained SDS-PAGE gels of the solubility of GST-R1 and GST-FG in GST-lysis buffer showed that although GST-R1 and GST-FG were present in the pellets, they were not detected in the material loaded onto the column (Fig 4.3.2 A & B, lanes P & 1). As GST-R1 and GST-FG were not soluble in GST-lysis buffer, nothing bound to - and eluted from - the glutathione gel, and subsequently it was impossible to purify the recombinant GST proteins from bacteria transfected with pGEX-1 vector.

*4.3.2 Expression of recombinant material from pRSET-B vectors*

Expression of recombinant material from the pRSET-B vector resulted in the production of proteins fused with hexahistidine tags at their N-terminal. The production of recombinant hexahistidine R1 and FG (hR1 and hFG) in BL21(DE3) pLysS bacteria was detected by Coomassie Blue staining of bacterial pellets loaded on SDS-PAGE gels. From here, the molecular size of recombinant hR1 was estimated to be 52 kDa and that of hFG to be 27 kDa (Figs 4.3.3 A & B, lanes 2, 4 & 6).

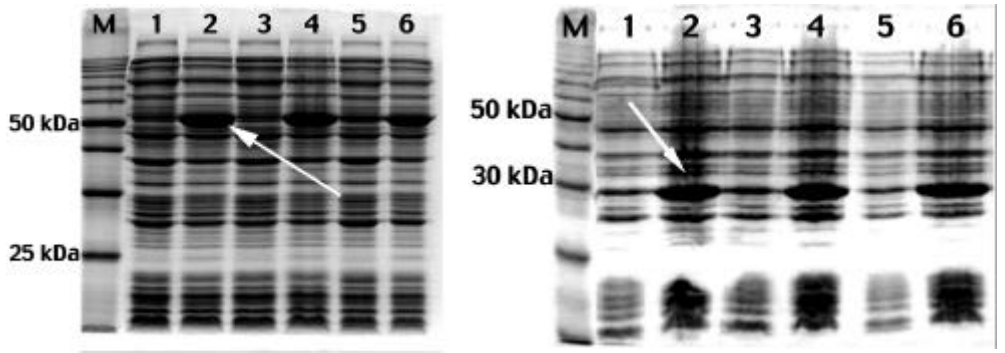


**Figure 4.3.3 Coomassie Blue stained SDS-PAGE gels of bacterial pellets**.
Expression of recombinant hexahistidine R1 (**A**) and FG (**B**) in BL21 bacteria. Lane **M (A & B)**, 10 kDa molecular marker. Lanes **1**, **3** and **5** represent pellets from non-induced and **2**, **4** and **6** from induced bacteria. Arrows in **A** & **B** give an example of the production of recombinant material with molecular sizes of 52 and 27 kDa respectively.

*4.3.3 Native conditions*

When induced bacteria, expressing either recombinant hR1 or hFG, were treated under native conditions, it was not possible to purify the recombinant proteins from a Ni-NTA agarose gel (Fig. 4.3.4 A & B, lanes 4 to 7). Recombinant hR1 was only detected in pellets from induced bacteria (Fig, 4.3.4 A, lanes P) and not in the

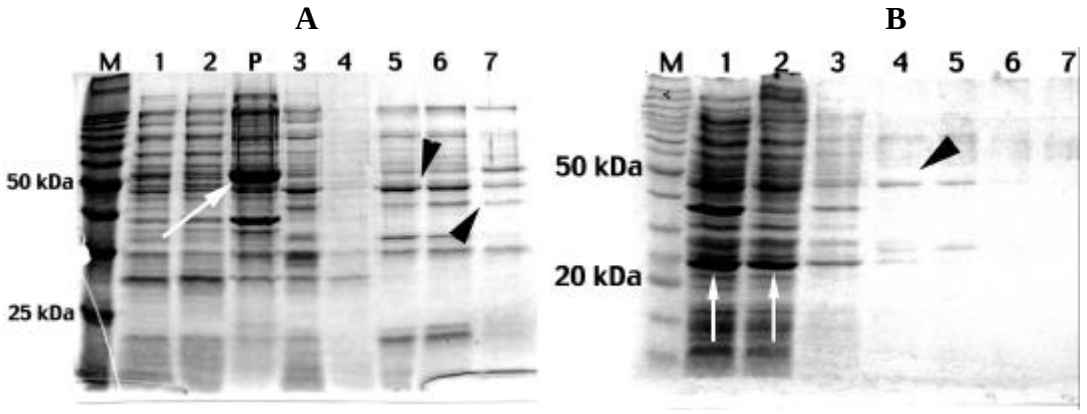


**Figure 4.3.4 Coomassie Blue stained SDS-PAGE gels of eluates from the Ni-NTA gel under native conditions**. Recombinant hexahistidine R1 (**A**) and FG (**B**). Lane **M**, 10 kDa molecular marker. Lane **P**, pellet from induced bacteria. The numbered lanes represent: **1**; solution loaded onto column, **2**; run-through from column, **3**; native His-washing buffer and **4** to **7**; eluates from the Ni-NTA gel. White arrow in **A** shows expression of recombinant material with a molecular size of 52 kDa. White arrows in **B** show recombinant FG in both the solutions loaded onto the column and the flow-through. Arrowheads in **A** & **B** indicate elution of proteins associating with the Ni-NTA gel. In both **A** and **B** it can be observed that certain bacterial proteins associate with the gel and are present in the eluates (arrowheads).

native homogenate as it remained in inclusion bodies under native lysis-conditions. In contrast, recombinant hFG was detected in the native homogenate (Fig. 4.3.4 B, arrows) but the majority remained as inclusion bodies. However, the soluble part of recombinant hFG was still unable to bind to the Ni-NTA gel (Fig. 4.3.4 B, lanes 4 to 7). In addition, binding of hFG to the Ni-NTA gel was absent when pellets were processed under denaturing conditions, dialysed against native buffer to renature the protein and subsequently incubated with the Ni-NTA gel (Fig 4.3.5, lanes 7 & 8). When using an NTA agarose gel where $Ni^{2+}$ ions had been exchanged for $Cu^{2+}$ ions, enabling stronger interaction between the histidine amino

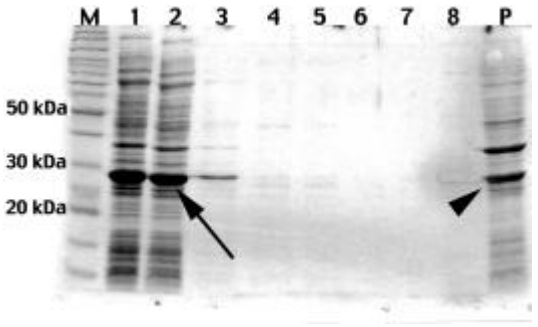


**Figure 4.3.5 Coomassie Blue stained SDS-PAGE gel of bacterial pellets lysed under denaturing conditions and dialysed against native buffer**.
Lane **M**, 10 kDa molecular marker. Lane **P**, pellet from induced bacteria. The numbered lanes represent: **1**; solution loaded onto column, **2**; run-through from column, **3**; native His-washing buffer and **4** to **8**; eluates from the Ni-NTA gel. Arrowhead shows the expression of recombinant material in the bacterial pellet. Arrow indicates the presence of recombinant hexahistidine FG in the flow-through. No proteins were detected in the eluates.

acids and the NTA agarose gel, it was not possible to purify recombinant hFG (data not shown).

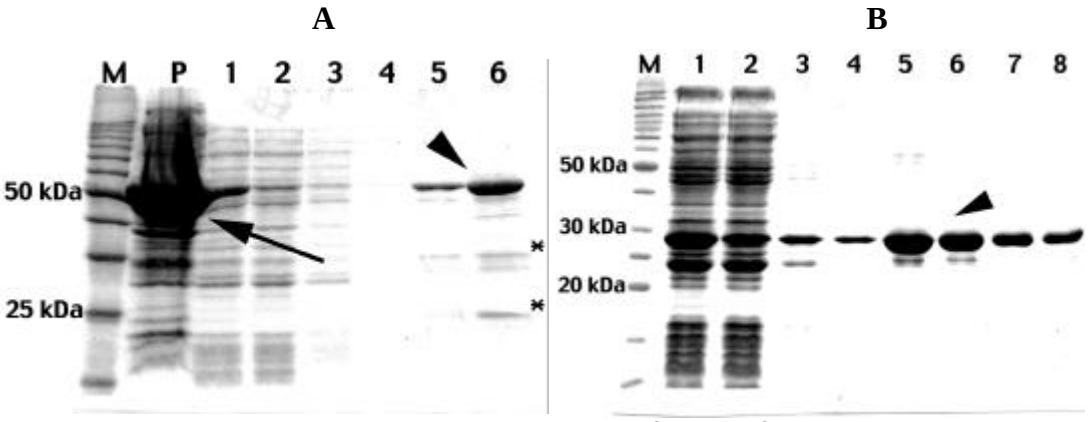


**Figure 4.3.6 Coomassie Blue stained SDS-PAGE gels of eluates from the Ni-NTA gel under denaturing conditions**. Detection of recombinant hexahistidine R1 (**A**) and FG (**B**). Lane **M (A & B)**, 10 kDa molecular marker. Lane **P**, pellet from induced bacteria. The following lanes represent: **1**; solution loaded onto column, **2**; run-through from column, **3**; denaturing His-washing buffer, **4** to **8**; eluates from the Ni-NTA gel. Arrow in **A** shows expression of recombinant R1 in the bacterial pellet. Arrowheads in **A** & **B** indicate the elution of recombinant material from the Ni-NTA gel. Asterisks in **A** show then presence of contaminating proteins in the eluates.

*4.3.4 Denaturing conditions*

Purification of both recombinants, hR1 and hFG, was only possible under denaturing conditions (Fig. 4.3.6 A, lanes 5 & 6 and Fig. 4.3.6 B, lanes 5 to 8). Both hR1 and hFG bound strongly to the Ni-NTA gel and eluted mainly with concentration of imidazole higher than 100 mM. Purification of recombinant hFG resulted in an almost completely pure protein (Fig. 4.3.6 B, lanes 7 & 8) whereas some contaminating proteins were present after purification of hR1 (Fig. 4.3.6 A). Dialysis of purified recombinant hFG against 3 M sodium thiocyanate in coupling buffer resulted in some protein precipitation. Consequently, a maximum of 1 to 2 mg recombinant material could be coupled to CNBr-activated agarose, as determined by Coomassie Blue staining of SDS-PAGE gels (data not shown).

*4.3.5 Elution of material from affinity column*

The amount of material eluted from the recombinant hFG affinity column, after the homogenate of pig cortex had been applied, was very low and proteins could only be detected by silver staining. On large SDS-PAGE gels, the homogenate showed proteins ranging from less than 20 kDa to more than 500 kDa, with the majority being between 30 and 200 kDa (Fig 4.3.7, part A - lane 3). Evaluation of the

washes showed the disappearance of lower weight proteins with increasing salt concentration (Fig. 4.3.7, lanes 5 to 10). Proteins interacting with the recombinant hFG column were eluted by high pH. Three predominant bands, with molecular sizes of 70 kDa, 300 kDa and > 600 kDa, appeared repeatedly throughout independent experiments (Fig. 4.3.7, part B - lanes 10 to 12). After two additional steps of affinity purification, no protein appeared to predominate when evaluated on large SDS-PAGE gels and improvement in specific tenascin-binding activity was also not observed (data not shown).

The high molecular weight proteins detected on large silver stained SDS-PAGE gels were not present when eluates were analysed by 2D-elecrophoresis. Nevertheless, three groups of proteins were detected on the acidic part of the silver

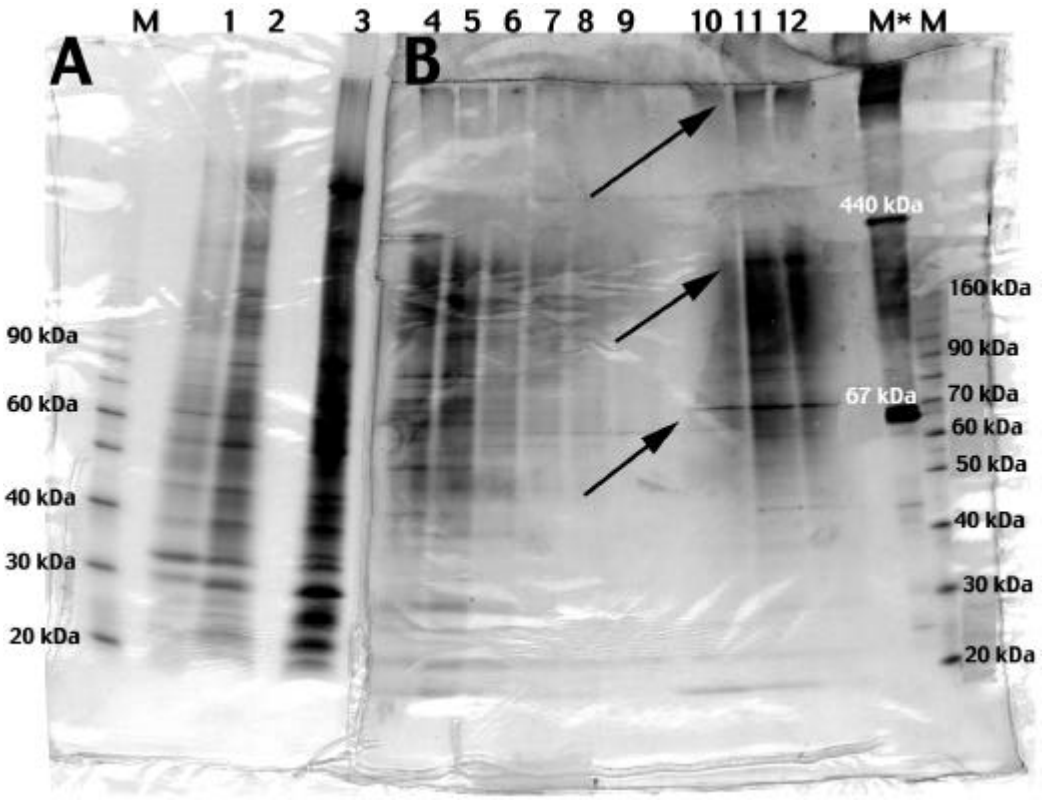


**Figure 4.3.7 Large gradient SDS-PAGE gel of homogenated pig cortex, washes and eluates from FG column**. Coomassie Blue staining of the part of the gel containing pig cortex homogenates (**A**). Silver staining of the part of the gel containing washes and eluates (**B**). Lane **M**, 10 kDa molecular marker. Lane **M***, heavy protein marker (CibcoBRL). The numbered lanes represent: **1**; homogenate of pig cortex, **2**; semisolid liquid present below homogenate of pig cortex after centrifugation, **3**; pellet after centrifugation, **4** to **9**; washes with increasing salt concentrations and **10** to **12**; elutions from column by high pH. Arrows (**B**) indicate three predominant bands with sizes of 70, 300 and >600 kDa in eluates. Proteins with lower molecular sizes disappear as concentrations of NaCl increases in the washing buffer.

stained 2D gel. The protein with the highest molecular weight gave rise to three equidistant spots, with the more basic being the predominant one (Fig. 4.3.8). The smallest of the three proteins gave rise to two spots (curved arrow) whereas the last protein only gave rise to one spot (Fig. 4.3.8). On the basic part of the 2D gel, proteins

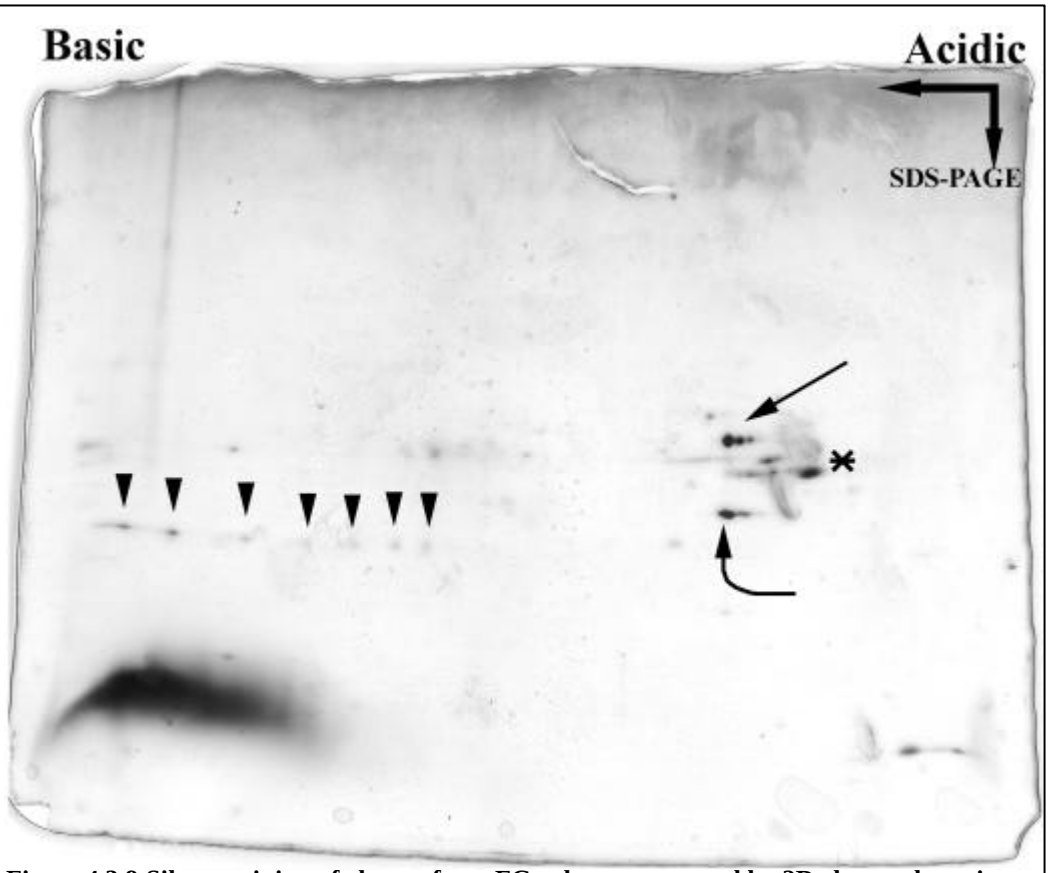


**Figure 4.3.8 Silver staining of eluates from FG column separated by 2D electrophoresis**. The straight arrow indicates a phosphorylated protein comprised of three spots with the distance of one charge unit between them. The curved arrow shows a phosphorylated protein comprised of two spots that are separated by one charge unit. The asterisk displays the staining pattern for a protein without a complex phosphorylation pattern. The arrowheads point to a protein with complex elution pattern different from the one observed for the phosphorylated proteins. The distance between these spots and the constant molecular size of the protein indicates a protein containing multi-charged groups such as $SO_4^{2-}$.

with more complex elution patterns could be observed (Fig. 4.3.8).

*4.3.6 Enzymatic digestions and fluorometric measurements*

Digestion of eluates from the recombinant hFG column, with either elastase[g], collagenase type II, hyaluronidase or chondroitinase ABC, caused no change in the

[g] The enzyme elastase digests both elastin and collagen type IV repeats (Lawrence, 1995).

migration pattern or size of bands when they were evaluated on silver stained SDS-PAGE gels (data not shown).

Monitoring the tenascin-R-binding activity of eluted samples was performed by measuring the emission of solutions from Ni-NTA HisSorb wells that were incubated with either homogenisation buffer C, FITC labelled eluate or recombinant hFG combined with FITC labelled eluate (Table 4.3.1).

| **Table 4.3.1** Fluorometric measurements | *Excitation* | *Emission* | *Slit-width* | *Av-I*[1] | *SD*[2] | *Numbers* |
|---|---|---|---|---|---|---|
| Recombinant hFG-eluate | 494 nm | 520 nm | 10 nm | 16.74 | 4.25 | 9 |
| Eluate | 494 nm | 520 nm | 10 nm | 11.84 | 3.10 | 8 |
| Hom. buffer C | 494 nm | 520 nm | 10 nm | 1.18 | 0.50 | 7 |

[1]Av-I; average intensities, [2]SD; standard deviation

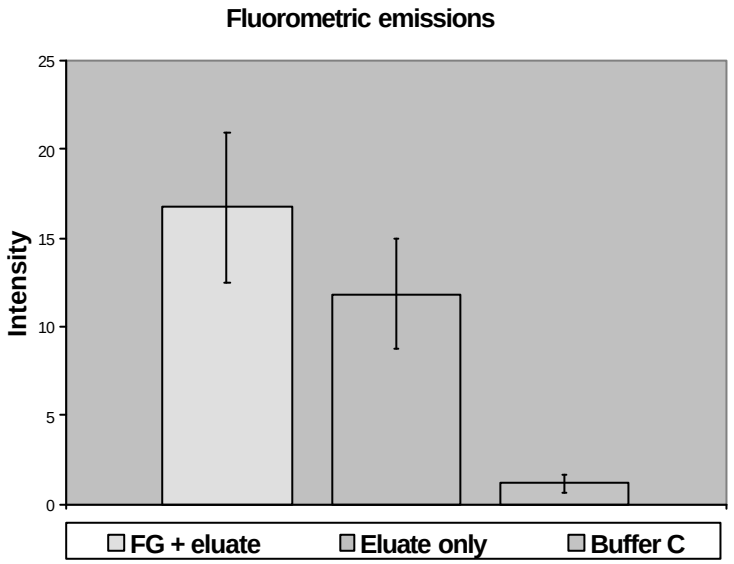


**Fig. 4.3.9** Graphic representation of measured intensities shown as absolute measured values. Bars = standard deviations.

Evaluation of the measured intensity between FITC labelled eluate and combined recombinant hFG - FITC labelled eluate revealed no statistical significant difference (Fig. 4.3.9). In addition, it was not possible to detect any eluted fraction with a higher biological activity using this method.

# 5. Expression of recombinant protein in yeast cells

## 5.1 Introduction

As it was not possible to produce large amounts of soluble recombinant human TN-R FG using a bacterial expression system, a system more likely to yield correctly folded recombinant material was chosen. One reason that the FG fragment of human TN-R aggregated and formed inclusion bodies when it was expressed by a bacterial host could be the lack of carbohydrates that may be needed for proteins to fold into their correct three-dimensional structures (Creighton, 1993). Based on the primary structure[h] of a protein, a full prediction of where and what kinds of carbohydrates are attached during processing in the endoplasmatic reticulum (ER) and Golgi apparatus is still impossible. The most predictable type of glycosylation is the attachment of N-linked carbohydrates, which mainly occurs on aspartate amino acids in the sequence Asn-Xxx-Ser/Thr/Cys (Creighton, 1993). The exact sites responsible for attachment of O-linked carbohydrates are less well described and most likely not predictable from the protein sequence at all. Nonetheless, it is known that O-linked carbohydrates are attached to serine or threonine amino acids. An investigation of the sequence of FG-knob from human TN-R showed that it contains one potential site for N-linked glycosylation (Asn-Gly-Ser) and 25 serine and 28 threonine amino acids. Although Zamze and colleagues did not show where the different carbohydrates were attached to mouse TN-R, they did show that the most abundant carbohydrates on TN-R are neutral N-linked oligosaccharides and O-linked sialylated structures (Zamze et al., 1999).

Therefore the yeast *Pichia pastoris* was chosen as an alternative expression system (Invitrogen, 1997a). The heterologous expression and subsequent secretion of proteins by *P. pastoris* has the advantage that *P. pastoris* secretes very low levels of native protein (Invitrogen, 1997a). *P. pastoris* has also been shown to perform N-linked glycosylation on similar sites as in higher eucaryotic cells (Asn-X-Ser/Thr) and not to hyperglycosylate proteins as has been observed in *S. cerevisiae* (Invitrogen, 1997a).

[h] The 'primary structure' is a synonym for the amino acid sequence

## 5.2 Materials and methods

### *5.2.1 Recombinant DNA technology*

#### *5.2.1.1 Polymerase chain reaction*[i]

To amplify the human tenascin-R FG fragment, PCR was performed with a plasmid containing the human tenascin-R R1 cDNA fragment as template (kindly provided by Dr. Zardi, Geneva; see Carnemolla et al., 1996). Primers were purchased from Microsynth and used at a final concentration of 0.4 pmol/µL. The PCR was performed in a Peltier Thermal Cycler DNA Engine (PTC-200) as illustrated in figure 5.2.1. One unit of Pfu DNA polymerase (Promega), primers, 200 ng of template plasmid and 0.2 nmol/µL of dNTPs were mixed in 1 x Pfu-buffer (Promega). Following the PCR, the sample was loaded on a 1% agarose gel and purified using a QIAEX II gel extraction kit (Qiagen).

94°C for 2 min.

**10 cycles at:**
94°C for 30 sec.
56°C for 45 sec.
72°C for 3 min.

**30 cycles at:**
94°C for 30 sec.
54°C for 45 sec.
72°C for 3 min.

72°C for 5 min.

**Figure 5.2.1** PCR program

The sequences for the primers were:

FG-F-EcoR1 : $^{5'}$TGAATTC **GAG** CTG AGC CAG AAA TTA C$^{3'}$

FG-R-Xba1 : $^{5'}$TTCTAG**A** **AA** CTG TAA GGA CTG CCG T$^{3'}$

The FG-F-EcoR1 was used as the forward primer and FG-R-Xba1 as the reverse primer. The position of the restriction sites for the endonucleases EcoR1 and Xba1, included in the primer sequence, are underlined. The first and last codons in tenascin-R are indicated in bold.

[i] See Saiki et al., 1988

*5.2.1.2 cDNA cloning and construction of expression vectors*

The purified PCR product and the plasmids pBluescript II KS +/- and pPICZαA (Invitrogen) were digested for 1 hr at 37°C with the restriction endonucleases EcoR1 (Boeringer Mannheim) and Xba1 (Amersham) in buffer H (Boeringer Mannheim). All digested products were purified from 1% agarose gels using the QIAEX II kit. Unless otherwise stated all media contained low salt (5 g/L) and all centrifugations were performed at 13,000 rpm in a Micro Centaur table centrifuge. Approximately 20 ng digested pBluescript II and 50 ng tenascin-R FG cDNA together with 2 units T4 DNA ligase (Fermentas) in 1 x T4 DNA ligase buffer (GibcoBRL) were placed for 3 hrs at room temperature. Subsequently, tubes were placed for 5 min. at 56°C, transferred on ice, 100 µL chemical competent XL-1 Blue bacteria (Promega) were added and the mixture was placed on ice for 20 min. The bacteria were given a heat shock at 42°C for 45 sec. and returned on ice for 5 min., after which 1 mL LB-medium (without antibiotics) was added and the tube placed at 37°C for 1 hr. The solution was centrifuged and the pellet re-suspended in 50 µL LB-medium, after which 10 µL 0.1 M IPTG and 80 µL 20 mg/mL X-GAL were added and the tubes content plated on LB-agar plates containing 50 mM ampicillin (Sigma). This makes it possible to distinguish clones containing insert as white and clones without as blue. Plates were then incubated overnight at 37°C. The following day ten white clones were picked with a sterile toothpick and placed individually in separate 14 mL polystyrene tubes along with 3 mL low salt LB-medium containing 25

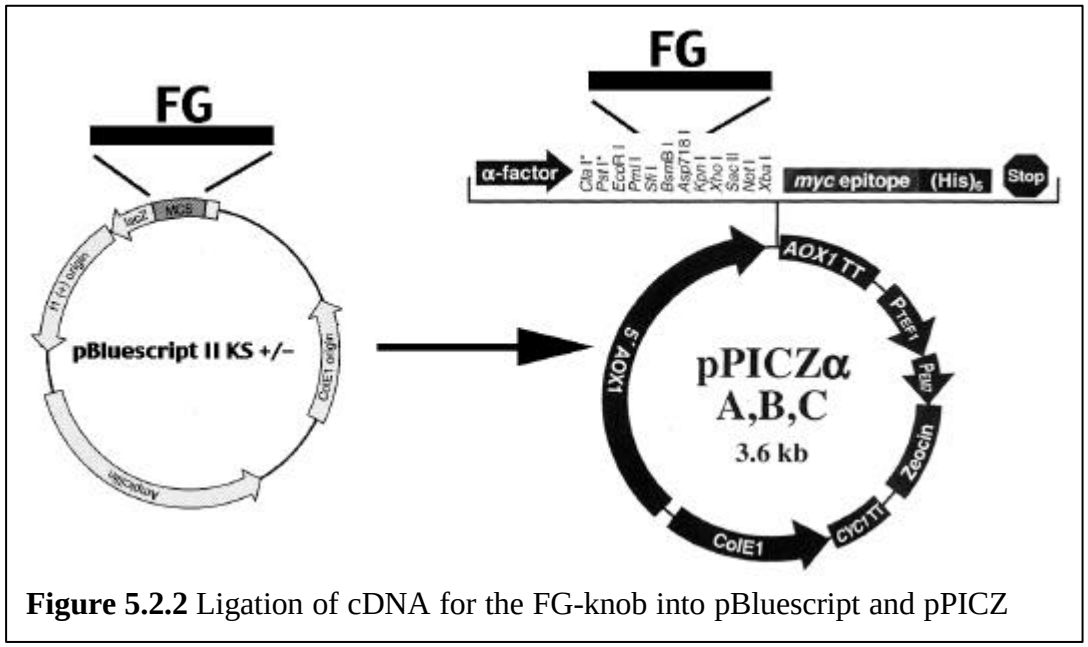


**Figure 5.2.2** Ligation of cDNA for the FG-knob into pBluescript and pPICZ

μg/mL Zeocin (Invitrogen). The tubes were then placed in an orbital shaking incubator overnight at 37°C. Plasmids were extracted from the bacteria as described by (Feliciello and Chinali, 1993) and in section **4.2.1.3** and digested with EcoR1 and Xba1 to retrieve the inserted FG cDNAs, which were subsequently ligated into pPICZαA vector as described above (for a schematic overview of the vectors see Fig 5.2.2). XL-1 blue bacteria were transformed with the ligation mixture and plated on LB-agar plates containing 100 μg/mL Zeocin from where clones were chosen and plasmid DNA extracted as outlined previously.

*5.2.2 DNA sequencing*

All enzymes and solutions (except plasmid, primer, $ddH_2O$, NaOH, NaOAc and absolute ethanol) were provided in the T7 Sequenase v. 2.0 DNA sequencing kit (Amersham) and the sequencing reactions were performed according to the protocol supplied by the manufacturer.

To 8 mL extracted pPICZαA yeast expression vector containing the human tenascin-R FG fragment (pPICZαA-FG) was added 2 μL 2 M NaOH and the mixture incubated at room temp. for 10 min., after which it was heated to 37°C for 5 min. FG-F-EcoR1 primer (1 μL) was added together with 2 μL 3 M NaOAc, 7 μL $ddH_2O$ and 50 μL absolute ethanol and placed at -70°C for 5 min. and subsequently centrifuged for 10 min. at 13,000 rpm. The pellet was re-suspended in 10 μL 1 x sequencing buffer. Two solutions, the first comprising of 7 μL sequence dilution buffer, 0.5 μL pyrophosphatase and 1 μL T7 Sequenase v2.0 DNA polymerase (enzyme mixture) and the second composed of 2 μL dGTP label mix. with 8 μL $ddH_2O$ (label mixture) were prepared. Dithiothreitol (1 μL, DTT) together with 0.5 μL $^{35}$S-dATP (Hartmann), 2 μL of the enzyme mixture and 2 μL of the label mixture were combined and added to the 1.5 mL Eppendorf tube containing the re-suspended vector. From this tube, 3.5 μL solution was removed and added at an interval of 30 sec. to each of four individual tubes, marked G, A, T & C, already containing 2.5 μL of the appropriate dNTP solution (G, A, T & C respectively). These marked tubes were placed for 3 min. at room temp. before being moved to 37°C for 5 min. The reaction was stopped by adding 4 μL stop-solution and the samples were stored at -20°C.

*5.2.2.1 DNA sequencing gel*

Two large glass plates, first cleaned in absolute ethanol, were treated with dimethyldichlorosilane solution (Repel-Silan, LKB-produkter AB), cleaned with 70% ethanol and assembled in a SA-32 casting boot (LIFE Technologies). To an acrylamide solution (40% acrylamide 19:1, 1 x TBE, 7 M urea), APS (Fluka) and TEMED (Fluka) were added. The solution was degassed, poured into already assembled glass plates, a comb placed into the sequencing gel to introduce small wells and the solution left to polymerise for 1 hr. Subsequently, the gel was pre-run in 0.6 x TBE for 15 min. at 2,000 V & 60 W in a model SA adjustable sequencing gel electrophoresis system (BRL Life Sciences). During the pre-run, the frozen samples were heated at 75°C for 5 min. To each well 2 µL of sample was applied and the gel was left to run for 2 to 3 hrs at 70 W. After the run, the electrophoresis solution was discarded into appropriate radioactive material containers, glass plates were separated and the gel fixed in distilled water containing 10% acetic acid and 10% ethanol. The gel was placed on wet 3M paper and dried for 3 hrs in a gel dryer under vacuum. In a dark room, the dried gel was placed in a holding cassette, an X-Omat AR film (Kodak) was placed on top of it and exposed overnight. The following day the autoradiogram was developed in ILFORD PQ universal developer and fixed in ILFORD Hypam fixator.

*5.2.3 Transformation of Pichia pastoris with pPICZαA*

Solutions I, II & III for the production of easy-competence *Pichia pastoris* yeast stains were supplied by Invitrogen. *Pichia pastoris* yeast strain KM71 and GS115 were grown overnight in 10 mL YPD-medium (yeast extract peptone dextrose) and placed in 150 mL YPD-medium and rotated at 30°C until an $OD_{600}$ of 0.8 was reached (all performed in Erlenmeyer flasks). The medium was centrifuged for 5 min. at 500 g, pellets re-suspending in 10 mL solution I, centrifuged and pellets re-suspended in 1 mL solution I, from where 60 µL aliquots were prepared and stored at -70°C.

A total of 5 µg pPICZαA vector, containing the human FG fragment of tenascin-R, was linearised by digestion with the endonuclease SacI (Fermentas) in buffer H. Agarose gel electrophoresis was performed on the digested product and the linearised plasmid was purified from the agarose gel using the QIAEX II kit. To two

tubes containing a mixture of 5 µg of purified vector and 50 µL competent *Pichia pastoris* (KM71 or GS115), were incubated for 10 min. at 30°C and 1 mL solution II was added. The tubes were incubated at 30°C for 1 hr and intermittently vortexed every 15 min., where after they were placed at 42°C for 10 min. The content of each tube was divided into two separate tubes and placed together with 1 mL of YPD medium for 1 hr at 30°C to allow expression of Zeocin resistance. Solutions were centrifuged for 5 min. at 3,000 g, supernatant discarded and each pellet re-suspended in 500 µL solution III. The appropriate KM71 or GS115 mixtures were pooled and centrifuged for 5 min. The resulting two pellets were each solubilised in 100 µL solution III, plated on YPDS plates containing 100 µg/mL Zeocin and incubated for 3 days at 30°C.

*5.2.3.1 Determination of Mut phenotype ($Mut^+$/$Mut^S$)*

One hundred Zeocin-resistant *Pichia pastoris* GS115 transformants were independently picked using sterile toothpicks and streaked first on MMH (minimal methanol with histidine) and subsequently on MDH (minimal dextrose with histidine) plates. On these plates were also placed positive and negative controls supplied by Invitrogen (GS115/$Mut^S$ albumin and GS115/pPICZ/*lac*Z($mut^+$) respectively). The plates were incubated at 30°C for 2 days after which clones growing better on MDH than on MHH plates were streaked onto MDH plates to obtain single colonies.

*5.2.4 Expression of recombinant material, affinity purification and Western blot*

*5.2.4.1 Small-scale protein expression and affinity purification*[j]

Overnight cultures of two KM71 and GS115 clones, containing the pPICZαA-FG vector and of the correct Mut phenotype, together with positive and negative controls, were prepared in buffered minimal glycerol medium containing histidine (BGMH). Expression of recombinant material was induced by mixing 5 mL overnight culture with 20 mL buffered minimal methanol medium with histidine (BMMH) and adding methanol to a final concentration of 0.5%. Methanol was supplemented every 24 hrs of incubation. To test the expression efficiency, 1 mL of

[j] See Pharmacia, 1993 and Scopes, 1994

expression cultures were removed at different time points (0, 4.5, 14, 24, 36, 48, 57, 72 and 96 hrs after initial induction) and kept in 1.5 mL Eppendorf tubes. Cultures were centrifuged and pellets and supernatants separated. These pellets were re-suspended in 50 µL 1 x Laemmli loading buffer, sonicated for three times 30 sec. and stored until loaded on small 12% SDS-PAGE gels. The pH of the supernatants was controlled (between 7.0 to 8.1), 100 µL washed Ni-NTA (nickel-nitrotriacetic acid) agarose gel (Qiagen) was added, and the mixtures incubated under rotation for 1.5 hr at room temp. Before being centrifuged for 10 min. at 10,000 rpm and re-suspended in 100 µL dHis washing solution, the Ni-NTA gel was washed twice in dHis washing buffer. Subsequently, the content of the tubes were incubated 5 min. in dHis elution buffer, centrifuged and the supernatants mixed with 6 x Laemmli loading buffer. All samples were heated for 2 min. at 94°C before loading on small SDS-PAGE gels, prepared as previously described, and stained with Coomassie Brilliant Blue R-250 solution.

*5.2.4.2 Small-scale protein expression and Western blotting*[k]

Transformed GS115 and KM71 clones, together with controls, were induced with methanol to express recombinant protein as described in section **5.2.4**. After centrifugation pellets were prepared for SDS-PAGE whereas supernatants were precipitated by adding 100% trichloroacetic acid (TCA, Fluka) to a final concentration of 10% (v/v). This mixture was placed on ice for 30 min. and subsequently centrifuged for 10 min. at 13,000 rpm. Pellets were re-suspended in 50 µL 1 x Laemmli loading buffer and liquid ammonia (25%) was added until the solution became basic (turned blue). The samples (pellets and precipitated supernatants) were applied to small 12% SDS-PAGE gels and run as previously described. The gels were either stained with Coomassie Brilliant Blue R-250 or assembled together with a Hydrobond-ECL nitrocellulose membrane (Amersham) and transferred (1 hr at 80 W in blotting buffer) using a Mini Protean II blotting chamber (Hoefer Pharmacia). Following the protein transfer, nitrocellulose membranes were briefly washed in $ddH_2O$ and placed overnight at 4°C in 1 x Tris-buffered saline solution containing 0.1 % triton-X 100 (TBS-T) with 1% skimmed milk (Rapilait, Migros). The following day, blots were incubated for 2 hrs in 10 mL TBS-T together

[k] See Pierce, 1998

with a mouse monoclonal antibody raised against the Myc-epitope (Invitrogen, 1:5,000). Subsequently, blots were washed three times in 10 mL TBS-T and placed for 2 hrs in 10 mL TBS-T containing biotinylated goat anti-mouse antibody (Vector, 1:10,000). Blots were then washed as previously described and incubated using the avidin-biotin peroxidase method for 30 min. in 10 mL TBS-T containing (pk-4000 ABC kit, Vectastain). After extensive washes, the blots were placed, in a dark room, in 10 mL enhanced chemiluminescence (ECL) SuperSignal substrate (Pierce) for 2 min. Subsequently, the blots were placed in a cassette, a sheet of Saran wrap placed on top, excessive liquid removed, everything covered by a Hyperfilm-ECL film (Amersham) and exposed for time intervals ranging from 5 sec. to 5 min. The films were developed in ILFORD PQ universal developer and fixed in ILFORD Hypam fixator.

## 5.3. Results

### *5.3.1 Analysis of control expression*

The GS115 yeast strain transfected with a control vector (GS115/Mut$^S$-albumin) supplied by Invitrogen, showed secretion of a protein with a molecular size similar to the one expected for albumin (67 kDa). Albumin was first detected after 14 hrs of incubation with the amount increasing over time (Fig. 5.3.1). After 48 hrs, proteins of lower molecular sizes, probably constituting degradation products, were also observed (Fig. 5.3.1).

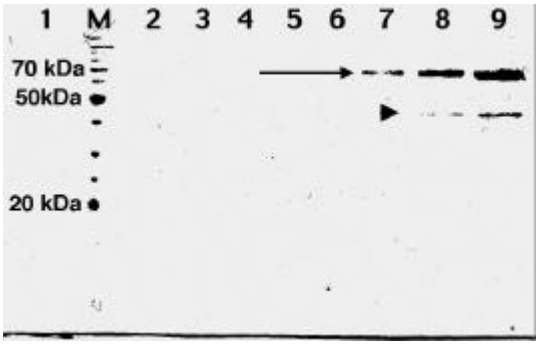


**Figure 5.3.1 Coomassie stained SDS-PAGE gel of Ni-NTA purified proteins from medium of GS115/Mut$^S$-albumin transfected GS115 yeast cells.** All numbered lanes, except lane 1, represent induced growth. Lane **M**, 10 kDa molecular marker. Lane **1**, eluate from medium before induction with methanol. The following lanes represent elutions after : **2**; 4.5 hrs, **3**; 14 hrs, **4**; 24 hrs, **5**; 36 hrs, **6**; 48 hrs, **7**; 57 hrs, **8**; 72 hrs and **9**; 96 hours of induction. Arrow shows the presence of albumin (67 kDa) in the eluate from the medium. It can be observed that the amount of purified protein increases in a time-dependent manner. Arrowhead indicates the appearance of degradation products from albumin.

### *5.3.2 Expression in KM71 yeast cells*

Analysis of pellets from the low expressing yeast strain KM71 transfected with pPICZαA-FG, on Coomassie stained SDS-PAGE gels, revealed a protein with a relative molecular size of 27 kDa. These results fits well with the expected size of 24.5 kDa for recombinant FG fused with the Myc-epitope (Fig. 5.3.2 A). The amount of protein increased in a time-dependent manner, reaching maximum after 96 hrs of induction with methanol (Fig. 5.3.2 A, lane 9). It was impossible to detect any

secreted protein in eluates from Ni-NTA agarose gel incubated with medium from transfected KM71 yeast cells (Fig. 5.3.2 B, lanes 2 to 9). However, on Western blots, eluates from KM71 yeast cells transfected with pPICZαA-FG revealed secreted proteins containing the Myc-epitope (Fig. 5.3.3). After 24 and 36 hrs of induction,

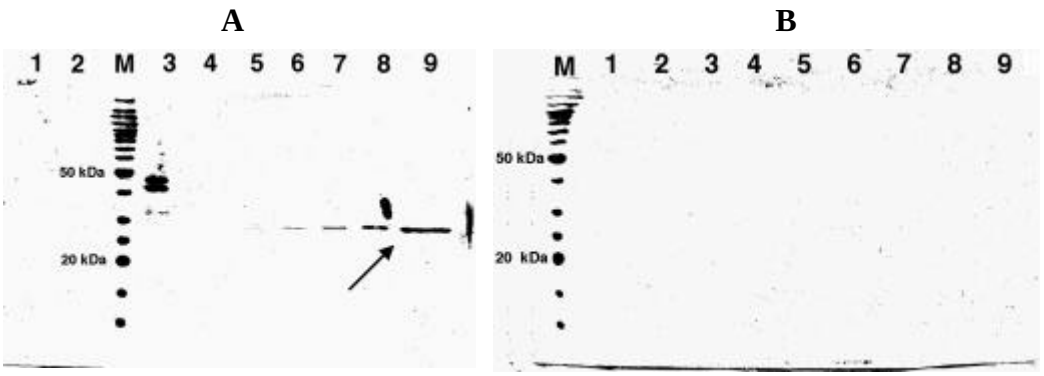


**Figure 5.3.2 Coomassie blue stained SDS-PAGE gel of pPICZa A-FG transfected KM71 yeast cells.** Coomassie stained gel of pellets (**A**) and eluates from the Ni-NTA gel (**B**) of transfected KM71 yeast cells at different time intervals. All numbered lanes, except lane 1, represent material induced with methanol. Lane **M (A & B)**, 10 kDa molecular marker. Lane **1**, before induction with methanol. The following lanes represent material after: **2**; 4.5 hrs, **3**; 14 hrs, **4**; 24 hrs, **5**; 36 hrs, **6**; 48 hrs, **7**; 57 hrs, **8**; 72 hrs and **9**; 96 hours of induction. Arrow in **A** shows the presence of a protein with a relative molecular size of 27 kDa. Expected size of recombinant FG fused to the Myc-epitope is 24.5 kDa. No significant amount of purified secreted protein can be detected in **B**.

proteins of 27 kDa were detected on Western blots (Fig. 5.3.3). After 48 hrs of induction, the size of the band had shifted to 35 kDa (Fig. 5.3.3). Secreted Myc-containing proteins could not be detected in non-induced material or at any other time points of induction.

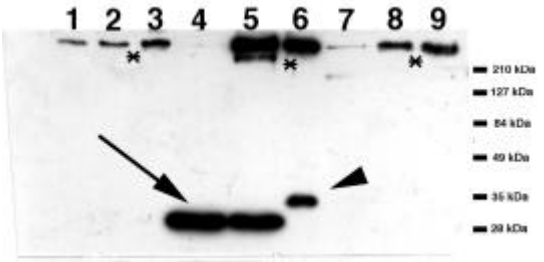


**Figure 5.3.3 Western blot of Ni-NTA purified proteins secreted by pPICZa A-FG transfected KM71 yeast cells.** Lanes 1, 7, 8 and 9 represent eluates from non-induced material. The remaining lanes (2 - 6) represent material induced with methanol. Lane **M**, 10 kDa molecular marker. Lane **1**, eluate from medium before induction with methanol. The following lanes represent eluates after **2**; 4.5 hrs, **3**; 14 hrs, **4**; 24 hrs, **5**; 36 hrs, **6 & 7**; 48 hrs, **8**; 57 hrs, and **9**; 72 hours of growth. Arrow indicates the detection of a secreted protein containing the Myc-epitope with a size of 27 kDa. Arrowhead shows secreted protein of a slightly larger size at $t_{48}$ after induction. No protein was detected from non-induced yeast cells. Asterisks indicate proteins precipitated at the border between stacking and separation gel resulting in cross-reaction with the applied antibodies.

*5.3.3 Expression in GS115 yeast cells*

Investigation of pellets from the high expressing yeast strain GS115, transfected with pPICZαA-FG showed a higher background expression of proteins

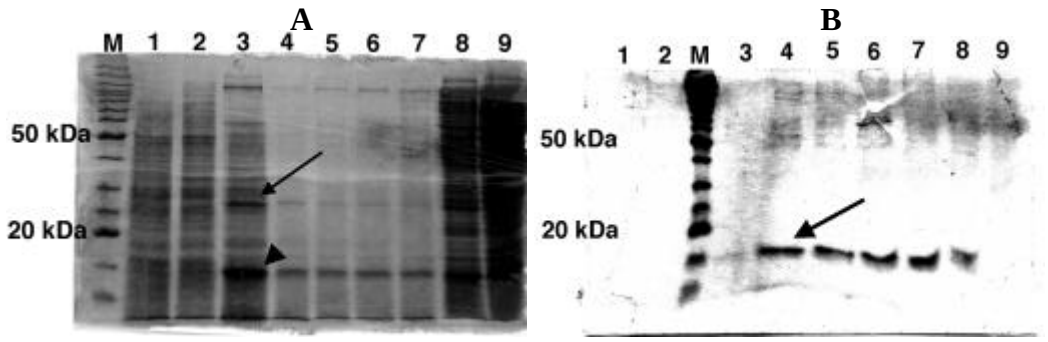


**Figure 5.3.4 Coomassie Blue stained SDS-PAGE gel of pPICZa A-FG transfected GS115 yeast cells.** Coomassie stained gels of pellets (**A**) and eluates from the Ni-NTA gel (**B**) of transfected GS115 yeast cells at different time intervals. All numbered lanes, except lane 1, represent material from induced material. Lane **M (A & B)**, 10 kDa molecular marker. Lane **1**, material before induction with methanol. The following lanes represent material after **2**; 4.5 hrs, **3**; 14 hrs, **4**; 24 hrs, **5**; 36 hrs, **6**; 48 hrs, **7**; 57 hrs, **8**; 72 hrs and **9**; 96 hours of induction. Arrow in **A** shows the presence of a protein with a relative molecular size of 27 kDa in pellets between $t_{14}$ and $t_{96}$ hrs of induction. Arrowhead in **A** indicates the presence of a protein with a size of approximately 10 kDa. The latter protein is also observed in eluates in **B** (arrow) at induction intervals ranging from $t_{14}$ to $t_{72}$.

than KM71 yeast cells. Between 14 and 96 hrs of induction with methanol, two proteins of roughly 10 and 27 kDa could be distinguished on Coomassie stained SDS-PAGE gels (Fig. 5.3.4 A). In eluates from medium incubated with Ni-NTA agarose gel, the smaller protein appeared after 14 hrs of induction and could be detected, in constant amounts, until 96 hrs (Fig. 5.3.4 B). The smaller sized protein was detected between 14 and 57 hrs after induction but later disappeared although the total amount of proteins increased. On Coomassie stained SDS-PAGE gels, the larger protein was not detected in the medium at any of

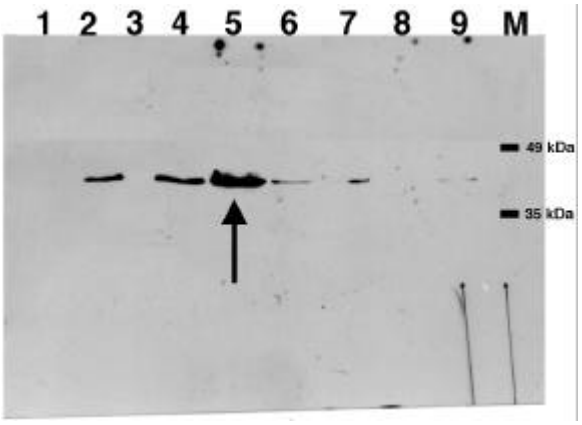


**Figure 5.3.5 Western blot of Ni-NTA purified proteins secreted by pPICZa A-FG transfected GS115 yeast cells.** Lanes 1, 3 and 8 represent eluates from non-induced yeast. The remaining lanes (2, 4 - 7 & 9) represent material induced with methanol. Lane **M**, 10 kDa molecular marker. Lane **1**, eluate from medium before induction with methanol. The following lanes represent eluates from the Ni-NTA gel incubated with medium grown for **2** & **3**; 4.5 hrs, **4**; 14 hrs, **5**; 24 hrs, **6**; 36 hrs, **7**; 48 hrs and **8** & **9**; 57 hours. Arrow indicates the purification of a secreted protein containing the Myc-epitope with a molecular size of 40 kDa.

the examined time points. Secreted proteins containing the Myc-epitope were detected on Western blots of medium from transfected GS115 yeast cells (Fig. 5.3.5). Eluates, from medium incubated with Ni-NTA agarose gel, revealed bands corresponding to proteins with a molecular size of 40 kDa. Proteins were detected, in variable amounts, between 4.5 and 57 hrs after initial induction with methanol. On Western blots, the highest band intensity was observed 36 hrs after induction where after the intensity decreased (Fig. 5.3.5, lane 6).

# 6. Expression of recombinant proteins in mammalian cells

## 6.1 Introduction

As purification of soluble recombinant human TN-R protein using either bacterial or yeast expression systems were not accomplished, another approach was chosen focusing on the expression of the FG-knob in a transformed mammalian cell line. Cos-1/M6 cells, which are SV40 transformed Simian fibroblasts from green monkeys, were chosen for two reasons. Firstly, they do not express the CNS restricted extracellular matrix molecule TN-R or potential biological ligands for TN-R and secondly they respond well to Zeocin treatment. The pSecTag2 vector (Invitrogen) promised to be a suitable expression vector since it contained a signal peptide enabling secretion of produced material. Moreover, using primate cell lines, proteins with more 'natural' post-translational modifications than are produced in yeast may be expected. Native mouse TN-R contains a complex pattern of carbohydrates (Zamze et al., 1999) whereas *Pichia pastoris* mainly adds mannose residues (Invitrogen, 1997a). Although cDNA fragments ligated into the pSecTag2 vector give rise to proteins fused at the C-terminal with a hexahistidine tag, the method of choice was to express the recombinant FG fragment as a chimeric protein together with GST. The motivation for this was that the addition of GST (known to easily fold into a soluble protein) could result in a soluble GST-FG protein.

## 6.2 Material and methods

### *6.2.1 Recombinant DNA technology*

#### *6.2.1.1 Polymerase chain reaction*[1]

To amplify the cDNA for cloning into the pSecTag2 C vector (Invitrogen), PCR was performed using the pGEX-1 plasmid, containing human tenascin-R FG fragment, as template. The primers were purchased from Microsynth, Switzerland and used at a final concentration of 0.4 pmol/µL. The PCR was performed in a Peltier Thermal Cycler DNA Engine (PTC-200). One unit of Pfu DNA polymerase (Promega), primers, 200 ng of template plasmid and 0.2 nmol/µL of dNTPs were mixed in 1 x Pfu-buffer (Promega) and the PCR was performed as described in figure 6.2.1. The PCR resulted in the production of cDNA where GST was fused to the 5' end of tenascin-R FG (GST-FG). Following the PCR, the sample was loaded on a 1% agarose gel and purified by the aid of the QIAEX II gel extraction kit (Qiagen).

94°C for 2 min.

**10 cycles at:**
94°C for 30 sec.
60°C for 45 sec.
ΔT=0.1°C/cycle
72°C for 3 min.

**30 cycles at:**
94°C for 30 sec.
58°C for 45 sec.
ΔT=0.1°C/cycle
72°C for 3 min.

72°C for 5 min.

**Figure 6.2.1** PCR program

The primer sequences were:

pSec-Hind-F : $^{5'}$TACGAAGCT **TTG** TCC CCT ATA CTA GGT TAT TG$^{3'}$

pSec-Eco-R : $^{5'}$GG **AAT** TCT CAG AAC TGT AAG GAC TGC C$^{3'}$

The position of the restriction sites for the endonucleases Hind III and EcoR1 included in the primer sequences are underlined. The first codon in GST and the stop codon in tenascin-R FG are indicated in bold.

#### *6.2.1.2 cDNA cloning and construction of expression vectors*

Both the purified PCR product and the plasmids pBluescript II KS +/- and pSecTag2 C (Invitrogen) were digested for 1 hr at 37°C with the restriction

[1] See Saiki et al., 1988

endonucleases EcoR1 and Hind III in buffer B (all Boeringer Mannheim). Digested products were purified from 1% agarose gels using the QIAEX II kit. Unless otherwise stated, all media contained 50 mM ampicillin and all centrifugations were performed at 13,000 rpm in a Micro Centaur table centrifuge. Approximately 20 ng digested pBluescript II and 50 ng GST-FG cDNA together with 2 units of T4 DNA ligase (Fermentas) in 1 x T4 DNA ligase buffer (GibcoBRL) were kept for 3 hrs at room temp. Subsequently, tubes were placed for 5 min. at 56°C, transferred on ice, 100 µL chemical competent XL-1 Blue bacteria (Promega) were added and the mixture was placed on ice for 20 min. The mixture was heated at 42°C for 45 sec., returned on ice for 5 min. before adding 1 mL LB-medium without antibiotics, and incubating at 37°C for another hr. Subsequently, the solution was centrifuged and the pellet re-suspended in 50 µL LB-medium, after which 10 µL 0.1 M IPTG and 80 µL 20 mg/mL X-GAL were added and the tubes content plated on LB-agar plates containing 50 mM ampicillin (Sigma), which were kept at 37°C overnight. The presence of IPTG and X-GAL makes it possible to distinguish clones with insert as white and clones without as blue. The following day, using sterile toothpicks, 10 white colonies were picked, placed in 14 mL polystyrene tubes containing 3 mL LB-medium and incubated overnight at 37°C in an orbital shaking incubator (200 rpm). As described by (Feliciello and Chinali, 1993) and in section **4.2.1.3**, plasmids were extracted from the bacteria and four plasmid mini-preparations were chosen for DNA sequencing performed as previously described. One of the sequenced plasmids, shown to contain the appropriate insert, was digested with the endonucleases EcoR1 and Hind III to retrieve the GST-FG cDNAs. The insert was purified from agarose gel

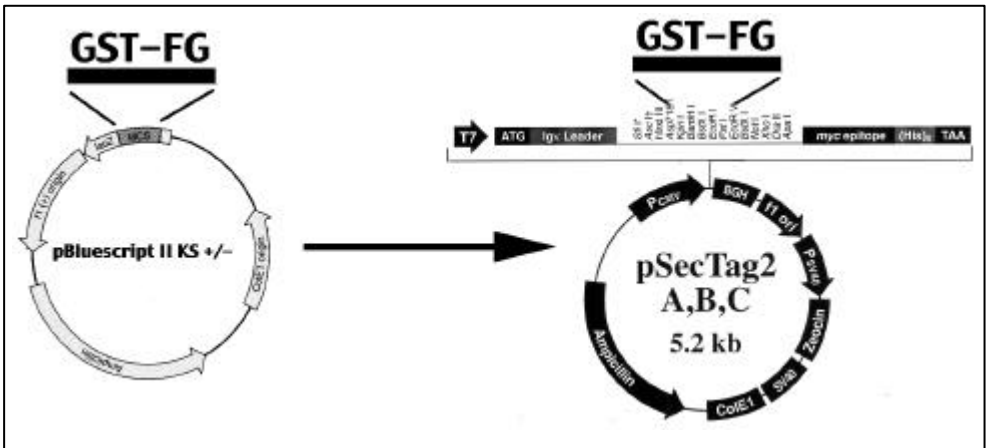


**Figure 6.2.2** Ligation of the cDNA for GST-FG into pSecTag2A

and subsequently ligated into a previously digested pSecTag2 C vector (for a schematic overview of the vectors see Fig. 6.2.2). XL-1 blue bacteria were transformed with the pSecTag2 C/GST-FG ligation and plated on low salt LB-agar plates containing 25 μL/mL Zeocin (Invitrogen). Several clones were chosen and mini-preparations of plasmid DNA were performed. Digestion of the mini-preparations with Hind III and EcoR1 were evaluated on 1% agarose gels. A maxi-preparation of one pSecTag2 C/GST-FG plasmid, containing the appropriate GST-FG cDNA, was performed according to the protocol supplied by the manufacturer (Nucleobond, AX500).

### *6.2.2 General cell culture techniques*[m]

Cos-1/M6 p25 cells (kindly provided by Dr. Bonaiti, Geneva) were propagated as a monolayer at 37°C in an automatic $CO_2$ incubator (Forma Scientific) in 50 mL culture flasks (Milan) or 35 mm microtiter wells (Nalgene Nunc Int.). Dulbecco's Modified Eagle's Medium (DMEM, GibcoBRL) with or without 10% foetal calf serum (FCS, GibcoBRL) and containing 2 mM glutamine, penicillin and streptomycin (10,000 U, 10,000 μg/ml) was used. The cells were trypsinised by first removing the growth medium followed by a brief wash in excess of sterile PBS containing 0.25% trypsin and 0.02% EDTA. The cells were left for 1 min. at room temp., excess solution aspirated, and subsequently placed at 37°C until the cells began to detach from the plastic and started to round up. The cells were re-suspended in 5 mL DMEM containing 10% FCS and split in a ratio of 1:10 in a 50 mL culture flask or into microtiter wells.

Cells for storage were, after trypsination, re-suspended in DMEM containing 10% FCS at a concentration of 5 x $10^6$ cells per mL, centrifuged and re-suspended at 2 x $10^6$ cells per mL in freezing medium (90% FCS, 10% glycerol (v/v)). The suspension of cells was dispensed in 1 mL aliquots, cooled to –80°C for 24 hrs in polystyrene containers and transferred to liquid nitrogen.

#### *6.2.2.1 Transfection of the Cos-1/M6 cell line*

Before obtaining stable transfected Cos-1/M6 cells, their susceptibility to Zeocin was determined. Cells were plated at 8 x $10^4$ cell/well in 35 mm wells, grown

[m] See Celis et al., 1995

until 50% confluency before different concentrations of Zeocin diluted in DMEM were applied (0.0, 0.1, 0.2, 0.3, 0.5 and 1.0 mg/mL). Viability of the cells was checked under an ID 02 light microscope (Zeiss). After nine days at 37°C, with the medium being changed every third day, the remaining cells were trypsinised and the concentration was estimated using a hemocytometer.

A positive control vector (pSecTag2/PSA) secreting the prostate-specific antigen (PSA) fused C-terminally with the Myc-epitope was supplied by Invitrogen. Cos-1/M6 cells plated one day prior to the transfection experiment and having reached 50% confluency in 35 mm wells were used. Into a sterile 1.5 mL Eppendorf tube 97 µL DMEM without FCS and 3 µL FuGENE 6 (Boehringer Mannheim) per 35 mm well were added. This mixture was incubated for 5 min. at room temp. then added dropwise either 2 µg pSecTag2 C, pSecTag2/PSA or pSecTag2 C/GST-FG vectors in separate Eppendorf tubes. These tubes were incubated for 15 min. at room temp. and the transfection mixture added dropwise to the Cos-1/M6 cells. After two days at 37°C, the medium was changed into DMEM containing 10% FCS and cells were incubated for another 2 days. Cells were then trypsinised and split into Zeocin containing DMEM (10% FCS, 0.5 mg/mL Zeocin) and changed every second day for the following 10 days. Stable transfected clones were plated into 96 wells using limited dilution to obtain single colonies and were propagated in DMEM containing 10% FCS and 0.25 mg/mL Zeocin. Medium was changed every third day. Aliquots of all non-transfected and stable transfected Cos-1/M6 cells were prepared and stored in liquid nitrogen as described in section **6.2.2**.

*6.2.3 Protein expression, purification and Western blotting*[n]

Cos-1/M6 cells, stable transfected with either pSecTag2/PSA or pSecTag2 C/GST-FG, were incubated in 9 cm petri dishes together with 2 mL DMEM without FCS. The following day, 1 mL conditioned serum-free DMEM was removed and 60 µL were mixed with 2 x Laemmli loading buffer. The remaining medium was precipitated with a final concentration of 10% TCA and prepared for SDS-PAGE as described in section **4.2.3**. The remaining cells were re-suspended in 200 µL 1 x Laemmli loading buffer. Electrophoresis of SDS-PAGE gels and subsequent Western

[n] See Pharmacia, 1993, Scopes, 1994 and Pierce, 1998

blotting was performed as previously described. Processing of Western blots was performed as described below.

Cos-1/M6 cells, stable transfected with either pSecTag2/PSA or pSecTag2 C/GST-FG, were incubated in 35 mm wells together with 300 µL DMEM without FCS. The following day the 300 µL serum-free DMEM was removed and the cells were re-suspended in 50 µL 1 x Laemmli loading buffer. From the serum-free medium 30 µL was removed and mixed with 2 x Laemmli loading buffer. To the remaining 270 µL serum-free DMEM from the pSecTag2 C/GST-FG transfected cells was added 200 µL 1 x PBS containing 5 mM EDTA and 0.2% Triton-X 100 (Sigma), pH≥7.0, together with 200 µL washed glutathione sepharose 4B gel which was left under rotation at room temp. for 1 hr. Subsequently, the sepharose gel was rinsed 2 times in 10 min. in GST-washing buffer and eluted in 100 µL GST-elution buffer. Part of the elutions (15 µL) were mixed 1:1 in 2 x Laemmli loading buffer and the remaining sepharose gel was re-suspended in 50 µL 1 x Laemmli loading buffer. All samples were loaded on small SDS-PAGE gels, the proteins electrophoretically separated and transferred onto nitrocellulose membranes as previously described.

After the protein transfer, nitrocellulose membranes were blocked overnight in TBS-T containing 1% skimmed milk. The next day, membranes were incubated in 10 mL TBS-T containing either goat antibody against GST (Pharmacia, 1:10,000) or mouse monoclonal antibody against the Myc-epitope (Invitrogen; Evan et al., 1985; 1:5,000) for 2 hrs at room temp. Extensive washes preceded the 2 hrs incubation in 10 mL TBS-T containing either biotinylated horse anti-goat antibody (Vector; 1:10,000) or biotinylated anti-mouse antibody (Vector; 1:10,000) respectively. Subsequently, membranes were washed and the immunoreaction visualised using the avidin-biotin peroxidase method (pk-4000 ABC kit; Vectastain) and the ECL method as described in section **5.2.4.2**.

*6.2.4 Immunohistochemical staining of PFA-fixed stable transfected Cos-1/M6 cells.*

Unless otherwise stated all washes were performed twice for 15 min. in PBS and incubations in PBS containing 10% bovine serum. Sterilised round coverslips with a diameter of 15 mm were placed in 35 mm wells, covered with DMEM containing 10% FCS and trypsinised Cos-1/M6 cells (transfected with pSecTag2 C/GST-FG or non-transfected) were added. The following day, the medium was

aspirated and the cells fixed for 4 min. with 4% paraformaldehyde in PBS and subsequently washed. The coverslips were incubated with the antibody against the Myc-epitope (1:1,000 in PBS containing 10% bovine serum and 0.05% Triton-X 100) overnight at 4°C. Cells were washed prior to incubation for 2 hrs with the biotinylated anti-mouse antibody (Vector; 1:200) at room temp. After extensive washes, they were incubated for an additional 2 hrs in PBS containing Texas Red conjugated streptavidine (1:200; Molecular Probes), washed, air dried for 2 hrs at room temp., re-hydrated in distilled water and dried for an additional 30 min. at room temp. The coverslips were then mounted in SlowFade (Molecular Probes) onto 76 x 26 mm slides (Menzel) and sealed using clear varnish. Slides were visualised under an Axiophot fluorescence microscope (Zeiss) and photographed using a Spot camera™ (Diagnostic Instruments).

## 6.3 Results

*6.3.1 Detection of material using antibodies against GST*

The amount of recombinant GST-FG expressed from stable transfected Cos-1/M6 cells was low, and no protein was observed to predominate on either Coomassie Brilliant Blue R-250 or silver stained SDS-PAGE gels (data not shown). When proteins were transferred onto nitrocelluose membranes, and subsequently incubated with an antibody against GST, expression of two GST-containing proteins were detected in the cell-lysate from pSecTag2 C/GST-FG transfec-ted Cos-1/M6 cells (Fig. 6.3.1, lane 5). The proteins had a relative molecular mass of approximately 60 and 100 kDa. It was however not possible to detect any secreted recom-binant material in conditioned medium from these cells (Fig. 6.3.1, lanes 4 & 5). Expression of recombinant material could not be detected in cell-lysate or conditioned medium from Cos-1/M6 cells transfected with the control vector pSecTag2/PSA, supplied by Invitrogen (Fig. 6.3.1, lane 2).

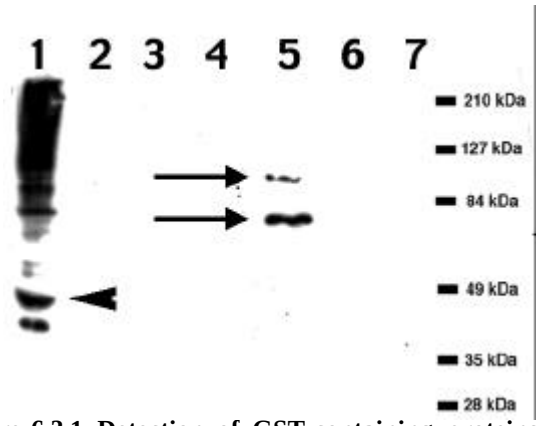


**Figure 6.3.1 Detection of GST-containing proteins by Western blotting**. The numbered lanes represent: **1**; cell-lysate of BL21 bacteria expressing GST-FG, **2**; TCA precipitate of serum–free medium from pSecTag2/PSA transfected cells, **3**; cell-lysate of pSecTag2/PSA transfected cells, **4**; serum-free medium of pSecTag2/PSA transfected cells, **5**; TCA precipitated serum-free medium of pSecTag2 C/GST-FG, **6**; cell-lysate of pSecTag2 C/GST-FG transfected cells and **7**; serum-free medium of pSecTag2 C/GST-FG transfected cells. Arrows indicate GST-containing proteins with a molecular size of approximately 60 kDa and 100 kDa in the cell-lysate of pSecTag2 C/GST-FG transfected cells, possibly representing glycosylated versions of GST-FG. Arrowhead shows band corresponding to GST-FG expressed in BL21 bacteria. Remaining immunoreactivity in lane 1 represents cross-reaction between the anti-GST antibody and bacterial proteins.

*6.3.2 Detection of material using antibodies against the Myc-epitope*

A Western blot incubated with an antibody against the Myc-epitope revealed two proteins containing the Myc-epitope in the cell-lysate of pSecTag2 C/GST-FG transfected Cos-1/M6 cells (Fig. 6.3.2, lane 6). These proteins were of a similar molecular size as those identified on Western blots incubated with the antibody against GST (Fig. 6.3.1 & 6.3.2). No secreted proteins were found in the conditioned medium of pSecTag2 C/GST-FG transfected cells when detecting the Myc-epitope (Fig. 6.3.2, lane 5). However, cells transfected with the control vector SecTag2/PSA secreted a protein with a size of approximately 55 kDa as can be seen on Western blots incubated with the antibody against the Myc-epitope (Fig. 6.3.2, lane 2). Although the calculated size for PSA is 25 kDa, a 55 kDa glycosylated protein was observed when PSA was expressed in a breast carcinoma cell line (Invitrogen, 1997c). Recombinant material was not detected in the cell-lysate of control-transfected cells.

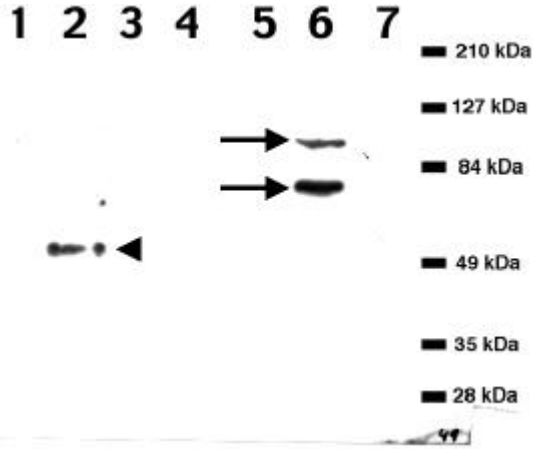


**Figure 6.3.2 Detection of Myc-containing proteins by Western blotting.** The numbered lanes represent: **1**; cell-lysate of BL21 bacteria expressing GST-FG, **2**; TCA precipitate of serum–free medium from pSecTag2/PSA transfected cells, **3**; cell-lysate of pSecTag2/PSA transfected cells, **4**; serum-free medium of pSecTag2/PSA transfected cells, **5**; TCA precipitated serum-free medium of pSecTag2 C/GST-FG, **6**; cell-lysate of pSecTag2 C/GST-FG transfected cells and **7**; serum-free medium of pSecTag2 C/GST-FG transfected cells. Arrows indicate proteins containing the Myc-epitope in the cell-lysate of pSecTag2 C/GST-FG transfected cells. Arrowhead shows a band corresponding to secreted PSA by pSecTag2/PSA transfected cells. The difference between the calculated molecular size of PSA (25 kDa) and the observed size (55 kDa) may arise because of glycosylation.

*6.3.3 Affinity purification and anti-GST detection*

On Western blots of eluates from glutathione sepharose 4B gel incubated with medium from pSecTag2 C/GST-FG transfected Cos-1/M6 cells, it was not possible to detect any secreted proteins fused to GST. Nevertheless, bands corresponding to proteins with sizes of either 60 and or 100 kDa were detected in the cell-lysate (Fig. 6.3.3, lane 6).

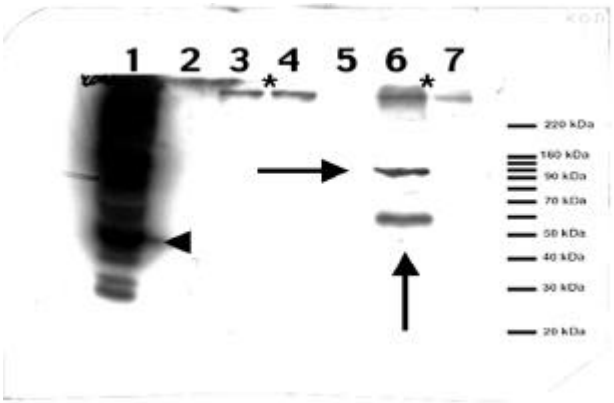


**Figure 6.3.3 Detection of GST-containing proteins by Western blotting**. The numbered lanes represent: **1**; cell-lysate of BL21 bacteria expressing GST-FG, **2**; elution from the glutathione sepharose 4B gel, **3**; serum-free medium after the addition of the glutathione sepharose 4B gel, **4**; serum-free medium before addition of the glutathione sepharose 4B gel, **5**; the glutathione sepharose 4B gel after elution, **6**; cell-lysate of Cos-1/M6 cells transfected pSecTag2 C/GST-FG and **7**; non-transfected Cos-1/M6 cells. Arrows indicate proteins of approximately 60 and 100 kDa in the cell-lysate of pSecTag2 C/GST-FG transfected cells, recognised by the antibody against GST. Arrowhead shows a band corresponding to GST-FG expressed in BL21 bacteria. Remaining immunoreactivity in lane 1 represents cross-reaction between the anti-GST antibody and bacterial proteins. Asterisks indicate bands arising from proteins aggregating at the border between stacking and separation gel leading to a cross-reaction with the applied antibodies.

*6.3.4 Immunohistochemistry*

Immunohistochemistry performed on 4% PFA fixed Cos-1/M6 cells (either mock transfected or transfected with pSecTag2 C/GST-FG) showed marked morphological differences when incubated with an antibody binding to the Myc-epitope. Mock-transfected Cos-1/M6 cells could not be distinguished from un-transfected cells

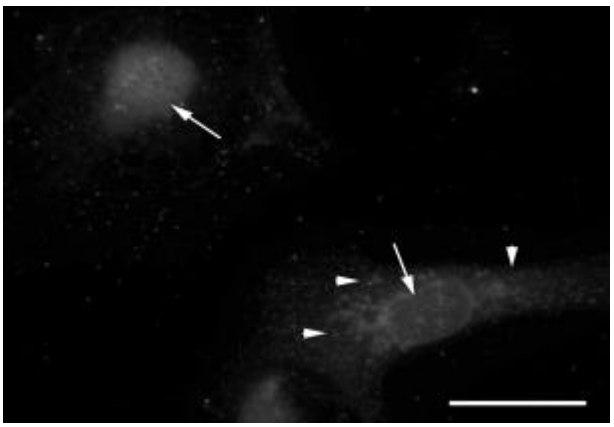

**Figure 6.3.4 Immunofluorescence image of finely spread mock-transfected Cos-1/M6 cells**. Cells show normal morphology with dispersed point-like immunoreactivity in the cytosol (arrowheads) and an overall staining of the nucleus (arrows). Scale bar = 50 µm.

when examined under a light microscope (not shown); nor did they show any difference in proliferation rates. Mock-transfected cells (see figure 6.3.4) showed weak point-like immunoreactivity in the cytosol and a general staining of the nucleus. Overall, strong immunoreactivity could not be observed in these cells. In Cos-1/M6 cells, stable transfected with pSecTag2 C/GST-FG, normal cell structures - such as nucleus and cytoplasm - were no longer detectable. Individual cells could no longer be identified as transfected cells clumped together forming large fibrous aggregates (Fig. 6.3.5). The anti-Myc immunoreactivity was seen covering these aggregates indicating the presence of the Myc-epitope in association with these structures (Fig. 6.3.5).

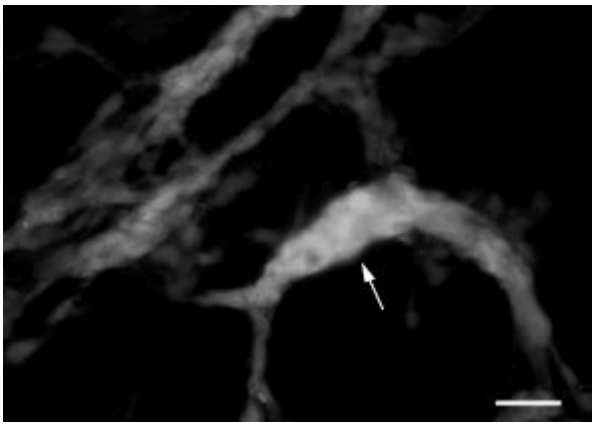

**Figure 6.3.5. Immunofluorescence image of pSecTag2 C/GST-FG transfected Cos-1/M6 cells.** Cos-1/M6 cells transfected with pSecTag2 C/GST-FG clump together forming large aggregates, leading to a disappearance of normal cell structures and an altered morphology. Arrow marks large fibrous aggregate. Scale bar = 50 µm.

# Discussion for section 4 to 6

# 7. Discussion

In these studies, TN-R has been further characterised in view of its role in the function of PNEMs found around GABAergic parvalbumin expressing interneurones. A number of techniques were applied to discover novel ligands for TN-R *e.g.* cDNA cloning, heterologous protein expression in various host cells such as bacteria, yeast and mammalian cell lines and the generation of a TN-R affinity column. The FG fragment is the most conserved domain in the tenascins (Erickson, 1993) and has been suggested to be the functionally dominant region (Elefteriou et al., 1999). This lead to the hypothesis that the FG domain might play an important role in mediating many of the effects observed for the native full length TN-R (Xiao et al., 1996), with the research focusing on this C-terminal fragment. However, problems arising from this work involved the general insolubility and precipitation of the FG-knob. The different techniques and methods employed to resolve this problem are further elucidated and discussed below.

### 7.1 Bacterial expression of recombinant material

Although the expression of different sized C-terminal TN-R fragments containing various affinity tags were induced under several temperature conditions, the recombinant proteins remained insoluble in native buffers. Furthermore, unsuccessful attempts were also made to obtain soluble chimeric proteins fused to calbindin by expressing the R1 and FG fragments in a pCal vector. Purification of bacterially expressed hFG was not possible under native conditions as none of the tags used were capable of inducing soluble folding of recombinant C-terminal TN-R fragments, although the tags themselves are generally believed to fold spontaneously into soluble forms (Scopes, 1994), concurring the insolubility of the FG-knob observed in both tenascin-R and tenascin-X (Norenberg et al., 1995; Elefteriou et al., 1999). All other previously studied tenascin domains have been shown to spontaneously fold into soluble forms (Norenberg et al., 1995; Elefteriou et al., 1999), indicating that the FG-knob needs additional factors such as other tenascin domains or carbohydrates to induce correct folding. Indeed, carbohydrates can play an essential role in determining the overall tertiary and quaternary structure of a protein

(Creighton, 1993). Analysis of the primary structure of the FG-knob from human TN-R showed that it contained one potential site for N-linked glycosylation (Asn-Gly-Ser) and 53 potential sites for O-linked glycosylation (serine or threonine; see also section **5.1**). Native mouse TN-R contains both N- and O-linked glycosylations (Zamze et al., 1999), but whether the FG-knob is glycosylated *in vivo* has yet to be determined. The observed insolubility of the FG knob may reflect some particular property of this part of TN-R in comparison to other TN-R domains, with this domain shown to be the most conserved in the tenascins (Erickson, 1993).

Under denaturing conditions[o], non-covalent bonds holding together the secondary, tertiary and quaternary structure of a protein are disrupted leaving the protein backbone in an unfolded state (Lawrence, 1995). Associations between hexahistidine tags and the Ni-NTA gel are nonetheless still feasible as interactions do not depend upon an overall structure, but upon interactions between individual histidine amino acids and the Ni-NTA gel (Scopes, 1994). Buffers containing primary, secondary or tertiary amino groups[p] cannot be used when coupling proteins to activated CNBr groups, as such amino groups react with them thereby blocking all active sites and leaving none for the proteins to couple to (Pharmacia, 1993). Purified recombinant hFG was only soluble in buffers containing 4 M or higher concentrations of urea, and precipitated when dialysed against a variety of native buffers. Analysis of the amino acid sequence of the FG-knob showed that it contains many charged amino acids (more than 20%) and precipitation could occur because of hydrophilic interactions between FG-domains. To overcome the precipitation in non-urea containing buffers, purified hFG was dialysed against buffers containing high concentration of chaotropic salts. High salt concentrations are believed to disrupt all non-hydrophobic interactions between proteins but also to increase the hydrophobic forces between them (Scopes, 1994). To avoid the latter, the chaotropic[q] salt sodium thioscyanate[r] (NaSCN) was chosen, as it has low 'salting out'[s] abilities according to the Hofmeister series (Scopes, 1994). This, combined with the fact that it does not

[o] Such as buffers containing urea
[p] Urea contains two primary amino groups
[q] Salts interacting directly with proteins thereby counteracting the 'salting out' properties
[r] Also termed sodium thiocyanide, sodium sulfocyanate and thiorhodanid
[s] 'Salting out', a decrease in solubility of proteins due to increased hydrophobic interactions as a result of high salt concentrations (Scopes, 1994).

contain any amino groups, is highly soluble, relatively non-toxic[t] and has no major buffering effect, made it an ideal salt for "solubilising" the FG fragment.

Examination of silver stained SDS-PAGE gels of proteins eluted from the TN-R affinity column revealed eluates composed predominantly of three different sized proteins. The large apparent size of the largest of the three affinity-purified proteins (> 600 kDa), together with recent reports of interactions between TN-R and CSPGs (Aspberg et al., 1995, 1997; Xiao et al., 1997; Milev et al., 1998) indicated a proteoglycan, whereas nothing could be extrapolated from the sizes of the other two proteins. Additional affinity purification of eluted proteins did not result in further predominance of any of the three proteins, which would otherwise have indicated a potential difference in binding affinities to the FG-knob. These three proteins could therefore not be distinguished using this method, either because the smaller proteins represented degradation fragments of the larger protein, or because they were independent proteins with binding affinities in the same range.

Investigation of eluates on 2D-PAGE gels showed that they contained both acidic and basic proteins, with sizes less than 100 kDa. The polyacrylamide pore size in the IPG strip excludes extremely large proteins (Pharmacia, 1994) and may be the reason that the high molecular weight proteins were not observed on the 2D-PAGE gels. On the acidic side of the 2D-PAGE gel, the proteins consisted of a dominating spot closely trailed by one or more less predominant ones indicating the proteins to be phosphorylated (Hames, 1990; Celis et al, 1995). These proteins were possibly comprised of cytosolic domains as phosphorylation has been shown to primarily occur intracellularly (Creighton, 1993). As most cytosolic proteins were removed during the preparation of the pig cortex homogenate, it is conceivable that these proteins consisted of degradation fragments of transmembrane proteins. The basic side of the gel revealed several spots separated by a relative large distance demonstrating that the proteins here contained multi-charged groups (Hames, 1990; Celis et al, 1995). Attachment of multi-charged groups such as $SO_4^{2-}$ may occur on tyrosine residues in proteins passing through the Golgi apparatus (Creighton, 1993). Furthermore, these multi-charged groups are an integrated part of the carbohydrate N-acetyl-D-galactosamine (GalNAc; Alberts et al., 1994), a common constituent of proteoglycans such as chondroitin sulphates and keratan sulphates (Alberts et al., 1994), found

[t] Danger class Xn; R 20/21/22-32 and S 13; see Lenga, 1985 and the searchable database KIROS at http://www.kemi.aau.dk/kiros/kiros.html

extensively in ECMs (Lodish et al., 1995). The protein on the basic side of the 2D-PAGE gel may therefore represent a degradation product of either a transmembrane or a secreted protein. The general insolubility of the FG-knob, even in buffers containing chaotropic salts, and the consequent low capacity of the affinity column may have been the reason for the low amount of purified proteins. Eluted proteins could only be visualised by silver staining of SDS-PAGE and 2D-PAGE gels thereby excluding the possibility of microsequencing the proteins (Celis et al., 1995).

PNEMs are rich in hyaluronic acid, chondroitin-bearing proteoglycans such as CSPGs and glycoproteins (Delpech et al., 1982; Bignami et al., 1992; Bruckner et al., 1994), with collagenous molecules also shown to associate with these entities (Murakami et al., 1999). Enzymatic digestion directed against elastin, collagen type II and IV repeats, hyaluronic acid and GalNAc carbohydrates, all constituents known to exist in many ECMs, revealed that no major change in protein migration pattern had occurred. This would indicate that the eluted proteins did not contain any sites recognised by the applied enzymes. Considering the many recent reports of interactions between TN-R and CSPGs (Aspberg et al., 1995, 1997; Xiao et al., 1997; Milev et al., 1998), a major family of proteoglycans in the BECM (Margolis and Margolis, 1993; Ruoslahti, 1996) characterised by containing GalNAc epitopes (Maeda et al., 1995), it was surprising that none of the eluated proteins belonged to this family. A reason could be that the eluted proteins comprised degradation fragments from larger proteins, which normally contain these sites. Nevertheless, many types of BECM proteins without these sites exist (Alberts et al., 1994; Weber et al., 1998), and the eluted proteins may therefore still represent matrix molecules.

The biological interaction between recombinant TN-R and eluted proteins was estimated by fluorometric measurements using FITC labelled eluates. A slight increase in intensities was observed when FITC labelled eluates were incubated together with the purified FG-knob in comparison to FITC labelled eluates alone. Nevertheless, a statistically significant difference was not found and it was not possible to validate whether the eluted proteins truly were comprised of TN-R binding proteins or just contaminating proteins associating non-specifically with the affinity column. Therefore, focus was placed on producing larger amounts of recombinant FG using other expression systems to overcome the general insolubility problem of the FG-fragment.

## 7.2 Expression of recombinant material in *P. pastoris*

Expression of recombinant FG-knob in KM71 and GS115 yeast cells resulted in the production of several proteins of different sizes. Analysis of pellets from transfected KM71 yeast cells revealed the expression of a protein with a size of 27 kDa, whereas two proteins of roughly 10 and 27 kDa predominated in pellets from transfected GS115 yeast cells. The calculated size of recombinant FG fused to the Myc-epitope was 24.5 kDa indicating that the recombinant proteins with sizes of approximately 27 kDa represented non-secreted full length chimera within the yeast cells. The 10 kDa protein detected in transfected GS115 yeast cells may either be due to degraded fragments of recombinant FG or to contaminating proteins associating with the Ni-NTA gel (see discussion below). Evaluation by Coomassie Blue staining of proteins eluted from Ni-NTA gel incubated with conditioned medium from both KM71 and GS115 yeast cells showed that secreted proteins were only detected in eluates from GS115 yeast cells. The fact that only the smaller recombinant protein (10 kDa) associated with the Ni-NTA gel indicated that the full length recombinant FG (27 kDa), observed in pellets from both KM71 and GS115 yeast cells, was either not secreted, present in non-detectable amounts or did not associate with the Ni-NTA gel. Nonetheless, by Western blotting, detection of Ni-NTA purified proteins present in conditioned medium were observed in both transfected KM71 and GS115 yeast cells. Proteins of either 27 or 35 kDa, containing the Myc-epitope, were detected in conditioned medium from transfected KM71 yeast cells, whereas GS115 yeast cells secreted a protein with a size of 40 kDa. The shift in size of proteins secreted from transfected KM71 yeast cells occurred after 48 hrs of induction, suggesting that a change in glycosylation pattern had occurred. It can be envisaged that the size difference may represent glycosylated (35 kDa) and non-glycosylated proteins (27 kDa), and that such a shift only occurs after a certain time of induction in KM71 yeast cells. The difference in size between recombinant FG detected in pellets (27 kDa) or in conditioned medium (40 kDa) in GS115 yeast cells, may also occur because of an addition of carbohydrates. Comparison of the different sizes of proteins secreted from transfected KM71 and GS115 (27/35 or 40 kDa) yeast cells indicated that the two yeast strains do not perform the same type of glycosylation. Whether the intracellular non-glycosylated recombinant FG with a size of 27 kDa, detected in both transfected KM71 and GS115 yeast cells, represents material yet to be post-translationally

modified (in ER or Golgi apparatus) or aggregated proteins, is still unclear. The 10 kDa secreted protein that was detected in conditioned medium from transfected GS115 yeast cells was not observed by Western blotting. These findings contradict each other because the protein associated with the Ni-NTA gel, suggesting that it contained the hexahistidine stretch. As recombinant proteins expressed using the pPICαA vector are fused C-terminally to the Myc-epitope followed by the hexahistidine tag (Invitogen, 1997a), it is unlikely that the 10 kDa protein could contain the hexahistidine stretch (840 Da) and not the Myc-epitope (2.5 kDa). It is therefore more likely that the observed 10 kDa protein represents a contaminating protein that is expressed by the GS115 and not KM71 yeast strain and associate with the Ni-NTA gel because of a high histidine content. Such proteins have frequently been observed in bacteria (Invitrogen, 1997b) and presumably exist in eukaryotic cells as well.

### 7.3 Mammalian protein expression

Two recombinant proteins were detected in cell-lysates of pSecTag2 C/GST-FG transfected Cos-1/M6 cells using antibodies against both GST and the Myc-epitope. The expected molecular size of recombinant GST-FG fused C-terminally to the Myc-epitope (without carbohydrates) is 50 kDa. As the antibodies did not recognise any of the proteins endogenously expressed in the Cos-1/M6 cells, the bands observed in material from transfected cells may represent recombinant proteins containing both the GST and the Myc-epitope suggesting them to be GST-FG. Several potential glycosylation sites exist in the FG-knob[u], and the size difference between the two forms of GST-FG (60 and 100 kDa) may have been due to differences in the glycosylation pattern. Variation in molecular size of TN-R arising from differences in glycosylation patterns has never previously been suggested in the literature, but two alternatively spliced isoforms have been described (of 160 and 180 kDa; Pesheva at al., 1989). The difference in size may therefore occur because the FG fragment is expressed in a cell line that is quite different from the neurone and glia populations known normally to express TN-R (Bartsch et al., 1993; Wintergerst et al., 1993). Unfortunately, no recombinant GST-FG was detected after affinity purification of

[u] See also sections **5.1** and **7.1**.

conditioned medium from transfected cells, which may have been due to a lack of sensitivity of the method used, or because the proteins were not secreted in a soluble form. However, as recombinant PSA was easily detected on Western blots, it seems unlikely that affinity purification of GST-tagged fusion proteins followed by Western blotting should not be sensitive enough to detect the recombinant protein (see discussion below).

Mock- and non-transfected Cos-1/M6 cells showed normal morphologies and cell structures. On the contrary, Cos-1/M6 cells transfected with the pSecTag2 C/GST-FG vector clumped together leading to the formation of large aggregates and the loss of normal cell structures. In transfected cells, the immunoreactivity around aggregated Cos-1/M6 cells indicated that secreted GST-FG associated with these structures. It is noteworthy, that although it cannot be excluded that such aggregation could occur because GST-FG molecules interacted with ECM proteins or receptors expressed *de novo* by the Cos-1/M6 cells, it seems more likely that the formation of these aggregates occurred because recombinant GST-FG molecules stuck together when secreted. This homophilic association then resulted in a pericellular aggregation of GST-FG at the surface of the Cos-1/M6 cells thereby knitting them together leading to the formation of large cell aggregates. Assembly of native TN-R monomers into dimers and trimers via the cysteine-rich N-terminal of the molecule has previously been reported (Pesheva et al., 1989; Norenberg et al., 1992). However, as interaction between FG domains in native TN-R has never been reported in the literature, it may be assumed that the aggregates observed here are simply due to a precipitation/aggregation of non-soluble GST-FG and not a biologically functional interaction.

### 7.4 Summary

The prokaryotic expression of recombinant proteins spanning the C-terminal part of TN-R resulted in the production of inclusion bodies rendering the proteins insoluble in native buffers. Renaturing of purified proteins was impossible in native buffers and only minor amounts of purified protein remained soluble in solutions containing high concentrations of chaotropic salts. This indicated that factors beyond the primary structure, such as glycosylation, are needed for the correct folding of the FG-knob. The overall insolubility of the FG-knob makes it very distinct in

comparison to other TN-R domains and this may reflect some still unidentified intrinsic function of this domain. Fragments of phosphorylated or differently modified proteins were purified from pig cortex using a TN-R affinity column. These proteins did not contain sites similar to common matrix components such as elastin, collagen type II or IV repeats and hyaluronic acid. It was also intriguing that these fragments did not belong to the CSPG family, suggesting that they may be transmembrane proteins or secreted glycoproteins.

When expressing recombinant FG in *P. pastoris* yeast cells it was clearly shown that recombinant FG could be generated and purified in a soluble form. The molecular size of the proteins indicated that they were glycosylated, but the quantity of soluble material was extremely low. Obtaining large amounts of recombinant FG from these yeast cells seemed not to be possible.

The expression of recombinant GST-FG in a Simian fibroblast cell line gave rise to two differently glycosylated proteins. These proteins, when secreted, stuck together leading to the formation of large cell/protein aggregates. Affinity purification of recombinant GST-FG was therefore not feasible using this method.

# Part B

# 8. Phosphacan immunoreactivity is associated with perineuronal nets around parvalbumin-expressing neurones.

**Anders Haunsø[1], Marco R. Celio[1], Renée K. Margolis[2], Pierre-Alain Menoud[1]**

[1]Institute of Histology and General Embryology and Program in Neuroscience, University of Fribourg, CH-1705 Fribourg, Switzerland

[2]Department of Pharmacology, State University of New York, Health Science Center, Brooklyn, New York 11203

**Published in: Brain Research 834 (1-2); 219-222 (1999)**

## 8.1 Abstract

A special feature of the extracellular matrix in adult brains of various species is the concentration of certain components around different sub-populations of neurones giving rise to net-like structures termed perineuronal nets. Recently, some of these components have been identified but the function of these nets has yet to be resolved. Using immunofluorescence microscopy we report here that phosphacan, a chondroitin sulphate proteoglycan, is an additional component of *Wisteria floribunda* labelled perineuronal nets surrounding parvalbumin-expressing neurones in rat cerebral cortex. Glycoproteins such as tenascin-C and R have been identified in perineuronal nets and the present detection of phosphacan immunoreactivity in the same entity is of potential physiological importance because of their previously described interactions.

## 8.2 Introduction

It is generally recognised that brain extracellular matrix (B-ECM) plays an important role in the development and maintenance of the central nervous system. B-ECM, which mainly consists of hyaluronan, glycoproteins and proteoglycans can influence the nervous system by binding growth factors and cell receptors, and by modulating cell adhesion and signalling (for review see Ruoslahti, 1996). A large part of potential signalling molecules in the B-ECM belongs to the chondroitin sulphate proteoglycan family (CSPGs) whose members tend to have distinct distribution patterns in the brain (Rauch et al., 1991; Lander et al., 1998). Phosphacan (reviewed in Margolis and Margolis, 1997), comprising the extracellular region of the receptor protein tyrosine phosphatase ζ/β (RPTP ζ/β), belongs to this family of CSPGs. Phosphacan is synthesised by astrocytes (Milev et al., 1994) and its localisation, carbohydrate and sulphate compositions are developmentally regulated in the nervous tissue (Meyer-Puttlitz et al., 1996). In embryonic and early postnatal rat brain, phosphacan immunoreactivity is distributed in the neuropil of the cerebral cortex and in the adult rat brain is localised mainly around multipolar non-pyramidal neurones (Maeda et al., 1995). CSPGs have been shown to be present in the perineuronal net (Celio and Blümcke, 1994) surrounding GABAergic interneurones expressing the calcium-binding protein parvalbumin (PV; Hartig et al., 1994; for an overview of PV distribution in the brain see Celio, 1990). In this report we show that phosphacan immunoreactivity is present in the perineuronal net surrounding PV-positive GABAergic interneurones in the adult rat cerebral cortex.

## 8.3 Material and Methods

Eight adult Wistar rats of either sex weighing ~ 300g were euthanised with carbon dioxide and perfused via the left ventricle with 150 ml of 4% (w/v) paraformaldehyde in PBS (0.147 M NaCl, 2.68 mM KCl, 1.76 mM $KH_2PO_4$ and 10.14 mM $Na_2HPO_4$; pH7.4). Brains were removed and placed for a further 1 hr in 4% paraformaldehyde, then transferred for an additional 1 hr in PBS and subsequently

incubated overnight at 4 °C in 18% (w/v) sucrose in PBS. Brains were frozen and cut, using a cryostat, into 40 µm thick horizontal sections. Prior to applying the primary antibodies the sections were washed in PBS for five minutes, post fixed for one minute in 4% (w/v) paraformaldehyde and subsequently washed again in PBS for two minutes. Double-immunolabellings were performed by incubating the sections with a rabbit polyclonal anti-phosphacan antibody (Milev et al., 1994; dilution 1:1,000) and either with the biotinylated lectin *Wisteria floribunda* agglutinin (WFA, Sigma) at a concentration of 20 µg/ml or with a mouse monoclonal anti-PV antibody (PV235; Swant) diluted 1:1,000. Free floating sections were incubated overnight at 4 °C in PBS containing 10% (v/v) bovine serum. Sections were rinsed three times ten minutes in PBS. All the following incubations were carried out at room temp in PBS containing 10% (v/v) bovine serum and all washes for three times ten minutes in PBS. Sections incubated with the anti-PV antibody were revealed with an anti-mouse Cy3™-conjugated antibody (Jackson Laboratories). Sections incubated with biotinylated WFA were revealed by a Cy2™-conjugated streptavidin (Jackson Laboratories). The anti-phosphacan antibody incubation was carried out as a two step reaction by first applying a goat anti-rabbit IgG antibody (Jackson Laboratories), followed by washes and subsequent incubated with a donkey anti-goat Cy2™-conjugated antibody (Amersham). The goat anti-rabbit antibody, the Cy2™ and Cy3™ -conjugated antibodies and the Cy2™ -conjugated streptavidin were all applied at dilutions of 1:100 for 2 hrs at room temp. After extensive washes sections were dried on slides for 2 hrs at room temp, re-hydrated in double distilled water, dried for thirty minutes and subsequently mounted in SlowFade™ (Molecular Probes), coversliped and sealed using clear nail varnish. Controls were carried out in the absence of the primary antibodies or the lectin. The slides were visualised under a Zeiss Axiophot fluorescence microscope, photographed using a Spot camera™ (Diagnostic instruments, Inc.), imported into Adobe Photoshop 3.0.5 where minor changes in brightness and contrast were performed and photographic plates were printed on a Kodak DS 8650 PS Color printer.

## 8.4 Results

Detailed analysis of phosphacan immunoreactivity in the adult rat cerebral cortex revealed a pericellular staining resembling perineuronal net-like structures, ensheathing the cell-body and major dendrites of non-pyramidal neurones. Neurones surrounded by phosphacan immunoreactivity were found in all layers of the cortex, except layer I, and were mainly distributed in the layers II, IV and VI. The immunofluorescence intensity varied from a strong staining in the deeper layers revealing both the contours of the cell body and dendrites, to an almost indistinct staining of the perimeter of a subclass of neurones in layer II. A difference in the density and intensity of positive neurones was also observed depending upon the region of the cerebral cortex, but this was not further studied. In double-staining experiments using both anti-phosphacan and anti-PV antibodies, it was shown that all

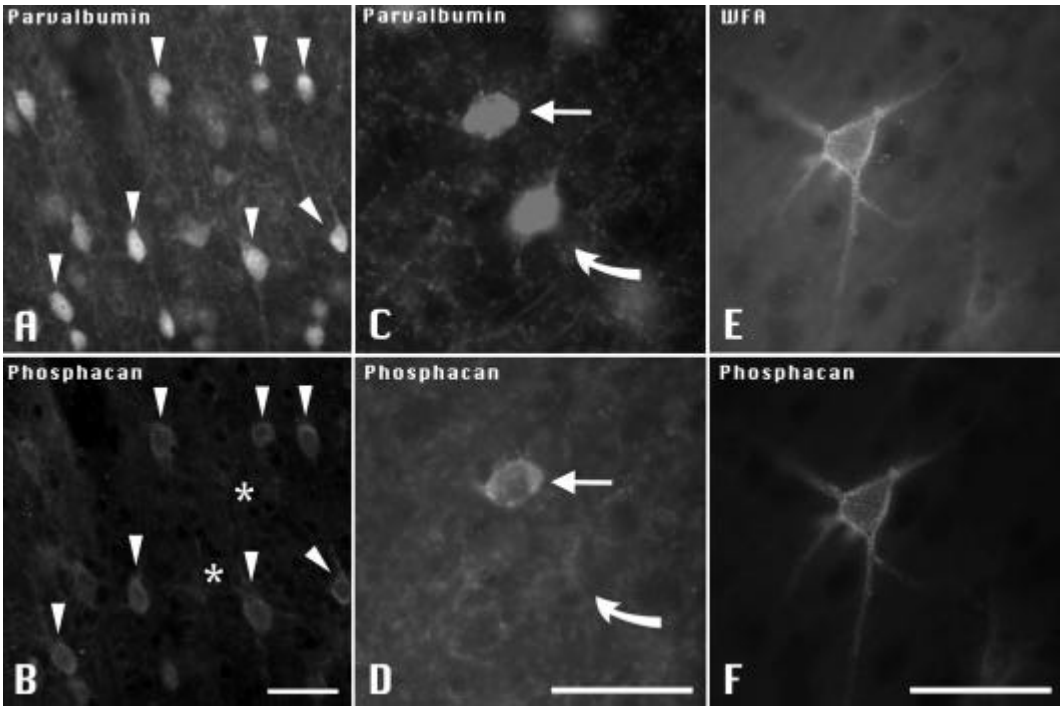


**Figure 8.4.1** Co-localisation of phosphacan immunoreactivity within perineuronal nets around parvalbumin expressing neurones in the cerebral cortex of adult rats. **A** and **B** show a double stained section incubated with anti-PV (A) and anti-phosphacan (B) antibodies. Some of the double stained cells in A and B are marked with arrow heads whereas the asterisks in **B** denote the position of faintly stained neurones in A that are out of focus. **C** and **D** depict a double stained section illustrating the lack of phosphacan immunoreactivity (curved arrow in D) around a PV-expressing neurone (C). **E** and **F** show a double stained section incubated respectively with WFA (E) and the anti-phosphacan antibody (F). Scale bars = 50 µm.

phosphacan immunoreactive neurones in the cerebral cortex were also PV-positive (Fig. 8.4.1 A, B). Very few PV-positive neurones were found without a phosphacan net (Fig. 8.4.1 C, D), but the variation in intensity of the phosphacan immunoreactivity made it difficult to distinguish negative from weakly stained cells. When sections were incubated concomitantly with WFA, a marker for the perineuronal net, and anti-phosphacan, we observed that phosphacan immunoreactivity was localised around the same sub-population of neurones as the perineuronal net (Fig. 8.4.1 E, F). In addition, there was a correlation between the intensity of the phosphacan immunoreactivity and that of WFA in the deeper cortical layers, but not in layer II where the phosphacan immunoreactivity was generally weak. Similar results were obtained when the monoclonal anti-phosphacan antibody 3F8 (Rauch et al., 1991) was applied (not shown).

## 8.5 Discussion

The amount of extracellular material detected in the brain is relatively low (Ruoslahti, 1996) when compared to the ECM of many other tissues. In addition, many if not all of the ECM components in the brain have restricted regional distributions and in addition some also tend to accumulate around specific sub-populations of neurones giving rise to net-like structures termed perineuronal nets (for review see Celio and Blümcke, 1994; Celio et al., 1998). ECM compounds such as hyaluronan (Bignami et al., 1992), neurocan (Matsui et al., 1998), tenascin-C (Celio and Chiquet-Ehrismann, 1993) and tenascin-R (Celio and Blümcke, 1994) are seen to accumulate around PV-expressing GABAergic interneurones (Hartig et al., 1992) comprising a proportion of the neurones surrounded by perineuronal nets. The distribution of PV-expressing neurones in the cerebral cortex (Celio, 1990) and their co-localisation with WFA labelled perineuronal nets is well established in the literature (Hartig et al., 1992; Brauer et al., 1993; Bruckner et al., 1994). CSPGs have been shown to constitute part of the perineuronal nets around PV-positive neurones (Hartig et al., 1994). Furthermore, using the monoclonal anti-phosphacan antibody 6B4, Maeda et al. (Maeda et al., 1995) have detected phosphacan immunoreactivity around certain multipolar non-pyramidal neurones in the adult rat cerebral cortex. In

this paper, we expand on these results by showing that phosphacan is one of the CSPGs in perineuronal nets and that it surrounds only PV-positive neurones in the cortex. The few PV-positive neurones we found not to be surrounded by phosphacan immunoreactivity were localised in the cortical regions where the intensity of the phosphacan immunoreactivity was generally weak. This made it difficult to determine if phosphacan immunoreactivity truly was absent around the PV-positive neurones or if the immunoreactivity was lower than could be detected. In the deeper layers of the cortex, where the intensity of the phosphacan immunoreactivity appeared to be strong, there was a perfect correlation between neurones surrounded by WFA and those surrounded by phosphacan immunoreactivity. Nevertheless, certain regions of the cortex had a low phosphacan immunoreactivity even though no apparent difference could be observed in the WFA staining. Here we suggest that the proportion between phosphacan and other CSPGs within perineuronal nets varies depending on region and layer of the cortex. The appearance of phosphacan immunoreactivity in WFA labelled perineuronal nets was not surprising as the former contains N-acetylgalactosamine carbohydrates (GalNAc, Maeda et al., 1995) which are recognised by WFA. Moreover, phosphacan is also known to bind to certain glycoproteins found in perineuronal nets such as tenascin-C (Milev et al., 1997) and tenascin-R (Milev et al., 1998). Therefore, the co-localisation of all three compounds in perineuronal nets suggests a potential physiological relevance for their interactions.

Perineuronal nets are thus not only heterogeneous in composition (Celio and Blümcke, 1994; Celio et al., 1998) but the proportion of their components vary depending upon the localisation within the cerebral cortex. Such regional differences in the composition of the ECM may reflect subdivisions of functionally defined areas. So far, the functions and the exact composition of perineuronal nets are still far from being determined (Celio and Blümcke, 1994) but the identification of phosphacan in this structure adds a further component to this special form of extracellular matrix and may enable us to better understand its role.

## 8.6 Acknowledgements:

This project was supported by the Desirée and Nils Yde Foundation and by Novartis. We are grateful to Dr. Merdol Ibrahim for his help, valuable advice and comments on this manuscript.

# 9. Morphology of Perineuronal Nets in Tenascin-R and Parvalbumin Single and Double Knockout Mice.

**Anders Haunsø[1], Merdol Ibrahim[1], Udo Bartsch[2], Maryse Letiembre[1], Marco R. Celio[1], Pierre-Alain Menoud[1]**

[1]Institute of Histology and General Embryology and Program in Neuroscience, University of Fribourg, CH-1705 Fribourg, Switzerland

[2]Zentrum für Molekulare Neurobiologie, Universität Hamburg, D-20246 Hamburg, Germany

**Published in: Brain Research 864 (1); 142-145 (2000)**

## 9.1 Abstract

Recently identified chondroitin sulphate proteoglycans in perineuronal nets include neurocan and phosphacan. However, the function and assembly of these components has yet to be resolved. In this study, we show morphological alteration in *Wisteria floribunda* labelled nets around cortical interneurones both in tenascin-R knockout and tenascin-R/parvalbumin double knockout mice. This alteration reflects the loss of phosphacan and neurocan from cortical nets in mice deficient in tenascin-R. No effect on the membrane related cytoskeleton, as revealed by ankyrinR, was observed in any of the mice. These results on mice lacking tenascin-R substantiate previously reported *in vitro* interactions between tenascin-R and phosphacan and neurocan.

## 9.2 Introduction

A special feature of the brain extracellular matrix (ECM; Ruoslahti, 1996) is the aggregation of certain components around specific sub-populations of neurones giving rise to net-like structures termed perineuronal nets of extracellular matrix (PNEMs; Celio et al., 1998). PNEMs are well characterised around cortical GABAergic parvalbumin immunoreactive (PV-IR) interneurones (Hartig et al., 1999) and are composed of hyaluronan, tenascin-C (Celio, 1993), -R (Celio and Blümcke, 1994) and defined chondroitin sulphate proteoglycans (CSPGs) such as brevican (Hagihara et al., 1999), neurocan (Matsui et al., 1998) and phosphacan (Haunso et al., 1999). However, neither function (Hartig et al., 1999) nor process of assembly of PNEMs has yet been determined (Celio et al., 1998). *In vitro* studies have shown binding between tenascin-R (TN-R) and members of the CSPG family (Milev et al., 1998; Hagihara et al., 1999) suggesting its involvement in the assembly and structure of PNEMs. In addition, the intracellular organisation of the ankyrin$_R$ membrane-related cytoskeleton (MRC) may also be involved in the formation of the lattice-like structure of PNEMs, by controlling the position of integral membrane proteins (Wintergerst et al., 1996) involved in forming the nets. In this report we show that TN-R is essential for attracting and/or retaining neurocan and phosphacan in cortical PNEMs as no pericellular staining was observed for these CSPGs when TN-R was lacking.

## 9.3 Material and methods

Mice lacking either TN-R (Weber et al., 1999) or PV (Schwaller et al., 1999) were used and double knockout mice for both TN-R and PV were generated by cross-breeding TN-R and PV single knockout mice. The genotype of TN-R, PV and PV/TN-R deficient mice were determined by Southern blotting as previously described (Schwaller et al., 1999; Weber et al., 1999). In total twelve adult mice ~ 30g, comprising three of each genotype - wild type (WT), PV knockout (KO), TN-R KO and PV/TN-R double KO - of either sex, were used in these experiments. Animals were sacrificed, brains dissected out and processed for immunohistochemistry as previously described (Haunso et al., 1999). Biotinylated *Wisteria floribunda*

agglutinin (WFA, Sigma) immunoreactivity (IR) was detected by applying the lectin at a concentration of 20 µg/ml and TN-R-IR by applying a 1:500 dilution of mouse anti-tenascin-R antibody (restrictin 23-14). Double-immunolabelling was performed by incubating sections with a mouse monoclonal anti-PV antibody (PV235; Swant) diluted 1:500 together with rabbit polyclonal antibodies against either phosphacan (Milev et al., 1994), neurocan (Milev et al., 1996) or ankyrin$_R$ (Lambert and Bennett, 1993), all diluted 1:1,000. Sections incubated with the anti-PV antibody were visualised with a fluoresceinisothiocyanate-conjugated (FITC; 1:200) anti-mouse antibody (Molecular Probes) and biotinylated WFA was visualised by Texas Red-conjugated streptavidine (Vector; 1:200). Detection of all rabbit polyclonal antibodies or the monoclonal TN-R antibody was carried out as two step reactions by first applying biotinylated goat anti-rabbit IgG antibodies (Vector; 1:200) or biotinylated horse anti-mouse IgG antibody (Vector; 1:200), respectively, followed by washes and subsequent incubation with Texas Red-conjugated streptavidine (1:200). Controls were carried out in the absence of primary antibodies or the lectin. Slides were analysed with a Bio-Rad 1024, argon/krypton confocal laser scanning fluorescence microscope (LSCM; Bio-Rad Microsciences Division Ltd). Both green and blue-lines of laser excitation were used and detected at 522nm for FITC and 680nm for Texas Red-labelled structures. Using a x60 oil immersion objective and real time zoom feature of the confocal program, captured optical sections of 0.2 µm thickness were superimposed and images transferred to Adobe Photoshop$^{TM}$ software where photographic plates were prepared and printed using a Kodak dye sublimation printer (DS 8650 PS).

## 9.4 Results

In both WT and TN-R KO animals, cortical PV-IR neurones had a normal pattern of distribution and normal pericellular staining was observed in WT and PV KO animals (not shown). Confocal analysis of individual WFA-labelled PNEMs revealed a lattice-like staining around cell soma and dendritic arborisations in both WT and PV KO animals (Fig. 9.4.1 A, B). However, in both TN-R KO and PV/TN-R KO animals WFA-labelled PNEMs around the cell soma showed punctuated immunolabelling (Fig. 9.4.1 C, D). Labelling along dendrites was also markedly

reduced or absent (Fig. 9.4.1 C, D). Despite this, no apparent change in the overall

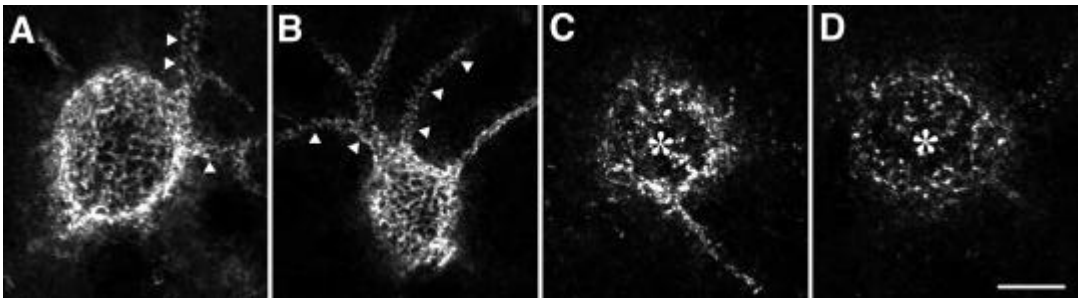


**Figure 9.4.1** Confocal images of WFA-labelled perineuronal nets in the cerebral cortex of WT (**A**), PV KO (**B**), TN-R KO (**C**) and PV/TN-R double KO (**D**). In both WT (**A**) and PV KO (**B**) mice the nets have a normal lattice-like morphology around soma and extend along dendritic aborisations (arrow heads). Nets were punctuated and disrupted around soma (asterisk) in TN-R KO (**C**) and to a similar extent in PV/TN-R double KO (**D**) mice. Labelling of nets along dendrites was generally absent in both genotypes. Scale bar = 20 μM.

distribution or density of cells with WFA-labelled nets was observed in any of the animals (as also shown by Weber *et al.* 1999). In WT and PV KO animals, double-immunofluorescence labelling using neurocan or phosphacan combined with PV-IR revealed a normal net-like staining pattern around cortical interneurones (Fig. 9.4.2 A, B, D, E). In TN-R deficient mice we observed a massively reduced and more diffusely distributed cortical neurocan-IR in mutant mice when compared to wild-type animals (Fig. 9.4.2 C), whereas no pericellular phosphacan-IR (Fig. 9.4.2 F) could be detected in any tenascin-R deficient mice. The ankyrin$_R$-IR MRC (characteristic for cortical PV-IR interneurones; Wintergerst et al., 1996) showed no morphological differences in any of the mice studied, even in neurones lacking PV or those showing altered neurocan and phosphacan PNEMs (Fig. 9.4.3).

## 9.5 Discussion

Many if not all ECM components in the brain show a restricted regional distribution (Rauch et al., 1991; Lander et al., 1998) with some accumulating around specific sub-populations of neurones giving rise to net-like structures termed PNEMs (for review see Celio and Blümcke, 1994; Celio et al., 1998). Recently, interactions between TN-R and defined CSPGs such as brevican (Aspberg et al., 1997), phosphacan (Milev et al., 1998), neurocan (Milev et al., 1998) and versican (Aspberg et al., 1995) have been shown *in vitro*. Furthermore, IR for brevican, phosphacan and

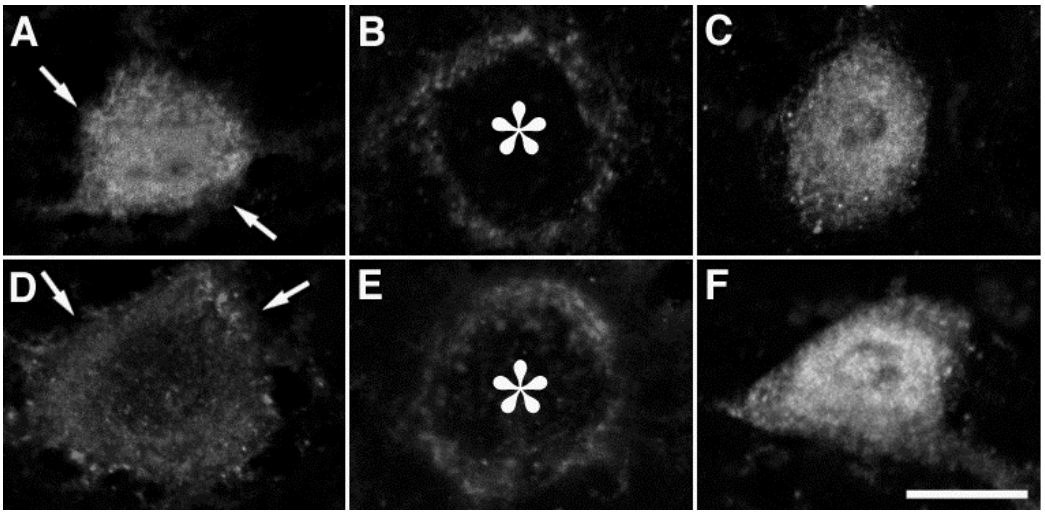


**Figure 9.4.2** Double confocal images of neurocan (**A-C**) and phosphacan (**D-F**) immunoreactivity around cortical interneurones. (**A**) Neurocan-IR (red, arrows) around a PV-labelled neurone (green) in WT. (**B**) Neurocan-IR (red) surrounding PV-negative (asterisk) neurone in PV KO. (**C**) PV-labelled neurone (green) lacking neurocan-IR around cell soma in TN-R KO. (**D**) Phosphacan-IR (red) around PV-labelled neurone (green) in WT. (**E**) Phosphacan-IR (red, arrows) surrounding PV-negative (asterisk) neurone in PV KO. (**F**) PV-labelled neurone (green) lacking phosphacan-IR around cell soma in TN-R KO. Scale bar = 20 μM.

neurocan together with TN-R (Celio and Blümcke, 1994) has also been associated with PNEMs (Matsui et al., 1998; Hagihara et al., 1999; Haunso et al., 1999), conferring physiological importance to their previously described interactions *in vitro*. In this paper, we report for the first time that the removal of a defined PNEM molecule can alter the distribution and levels of other specific components in perineuronal nets. We report that TN-R is needed for the correct assembly of PNEMs and when absent, CSPGs such as phosphacan and neurocan are no longer present, or in extremely low amounts, in cortical PNEMs, leading to a marked alteration in their appearance. The lectin WFA, used in this investigation, recognises N-acetylgalactosamine carbohydrates (Maeda et al., 1995) on both phosphacan and

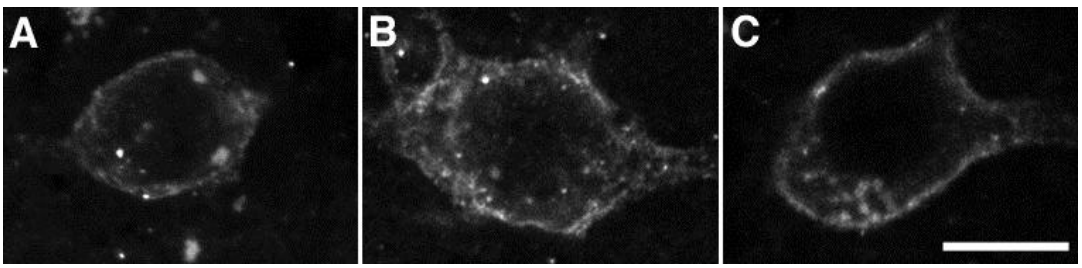


**Figure 9.4.3** Confocal images of ankyrin$_R$ membrane related cytoskeleton immunoreactivity in WT (**A**), PV KO (**B**) and TN-R KO (**C**) mice. Ankyrin$_R$-IR showed normal pattern of distribution and morphology in cortical neurones of all genotypes. Scale bar = 20 μM.

neurocan. The observed alteration in the WFA-labelled nets in mice lacking tenascin-R (as also reported by Weber *et al.* 1999) therefore reflects a significant reduction of the two investigated components and perhaps other CSPGs. It is noteworthy that in areas such as the cerebellum, olfactory bulb and spinal cord some neurocan-IR remained in tenascin-R deficient animals, but this was not investigated further. In contrast phosphacan-IR nets were not detected anywhere else in the CNS in these mice. This indicates that TN-R is not involved in determining which neurones form PNEMs but may be involved in attracting and/or retaining phosphacan and neurocan in cortical PNEMs. The MRC has been proposed as a prerequisite for the organisation of PNEMs and also to be involved in defining the area of synaptic contacts by keeping in register the overlaying PNEM (Celio and Rathjen, 1993; Wintergerst et al., 1996). The results presented here indicate that the MRC is more likely to be involved in determining the position of integral membrane proteins, rather than retaining the lattice-like structure of the PNEM. Evidence for this comes from the fact that the MRCs remain constant even though PNEMs have morphologically degenerated into a punctuated structure.

The lack of both PV and the alteration in morphology of PNEMs seemed not to have affected the distribution of individual cortical interneurones. It has been proposed that perineuronal nets are required for fast-spiking behaviour of GABAergic interneurones (Hartig et al., 1999). Modification of PNEMs could therefore influence the fast-spiking properties of these neurones or the distribution of synapses contacting their cell body, since the lattice-like structure of PNEMs defines the area of synaptic contacts (Celio and Blümcke, 1994). Together with a changed calcium homeostasis, this could modulate the inhibitory output from these GABAergic interneurones in mice lacking both TN-R and PV.

**9.6 Acknowledgements:**

We are grateful to Dr. M. Schachner for providing the tenascin-R knockout, Dr. B. Schwaller for providing the parvalbumin knockout mice, and to Dr. R.K. Margolis for the kind gift of antibodies against phosphacan and neurocan. This project was supported by the Desirée and Nils Yde Foundation and by Novartis.

# 10. Distribution and quantification of GABAergic inhibitory cortical interneurones in tenascin-R and parvalbumin single and double knockout mice.

## 10.1 Introduction

Parvalbumin (PV), calbindin-D28K and calretinin are calcium binding proteins which define non-overlapping sub-populations of GABAergic inhibitory interneurones in the cerebral cortex (Celio, 1986; Alcantara et al., 1996; Fujimaru and Kosaka, 1996). The PV-expressing inhibitory interneurones are further characterised by being surrounded by pericellular condensations of extracellular matrix (ECM) components forming a fine meshwork within the local neuropil (for reviews see Celio and Blümcke, 1994; Celio et al., 1998). These entities, termed perineuronal nets of extracellular matrix (PNEMs), together with PV, have been suggested as essential for sustaining the fast-spiking properties observed for these neurones (Hartig et al., 1999). Mice lacking PV have been shown to be more prone to seizures than wild type mice (Tandon et al., 1999). This change occurs although the 'previously PV positive' neurones still exist and can be observed using other markers for this sub-population of neurones (Naegele et al., 1988; Kosaka and Heizmann, 1989; Kosaka et al., 1989; Kosaka et al., 1990; Haunso et al., 2000). Another alteration impinging on this sub-population of cortical interneurones is observed in tenascin-R (TN-R) knockout (KO) mice. Here, morphological changes have been observed in PNEMs surrounding PV-immunoreactive (IR) neurones (Weber et al., 1999; Haunso et al., 2000). As both PV and PNEMs are thought to be critically involved in determining the properties of these neurones, changes herein may influence and modulate the behaviour of these animals. Any alteration in the GABAergic system may lead to change in neuronal inhibition resulting in physiological, morphological and behavioural abnormalities. Here, the distribution and number of GABAergic cortical interneurones in PV and TN-R single KOs and PV/TN-R double KOs is examined and it is shown that the overall inhibitory properties of these neurones remains intact in all animals.

## 10.2 Material and Methods

Mice lacking either PV (Schwaller et al., 1999) or TN-R (Weber et al., 1999) were used and double KO mice deficient for both PV and TN-R were generated by cross-breading PV and TN-R single KOs. The genotypes were determined as previously described (Haunso et al., 2000). In this study, eight adult mice ≈30 g,

comprising two of each genotype – wild type (WT), PV KO, TN-R KO and PV/TN-R KO – of either sex, were used. Animals were sacrificed, brains dissected out and processed for immunohistochemistry as previously described (Haunso et al., 1999). Glutamic acid decarboxylase (GAD), the GABA synthesising enzyme, was visualised as a marker for the whole GABAergic system (Kaufman et al., 1986). Double-immunolabelling was performed by incubating 60 μM cryostat sections with a mouse monoclonal anti-PV antibody (PV235; Swant) diluted 1:500 together with a rabbit polyclonal anti-GAD antibody (Chemicon; 1:250). Incubation with primary antibodies was performed over night at 4° C as floating sections in PBS (0.147 M NaCl, 2.68 mM KCl, 1.76 mM $KH_2PO_4$ and 10.14 mM $Na_2HPO_4$; pH7.4) containing 10% bovine serum. All washes were performed for 3 times 10 min. in PBS and incubations with secondary antibodies for 1 hr at room temp in PBS containing 10% bovine serum. Sections incubated with anti-GAD antibodies were incubated with a biotinylated goat anti-rabbit antibody (Vector; 1:200) followed by Texas Red-conjugated streptavidine (Vector; 1:200). Anti-parvalbumin antibodies were visualised with a fluorescein isothiocyanate-conjugated (FITC; 1:200) anti-mouse antibody (Molecular Probes). Following the incubations, sections were washed, placed on slides and subsequently left to dry at room temp. for 2 hrs. After drying, the sections were re-hydrated in double distilled water, dried for an additional 30 minutes, coversliped in SlowFade (Molecular Probes) and sealed using clear nail varnish. Staining in the sections was analysed and images captured using a Bio-Rad 1024, argon/krypton confocal laser scanning fluorescence microscope (LSCM; Bio-Rad Microsciences Division Ltd.). Both green and blue-lines of laser excitation were used and detected at 522 nm for FITC and 680 nm for Texas Red-labelled structures. Using x10 and x20 objective and real-time zoom features of the confocal program, captured optical sections of 0.5 μm thickness were superimposed and images transferred to Adobe Photoshop™ software where photographic plates were prepared. GAD-immunoreactive (GAD-IR) interneurones were quantified in cerebral cortices of WT, PV KO, TN-R KO and PV/TN-R double KO mice. For each mouse, GAD-IR cell bodies were counted in two or three sections with four fields per section. The quantification was performed in a genotypic-blinded fashion and all immunostained cell bodies were counting throughout the field using a x20 objective. Each field was chosen randomly within the cerebral cortex and the average cell number per field used in statistical evaluations.

## 10.3 Results

GAD-IR cortical interneurones showed a normal pattern of distribution and intensity throughout all the CNS in the investigated animals (data not shown). GAD-IR interneurones and their neuropil were present in all parts of the neocortex and showed normal intensity, density and distribution in all KO animals when compared to wild type mice (Fig. 10.3.1, A-D). The number of GAD-IR cortical interneurones were quantified in all mice genotypes and as can be seen in table 10.3.1 and figure 10.3.2, no significant differences could be observed in either of the different genotypes.

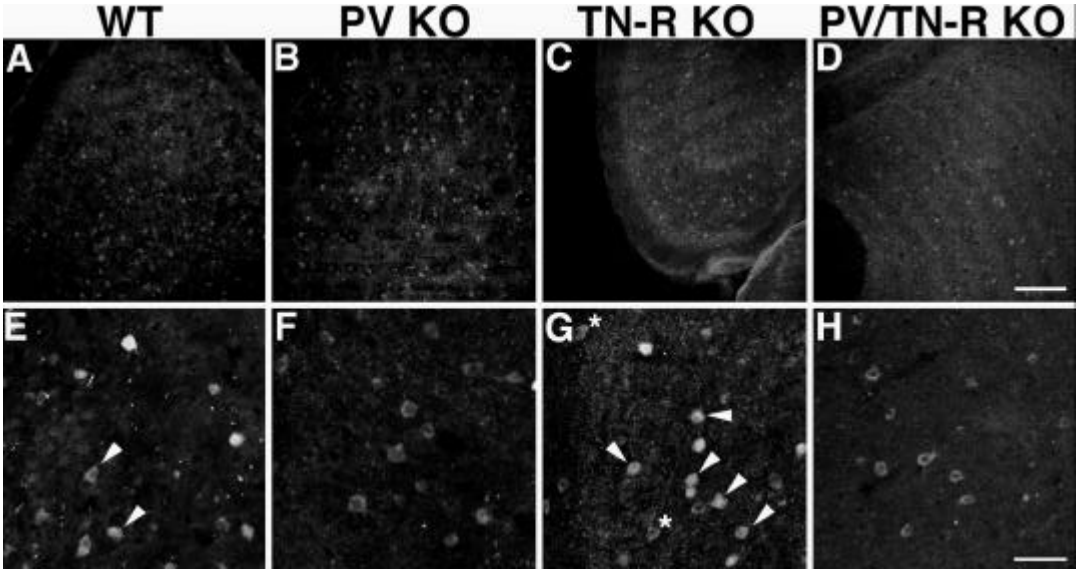


**Figure 10.3.1** Confocal images of glutamic acid decarboxylase (GAD) labelled (A - D) and combined parvalbumin (PV) and GAD labelled (E-H) cortical interneurones in WT (A & E), PV KO (B & F), TN-R KO (C & G) and PV/TN-R double KO (D & H). Distribution and density of GAD labelled interneurones (red) seem unchanged in all mice genotypes (A - D). Co-localisation of GAD-IR and PV-IR is observed in some interneurones (E & G, arrows) whereas PV-IR is not observed in mice lacking PV (F & H). Some interneurones expressed GAD but not PV (E and asterisks in G). In some interneurones, the GAD-IR was so week that it appeared as if the neurones only expressed PV. Scale bar in D = 100 µM (for images A - D). Scale bar in H = 50 µm (for images E - H).

| **Table 10.3.1** GAD-IR | *Av. # GAD-IR cells*[1] | *SD*[2] | *Sections* | *Fields* | *# Mice* |
|---|---|---|---|---|---|
| WT | 111 | 15.64 | 6 | 24 | 2 |
| PV KO | 134 | 25.89 | 6 | 24 | 2 |
| TN-R KO | 95 | 24.37 | 4 | 16 | 2 |
| PV/TN-R KO | 129 | 20.07 | 6 | 24 | 2 |

[1]Av; average, [2]SD; standard deviation

Depending upon the cortical region, a varying degree of interneurones expressing both GAD and PV were observed in the cortex of WT and TN-R single KO animals whereas PV-IR was devoid in mice lacking PV (Fig. 10.3.1 F & H). As expected, a number of GAD-IR interneurones not expressing PV were observed in WT and TN-R KO animals (Fig. 10.3.1 E and asterisks in G), and also some interneurones expressing GAD but not PV (Fig. 10.3.1 E & G).

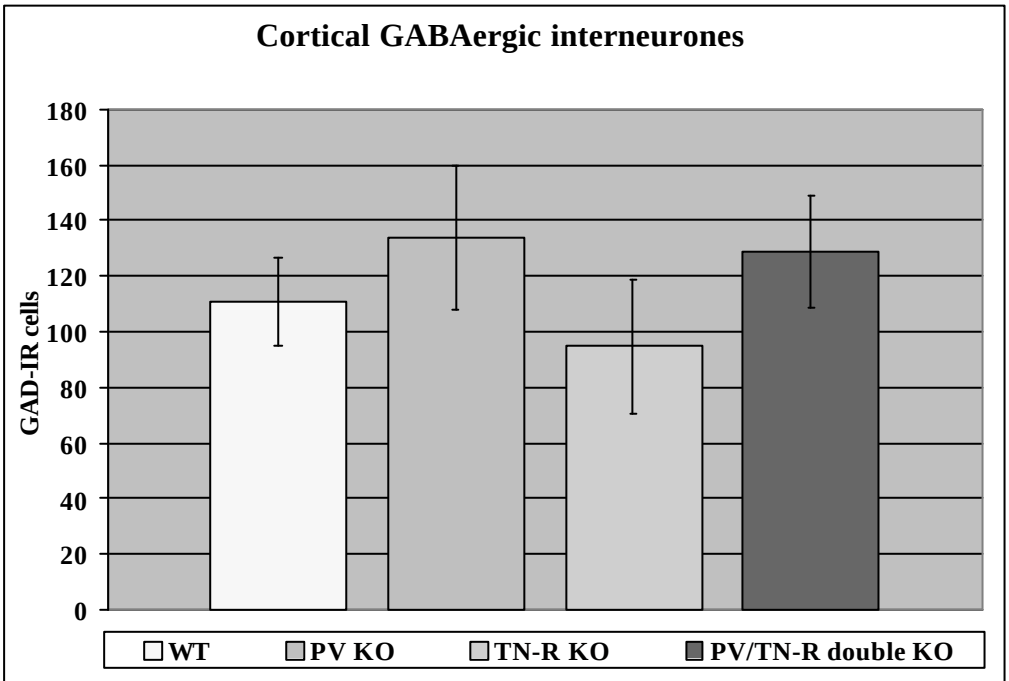


**Figure 10.3.2** Graph showing the average number of GAD-IR cortical interneurones in wild type (WT), parvalbumin (PV) and tenascin-R (TN-R) single knockouts (KO) and parvalbumin/tenascin-R double knockouts (PV/TN-R-KO). Bars = standard deviations.

## 10.4 Discussion

The output from the cerebral cortex, the cerebrofugal projections, arise from cortical pyramidal cells with these projection neurones being tightly controlled by nearby GABAergic interneurones associating with the pyramidal cells (Heimer, 1995). Calcium binding proteins are expressed in separate sub-populations of GABAergic interneurones in the neocortex (Baimbridge et al., 1992), the area of interest in this investigation. One large sub-population of cortical inhibitory interneurones expresses PV (Baimbridge et al., 1992), and are also characterised by having pronounced perineuronal nets of extracellular matrix (PNEMs; for review see Celio and Blümcke, 1994). Recently, an alteration in the release of GABA from the synaptic terminals of cortical interneurones has been observed in mice lacking parvalbumin (Drs M. Vreugdenhil and B. Schwaller, personal communication). These mice are also more susceptible to seizures, and it has been suggested that seizures occur because the lack of PV influences the GABAergic output and thereby induces the changes observed in these animals (Tandon et al., 1999). PNEMs have also been postulated to play an essential role in the functional properties of this sub-population of neurones and that modulations in these entities may influence the inhibitory function of these neurones (Hartig et al., 1999). Here, it is shown that the overall distribution and density of GABAergic cortical interneurones remain unchanged in mice lacking either PV, TN-R or both. Significant differences in the overall intensity of the GAD-IR in the genetically altered mice were also not observed, suggesting that the total amount of GAD enzyme remained unchanged in these neurones. Because the GAD-IR was quite weak in some cortical regions of WT and TN-R KO mice, the impression that some PV expressing interneurones did not express GAD was observed. Overall, no major changes in the cortical inhibitory system were observed in any of the genetically modified mice. Synaptic contacts impinging on cortical interneurones surrounded by PNEMs occur in the holes of the lattice-like net structures (Celio and Blümcke, 1994) and the distribution of these contacts may be altered in TN-R deficient mice as their PNEMs are markedly altered (Haunso et al., 2000). Lack of PV leading to a change in calcium homeostasis in cortical GABAergic interneurones, together with potential alterations in the distribution of synaptic endings on them, may lead to synergistic effects in the double KO animals, resulting in the modulation of the inhibitory output from these GABAergic interneurones.

Analysing such effects and potential behavioural changes in these double KO animals awaits further studies.

# 11. General discussion and summary

In these studies, perineuronal nets of extracellular matrix (PNEMs) found around GABAergic parvalbumin (PV) expressing interneurones have been further characterised in respect to the components comprising these nets and the role of tenascin-R (TN-R) in these entities. Although problems in affinity purification of TN-R fragments and identification and biochemical characterisation of TN-R ligands were encountered, novel findings with respect to PNEMs have been shown using combined immunofluorescence and confocal microscopic techniques. The morphological aspects of this study have given further insight into the possible functional role of TN-R in PNEMs.

## 11.1 Expression of recombinant material in *E. coli*

TN-R is an extracellular matrix molecule expressed exclusively in the central nervous system (Pesheva et al., 1989; Rathjen et al., 1991; Weber et al., 1999). A special feature of TN-R, and some of its known ligands, is their accumulation around certain sub-populations of neurones, forming PNEMs (Matsui et al., 1998; Wintergerst et al., 1996; Hagihara et al., 1999; Haunso et al., 1999). TN-R has been shown *in vitro* to promote neurite outgrowth and morphological polarisation of various neurones (Lochter and Schachner, 1993; Lochter et al., 1994). TN-R is also a repellent for growth cone advance (Pesheva et al., 1993; Taylor et al., 1993), promotes adhesion and differentiation of oligodendrocytes and astrocytes (Pesheva et al., 1989; Morganti et al., 1990; Pesheva et al., 1997) and has also been suggested as a modulator of fasciculation (Xiao et al., 1998). Different recombinant TN-R domains expressed in bacteria have been shown to mediate many of these properties and such domains have also been used to identify specific ligands for TN-R (Aspberg et al., 1997; Xiao et al., 1997).

Bacterial expression of the FG-knob from human tenascin-R led to the formation of inclusion bodies under all tested conditions, concurring similar observations in previous studies (Norenberg et al., 1995; Elefteriou et al., 1999), thereby rendering it insoluble in native buffers. Affinity purification of the FG-knob using hexahistidine tagged fusion proteins was nevertheless possible under denaturing

conditions, but the purified FG-knob remained insoluble in standard native buffers and only slightly soluble in buffers containing chaotropic salts. The general insolubility of the FG-knob probably occurred because this domain needs either additional TN-R domains or carbohydrates to fold correctly. Indeed, all members of the tenascin multi-gene family are glycoproteins (Chiquet-Ehrismann, 1995) and it has recently been shown that carbohydrates comprise 10 - 20% (w/w) of the observed relative molecular size for mouse TN-R (Zamze et al., 1999). Analysis of the amino acid sequence of the FG-knob from human TN-R revealed that it contains many potential sites for N- and O-linked glycosylation, indicating that this domain may be glycosylated in TN-R expressed *in vivo.* Fragments of phosphorylated or differently modified proteins were purified from pig cortex using a TN-R affinity column generated from the slight amounts of obtained soluble FG-knob. These proteins did not contain sites similar to common matrix components such as elastin, collagen type II or IV repeats or hyaluronic acid. Surprisingly, considering the many recent reports of interactions between TN-R and CSPGs (Aspberg et al., 1995, 1997; Xiao et al., 1997; Milev et al., 1998), these affinity purified protein fragments also did not belong to the CSPG family, one of the major BECM families, suggesting that they may be transmembrane proteins or secreted glycoproteins.

### 11.2 Expression of recombinant material in *P. pastoris*

Recombinant TN-R domains expressed in bacteria have frequently been used to determine the overall function, and specific ligands for tenascin-R (Aspberg et al., 1997; Xiao et al., 1996, 1997). The C-terminal domain of TN-R, the FG-knob, is probably expressed in an insoluble form in bacteria (Norenberg et al., 1995; Elefteriou et al., 1999) because other TN-R domains or carbohydrates are needed for the correct folding.

Analysing heterologous expression of the FG-knob in the yeast *P. pastoris* showed that the glycosylation pattern was different in the two strains, KM71 and GS115, since secretion of FG fusion proteins in these strains gave rise to proteins of different sizes. Moreover, the glycosylation pattern also changed during the induction period, in the KM71 strains, resulting in secretion of two differently sized proteins. In addition, it was observed that the majority of expressed protein was not secreted but remained within the yeast cells. Very low amounts of secreted proteins were detected

in conditioned medium from transfected yeast cells, and these quantities were insufficient to be used for the generation of an affinity column.

### 11.3 Expression of recombinant material in Cos-1/M6 cells

Expression of the FG-knob from human TN-R, as a secreted protein, in a mammalian cell line exposes the protein to the machinery in the endoplasmatic reticulum and Golgi apparatus responsible for folding and post-translational modifications (Creighton, 1993). Analysing heterologous expression of the FG-knob in a Simian fibroblast cell line, termed Cos-1/M6, clearly showed two differently glycosylated forms with a size difference of 40 kDa. Although TN-R is a glycoprotein, differences in glycosylation pattern has never been reported for this protein (Persheva et al., 1989; Zamze et al., 1999) and probably occurred here because it was expressed in a cell line quite different from the brain cells normally expressing TN-R (Bartsch et al., 1993; Wintergerst et al., 1993). The FG-knob was expressed as a secreted protein in the Cos-1/M6 cell line. Nonetheless, it was undetectable in conditioned medium because upon secretion homophilic interactions between recombinant GST-FG molecules lead to a pericellular aggregation around the host cells, thereby knitting them together and forming large cell aggregates. As homophilic interactions between FG domains in native TN-R have never been described before in the literature (see also section **7.3**), it may be assumed that the cell aggregations occurred because of a precipitation of non-soluble GST-FG at the surface of the host cells and not because of a biological functional interaction.

### 11.4 Phosphacan, a member of the CSPG family, is a constituent of PNEMs

Perineuronal nets of extracellular matrix (PNEMs) are lattice-like accumulations of brain extracellular matrix (BECM) components around GABAergic interneurones expressing the calcium binding protein parvalbumin (PV). These nets are generally believed to be composed of chondroitin sulphate proteoglycans (CSPGs; Margolis and Margolis, 1993; Ruoslahti, 1996) and glycoproteins (Celio and Blümcke, 1994) and recently, defined constituents belonging to these families have also been identified (Wintergerst et al., 1996; Matsui et al., 1998; Hagihara et al., 1999).

A specific member of the CSPG family, termed phosphacan, preferentially associates with both cortical and non-cortical PNEMs and constitutes one among several CSPGs making up these entities (Haunso et al., 1999). The identification of phosphacan in PNEMs *in vivo* provides functional and biological importance to its previously described interactions with other defined PNEM components *in vitro* (Aspberg et al., 1995, 1997; Xiao et al., 1997). It is noteworthy that the proportion phosphacan constituted of the CSPGs present in PNEMs varied depending upon region and cortical layer (Haunso et al., 1999). Thus, not only are PNEMs heterogeneous in composition (Celio et al., 1998) but the proportion of their components varies depending upon the localisation within the cerebral cortex. Such differences may reflect subdivisions of functionally defined areas and the identification of phosphacan in PNEMs may further help us to understand the role of these entities.

### 11.5 Loss of defined CSPG components in PNEMs of PV and TN-R single and double KO mice

Lecticans, a family of CSPGs forming large aggregates with hyaluronic acid (Aspberg et al., 1997), are the major components of BECM (Ruoslahti, 1996). Defined members identified in the lectican family comprise aggrecan, versican, brevican and neurocan and so far the two latter, together with a non-lectican CSPG, i.e phosphacan, have been identified in PNEMs (Matsui et al., 1998; Hagihara et al., 1999; Haunso et al., 1999). It has been shown *in vitro*, that all lecticans bind the BECM glycoprotein TN-R either through carbohydrate-protein or protein-protein interactions (Aspberg et al., 1995, 1997).

Investigation of PNEMs in parvalbumin (PV) and TN-R single and double knockout (KO) mice revealed that they remained normal in mice lacking PV, whereas TN-R deficient mice showed morphological alterations in these entities (Haunso et al., 2000). Thus, TN-R is essential for the correct formation of PNEMs and when it is absent, CSPGs such as phosphacan and neurocan were no longer present in cortical PNEMs leading to morphological changes in these entities in mice deficient for TN-R. Notable, in areas such as cerebellum, olfactory bulb and spinal cord some pericellular neurocan immunoreactivity (IR) remained in TN-R deficient mice whereas phosphacan-IR had completely disappeared (Haunso et al., 2000). This strongly

indicates that TN-R is essential for the attraction and/or retention of certain CSPGs in cortical PNEMs but that additional factors may also be present elsewhere in the CNS that are able to compensate for the lack of TN-R-mediated attraction of neurocan. PV-expressing cortical interneurones are characterised by the presence of a membrane-related cytoskeleton (MRC) composed, among others, of ankyrin$_R$ and spectrin (Wintergerst et al., 1996). MRCs assemble before the external PNEMs and it has been suggested that they form a prerequisite for the organisation of these nets. MRCs may function in defining the area in which synaptic contacts develop and impinge on these interneurones by keeping in register the overlaying PNEM (Celio and Rathjen, 1993; Wintergerst et al., 1996). As the MRC assembled normally in mice lacking either PV, TN-R or both (Haunso et al., 2000), the MRC is more likely to be involved in determining the position of integral membrane proteins and serve as focal points for the PNEMs rather than merely forming a template for their lattice-like structure.

### 11.6 GAD immunoreactive neurones in PV and TN-R single and double KO mice

Cortical interneurones are critically involved in modulating the corticofugal projections arising from pyramidal cell in the neocortex (Heimer, 1995), with a large sub-population of these cortical interneurones expressing PV (Baimbridge et al., 1992). These interneurones are surrounded by PNEMs (Celio and Blümcke, 1994) and it has been hypothesised that both expression of PV and the presence of PNEMs are crucial for sustaining the fast-spiking properties of these GABAergic interneurones (Celio and Blümcke, 1994; Hartig et al., 1999). Modulations in the properties of these inhibitory interneurones may lead to alterations in their GABAergic output thereby influencing the inhibitory cortical circuit.

Neither the lack of PV nor the alteration in morphology of PNEMs affected the distribution or density of inhibitory cortical interneurones, indicating that the overall inhibitory system remains intact in PV, TN-R and PV/TN-R KO mice. Nonetheless, slight modulations such as alterations in the release of GABA from the synaptic terminals of interneurones and an increased susceptibility to seizures has been observed in mice lacking parvalbumin (Drs M. Vreugdenhil and B. Schwaller, personal communication; Tandon et al., 1999; section **10.4**). Probably, these changes take place because of alterations in the calcium homeostasis and in the distribution of

synaptic terminals impinging upon the cell bodies, and it is perceivable that synergistic effects may occur in mice lacking both PV and TN-R, thereby further modulating the output from the sub-population of cortical inhibitory interneurones in these mice.

## 11.7 Conclusion

Taken together, these results indicate that the principal role for TN-R in relation to the PNEMs may be to attract and/or retain other matrix components. The intimate involvement of TN-R in the formation of the lattice-like structure of PNEMs is probably effectuated via the multimerisation of TN-R molecules leading to the formation of a scaffold onto which other PNEM components can assemble. TN-R is however not envisaged to be involved in determining which population of neurones form perineuronal nets of extracellular matrix, and is it self attracted to these neurones either by other putative matrix molecules or by still unidentified transmembrane receptors. The external PNEM and internal membrane-related cytoskeleton most likely interact via transmembrane proteins but the structures of the internal and external nets are formed independently.

It has been proposed that the intracellular cytoskeleton is involved in determining the position of transmembrane receptors by anchoring them to the actin filaments (Alberts et al., 1994; see also figure 11.7.1). The distribution of transmembrane receptors in the cell membrane is determined by factors such as the overall structure of the cytoskeleton and potential extracellular clues. Cytoskeleton associated proteins (CAPs), comprising among others ankyrin$_R$ and spectrin, are involved in determining the spatial formation of the cytoskeleton and are also mediating the interactions between the actin filament and catenins interacting with the cytosolic part of transmembrane receptors (Alberts et al., 1994). Here, it is proposed that PNEMs assemble, as certain BECM components bind to putative transmembrane proteins, specific for neurones forming PNEMs. Other BCEM components are then drawn to these neurones and are themselves responsible for attracting additional matrix molecules. The role of TN-R in the formation of PNEMs may be to form the corners in the observed lattice-like structures of the PNEMs via its ability to form dimers, trimers or multimers (see figure 11.7.1). Having multimerised, TN-R then attracts proteoglycans such as phosphacan and neurocan to the PNEMs, and these in

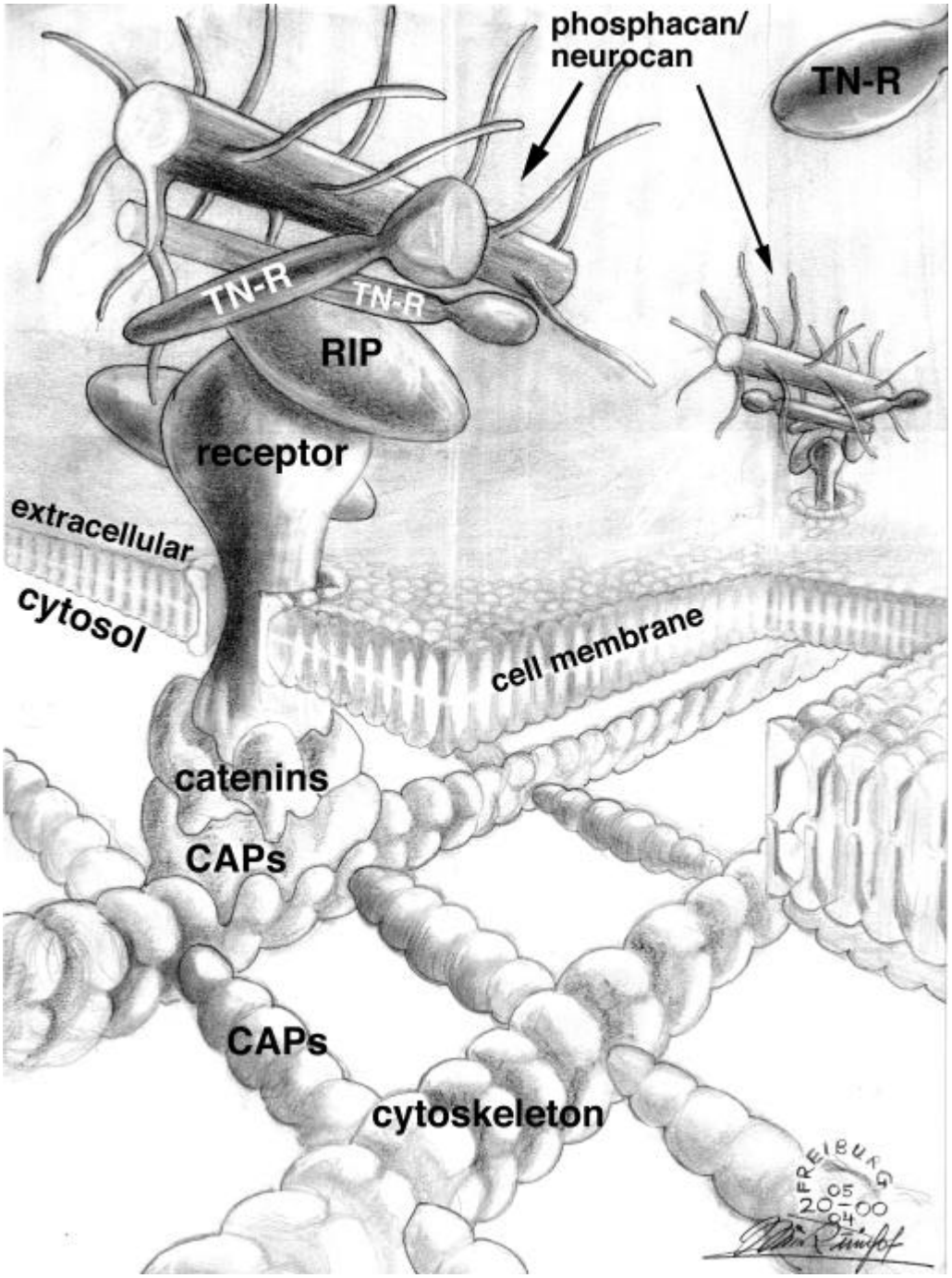


**Figure 11.7.1** Schematic drawing of intra- and extracellular nets and their potential interactions. The drawing has been simplified to only show two receptors and some of the molecules interacting with them. Abbreviations: Cytoskeleton associated proteins (CAPs), receptor interacting protein (RIP) and tenascin-R (TN-R). The general organisation of the cytoskeleton was modified from Alberts et al., 1994 and the hypothesis was kindly put to paper by Dr. Rienk Tuinhof.

turn attract other BECM components, e.g. hyaluronic acid. Many matrix molecules are modular proteins (Chiquet-Ehrismann, 1995; Bork and Koonin, 1996) and it can be envisaged that each PNEM component is involved in the attraction of several other components and that it is the synergistic effects of many constituents that ultimately

determines how strongly each component is bound within the nets. Nonetheless, here it has been shown that TN-R is essential for the attraction and/or retention of phosphacan and neurocan in cortical PNEMs, whereas other components may be able to compensate for the lack of TN-R-mediated attraction of neurocan to non-cortical PNEMs (Haunso et al., 2000). TN-R is most likely not the primary mediator of PNEM assembly, as some immunoreactivity for PNEM components is still observed around certain focal points on the cell membranes in TN-R deficient mice (Weber et al., 1999; Haunso et al., 2000). Probably, the lack of TN-R, and subsequent loss of phosphacan and neurocan, alters the strength with which several other components are attracted to PNEMs, thereby leading to the observed alteration in the overall morphology of these entities (see figure 11.7.1).

# 12. Appendix

**Phosphate-buffered saline solution (PBS)**

*1 x PBS* : 0.147 M NaCl; 2.68 mM KCl; 1.76 mM $KH_2PO_4$; 10.14 mM $Na_2HPO_4$; pH7.4

**Tris-buffered saline solutions (TBS)**

*1 x TBS* : 25 mM Tris-HCl, pH7.4; 0.137 mM NaCl; 2.7 mM KCl

*1 x TBS-T* : 1 x TBS; 0.1% Tween-20

**Tris-boric acid-EDTA buffer (TBE)**

*10 x TBE* : 108 g Trizma base; 53 g boric acid; 9.8 g EDTA; $ddH_2O$ until 1L

**Mini-preparation**

*solution I* : 50 mM Tris-HCl, pH7.5; 10 mM EDTA; 100 µg/mL RNase A

*solution II* : 0.2 M NaOH; 1% SDS

*solution III* : 60 mL 5 M potassium acetate; 12 mL glacial acetic acid; 28 mL $ddH_2O$

**Preparation of chemical competent bacteria**

Solutions

*TB solution* : 10 mM Pipes; 15 mM $CaCl_2$; 250 mM KCl; adjust to pH6.7 with 5 M KOH; add 55 mM MnCl; filter and store at 4°C

Procedure

Streak XL-1 blue bacteria (from a glycerol stock) on a LB plate and place it over night at 37°C. Pick 10 to 12 clones with a sterile tooth pick or an inoculation loop and place in 100 mL LB-medium (without antibiotics). Grow medium at 37°C in an orbital shaking incubator until $OD_{600}$ has reached approximately 0.45. Prior to centrifuging 10 min. at 2500 g, place the medium for 10 min. on ice. Resuspend the

pellet in 40 mL TB solution, incubate for 10 min. on ice and centrifuge at 2,500 g for ten minutes. Resuspend pellet in 10 mL TB containing 7% DMSO[v] (9.7 mL TB and 0.7 mL DMSO) and place on ice for 10 minutes. Gently tap the tube to resuspend the bacteria, make 300 µL aliquots in Eppendorf tubes and place them in liquid $N_2$. Store chemical competent bacteria at -70°C.

**Lennox L Broth base and agar (LB-medium / LB-agar)**

*1 x LB-agar* : 32 g Lennox L agar; dd$H_2O$ until 1 L

*1 x LB-medium* : 20 g LB-broth base; dd$H_2O$ until 1 L

**Dulbecco's Modified Eagle's Medium (DMEM)**

*1 x DMEM, serum-free*: 10 g DMEM w/1000 mg glucose; 3.7 g $NaHCO_3$; 5 mL 100 x glutamine (200 mM); 5 mL 100 x penicillin plus streptomycin (10,000 U; 10,000 µg/mL); pH7.4, dd$H_2O$ until 1 L

*1 x DMEM w/10% FCS*: 100 mL foetal calf serum; 10 g DMEM w/1000 mg glucose; 3.7 g $NaHCO_3$; 5 mL 100 x glutamine (200 mM); 5 mL 100 x penicillin plus streptomycin (10,000 U; 10,000 µg/mL); pH7.4; ddH2O until 1 L

**Solution for propagation of yeast cells**

*10 x YNB* : 134 g yeast nitrogen base w/ ammonium sulphate w/o amino acid; dd$H_2O$ until 1 L

*1 x BMGH* : 690 mL autoclaved dd$H_2O$; 100 mL 1 M potassium phosphate, pH6.0; 100 mL 10 x YNB; 2 mL 0.02% biotin; 100 mL 10% glycerol

*1 x BMMH* : 690 mL autoclaved dd$H_2O$; 100 mL 1 M potassium phosphate, pH6.0; 100 mL 10 x YNB; 2 mL 0.02% biotin; 100 mL 0.5% methanol

*MDH-plates* : 800 mL autoclaved dd$H_2O$; 100 mL 10 x YNB, 2 mL 0.02% biotin; 100 mL dextrose; 15 g agar

[v] Dimethyl sulfoxide

*MHH-plates* : 800 mL autoclaved dd$H_2O$; 100 mL 10 x YNB; 2 mL 0.02%; 100 mL 5% methanol; 15 g agar

*1 x YPAD* : 1% yeast extract; 2% peptone; 2% D-glucose

*YPDS-plates* : 1% yeast extract; 2% peptone; 2% D-glucose; 1 M sorbitol; 2% agar

**Tissue homogenisation buffers**

*hom. buffer A* : 0.4 M NaCl; 10 mM Tris-HCl, pH7.5; 1 mM EDTA; 1 mM EGTA; 0.02% $NaN_3$

*hom. buffer B* : 10 mM Tris-HCl, pH7.5; 2% Triton-X 100; 0.02% $NaN_3$

*hom. buffer C* : 10 mM Tris-HCl, pH7.5; 3 mM $CaCl_2$; 0.02% $NaN_3$

*hom. buffer D* : 1 M NaCl, 10 mM Tris-HCl, pH7.5; 1 mM EDTA; 1 mM EGTA; 0.02% $NaN_3$

*hom. buffer E* : 0.1 M diethanolamin, pH11; 0.1 M NaCl; 1 mM EGTA; 1 mM EGTA

**Buffers for purification of recombinant material**

Native buffers

*GST lysis buffer* : 1 x PBS

*GST washing buffer*: 1 x PBS; 0.1% Triton-X

*GST elution buffer*: 50 mM Tris-HCl, pH8.0; 5 mM reduced glutathione; 100 mM NaCl

*nHis lysis buffer* : 20 mM sodium phosphate, pH7.8; 500 mM NaCl

*nHis washing buffer*: 20 mM sodium phosphate, pH6.0; 500 mM NaCl

*nHis elution buffer*: 20 mM sodium phosphate, pH6.0; 0.2 M imidazole

Denaturing buffers

*dHis lysis buffer* : 8 M urea; 20 mM sodium phosphate, pH7.8; 500 mM NaCl; 5 mM imidazole

*dHis washing buffer*: 6 M urea; 20 mM sodium phosphate, pH6.0; 500 mM NaCl

*dHis elution buffer*: 6 M urea; 20 mM sodium phosphate, pH6.0; 0.2 M imidazole

**Sodium dodecylsulphate polyacrylamide gel electrophoresis gels (SDS-PAGE)**

Small SDS-PAGE gels (for two gels)

| *stacking gel* | **5%** | **3%** |
|---|---|---|
| 30% acrylamide/bis (29:1) | 810 µL | 480 µL |
| 0.5 M Tris-HCl, pH6.8 | 625 µL | 625 µL |
| SDS (10%) | 50 µL | 50 µL |
| APS (10%) | 25 µL | 25 µL |
| TEMED | 10 µL | 10 µL |
| $ddH_2O$ | 3.5 mL | 3.8 mL |
| $V_{TOTAL}$ | 5 mL | 5 mL |

| *separation gel* | **15%** | **12%** | **10%** | **8%** | **6%** | **3%** |
|---|---|---|---|---|---|---|
| 30% acrylamide/Bis (29:1) | 5 mL | 4 mL | 3.33 mL | 2.66 mL | 2 mL | 1 mL |
| 1.5 M Tris-HCl, pH9.2 | 3.75 mL | 3.75 mL | 3.75 mL | 3.75 mL | 3.75 mL | 3.75 mL |
| SDS (10%) | 100 µL | 100 µL | 100 µL | 100 µL | 100 µL | 100 µL |
| APS (10%) | 50 µL | 50 µL | 50 µL | 50 µL | 50 µL | 50 µL |
| TEMED | 20 µL | 20 µL | 20 µL | 20 µL | 20 µL | 20 µL |
| $ddH_2O$ | 1 mL | 2 mL | 2.66 mL | 3.33 mL | 4 mL | 5 mL |
| $V_{TOTAL}$ | 10 mL | 10 mL | 10 mL | 10 mL | 10 mL | 10 mL |

Large SDS-PAGE gels (per gel)

*stacking gel* : 3% gels, made as described above

| *separation gel* | **16%** | **4%** |
|---|---|---|
| 30% acrylamide/Bis (29:1) | 6.9 mL | 1.7 mL |
| 1.5 M Tris-HCl, pH9.2 | 4.7 mL | 4.7 mL |
| SDS (10%) | 126 µL | 126 µL |
| APS (10%) | 33 µL | 33 µL |
| TEMED | 5 µL | 5 µL |
| $ddH_2O$ | 1.2 mL | 6.4 mL |
| $V_{TOTAL}$ | 13 mL | 13 mL |

**Large SDS-PAGE gel for 2D-PAGE (per gel)**

| *separation gel* | **16%** | **4%** |
|---|---|---|
| 30 % acrylamide/PSA[w] (29:1) | 9.9 mL | 2.5 mL |
| 1.5 M Tris-HCl, pH9.2 | 4.6 mL | 4,6 mL |
| SDS (10%) | 200 µL | 200 µL |
| APS (10%) | 55 µL | 55 µL |
| TEMED | 4.6 µL | 4.6 µL |
| $Na_2S_2O_3$ (20 g/L) | 4.6 µL | 4.6 µL |
| $ddH_2O$ / glycerol[x] | 3.9 mL | 11.3 mL |
| $V_{TOTAL}$ | 19 mL | 19 mL |

**SDS-PAGE solutions**

*Coomassie Brilliant Blue R250*: 0.1 g Coomassie blue; 45 mL methanol; 10 mL glacial acetic acid, $ddH_2O$ until 1 L

*destainer* (1L) : 100 mL methanol; 100 mL glacial acetic acid; $ddH_2O$ until 1 L

[w] Piperazine diacrylamide (BioRad)

| | |
|---|---|
| *drying solution* : | 5% glycerol; 10% ethanol |
| *6 x Laemmli loading buffer*: | 7 mL 0.5 M Tris-HCl, pH6.8; 3 mL glycerol; 1 g SDS, few grains of bromphenol blue |
| *running buffer, 1 x*: | 0.025 M Tris-HCl; 0.192 M glycine; 0.01% SDS |
| *Western blotting buffer* : | 800 mL 1 x SDS-PAGE running buffer; 200 mL methanol |

[x] Distilled water for the 4% and 87% glycerol for the 16% acrylamide solution

# 13. Abbreviations

| | |
|---|---|
| **AD** | Alzheimer's disease |
| **APS** | ammonium peroxodisulfate |
| **BMGH** | buffered minimal glycerol medium containing histidine |
| **BMMH** | buffered minimal methanol medium containing histidine |
| **cDNA** | complementary DNA |
| **CHAPS** | 3-[(3-cholamidopropyl)dimethyl-ammonio]-1-propanesulfonate |
| **COS cells** | Simian fibroblasts transformed by SV40 |
| **CJD** | Creutzfeldt-Jacob disease |
| **CNS** | central nervous system |
| **dd$H_2O$** | double distilled water |
| **dHis** | denaturing hexahistidine |
| **DMEM** | Dulbecco's modified Eagle's medium |
| **DMSO** | dimethyl sulfoxide |
| **DNA** | deoxyribonucleic acid |
| **DTE** | 1,4-dithioerythiol |
| **DTT** | 1,4-dithiothreitol |
| **ECL** | enhanced chemiluminescence |
| ***E. coli*** | *Escherichia coli* |
| **EDTA** | ethylenediaminetetraacetic acid |
| **EGF** | epidermal growth factor |
| **EGTA** | Bis[2-aminoethylethene]-N,N,N',N' tetracacetic acid |
| **ER** | endoplasmatic reticulum |
| **FG** | fibrinogen like knob |
| **FITC** | fluorescinisothiocyanate |
| **FN** | fibronectin |
| **GABA** | γ-aminobutyric acid |
| **GAD** | glutamic acid decarboxylase |
| **GalNAc** | N-acetylgalactosamine |
| **GST** | glutathion-S-transferase |
| **h** | hexahistidine |
| **hFG** | hexahistidine fibrinogen like knob |

| | |
|---|---|
| **His buffers** | buffers used for purification of hexahistidine fusion proteins |
| **HIV** | human immunodeficiency virus |
| **hom.** | homogenisation |
| **IPG** | Immobiline DryStrip gels |
| **IPTG** | isopropyl β-D-thiogalactopyranoside |
| **IR** | immunoreactivity |
| **kDA** | kilodalton |
| **KO** | knockout |
| **LB** | Lennox L broth |
| **MDH** | minimal dextrose with histidine |
| **MHH** | minimal methanol with histidine |
| **MRC** | membrane related cytoskeleton |
| **MS** | multiple sclerosis |
| **nHis** | native hexahistidine |
| **NTA** | nickel-nitrotriacetic acid |
| **PAGE** | polyacrylamide gel electrophoresis |
| **PBS** | phosphate-buffered saline solution |
| **PNEM** | perineuronal net of extracellular matrix |
| **PNS** | peripheral nervous system |
| ***P. pastoris*** | *Pichia pastoris* |
| **PV** | parvalbumin |
| ***S. cerevisiae*** | *Saccharomyces cerevisiae* |
| **SDS** | sodium dodecylsulphate |
| **TBS** | Tris-buffered saline solution |
| **TBS-T** | Tris-buffered saline solution containing Triton-X 100 |
| **TCA** | trichloroacetic acid |
| **TEMED** | N,N,N',N' tetramethylethylenediamine |
| **TN-R** | tenascin-R |
| **Tris** | tris[hydroxymethyl]aminomethane hydrochloride |
| **TSE** | transmissible spongiform encephalopathie |

| | |
|---|---|
| **YNB** | yeast nitrogen base |
| **YPD** | yeast extract peptone dextrose |
| **YPDS** | yeast extract peptone dextrose |
| **X-Gal** | 5-bromo-4-chloro-3-indolyl-β-D-galactopyranoside |

# 14. References

**Alberts, B.** Bray, D., Lewis, J., Raff, M., Roberts, K. and Watson J.D (1994) *Cells in Their Social Context* in *Molecular Biology of the Cell*. Garland Publishing INC., New York, pp. 947-1009.

**Alcantara, S.,** de Lecea, L., Del Rio, J.A., Ferrer, I. and Soriano, E. (1996) Transient Colocalization of Parvalbumin and Calbindin D28k in the Postnatal Cerebral Cortex: Evidence for a Phenotypic Shift in Developing Nonpyramidal Neurons. *Eur J Neurosci*, **8**, 1329-39.

**Aspberg, A.,** Binkert, C. and Ruoslahti, E. (1995) The Versican C-Type Lectin Domain Recognizes the Adhesion Protein Tenascin-R. *Proc Natl Acad Sci U S A*, **92**, 10590-4.

**Aspberg, A.,** Miura, R., Bourdoulous, S., Shimonaka, M., Heinegard, D., Schachner, M., Ruoslahti, E. and Yamaguchi, Y. (1997) The C-Type Lectin Domains of Lecticans, a Family of Aggregating Chondroitin Sulfate Proteoglycans, Bind Tenascin-R by Protein-Protein Interactions Independent of Carbohydrate Moiety. *Proc Natl Acad Sci U S A*, **94**, 10116-21.

**Ausubel, F.,** Breat, R., Kingston, R.E., Moore, D.D., Seidman, J.G., Smith, J.A. and Struhl, K. (1995) *Short Protocols in Molecular Biology*. Wiley, pp. 10-38.

**Baimbridge, K.G.,** Celio, M.R. and Rogers, J.H. (1992) Calcium-Binding Proteins in the Nervous System. *Trends Neurosci*, **15**, 303-8.

**Bartsch, S.,** Bartsch, U., Dorries, U., Faissner, A., Weller, A., Ekblom, P. and Schachner, M. (1992) Expression of Tenascin in the Developing and Adult Cerebellar Cortex. *J Neurosci*, 12, 736-49.

**Bartsch, U.,** Pesheva, P., Raff, M. and Schachner, M. (1993) Expression of Janusin (J1-160/180) in the Retina and Optic Nerve of the Developing and Adult Mouse. *Glia*, **9**, 57-69.

**Belichenko, P.V.,** Hagberg, B. and Dahlstrom, A. (1997a) Morphological Study of Neocortical Areas in Rett Syndrome. *Acta Neuropathol (Berl)*, **93**, 50-61.

**Belichenko, P.V.,** Miklossy, J. and Celio, M.R. (1997b) HIV-I Induced Destruction of Neocortical Extracellular Matrix Components in AIDS Victims. *Neurobiol Dis*, **4**, 301-10.

**Belichenko, P.V.,** Miklossy, J., Belser, B., Budka, H. and Celio, M.R. (1999) Early Destruction of the Extracellular Matrix around Parvalbumin-Immunoreactive Interneurons in Creutzfeldt-Jakob Disease. *Neurobiol Dis*, **6**, 269-79.

**Bertolotto, A.,** Rocca, G. and Schiffer, D. (1990) Chondroitin 4-Sulfate Proteoglycan Forms an Extracellular Network in Human and Rat Central Nervous System. *J Neurol Sci*, **100**, 113-23.

**Bignami, A.,** Asher, R. and Perides, G. (1992) Co-Localization of Hyaluronic Acid and Chondroitin Sulfate Proteoglycan in Rat Cerebral Cortex. *Brain Res*, **579**, 173-7.

**Blackshaw, S.E.**, Brett, C.T., Curtis, A.S.G., Dow, J.A.T., Edwards, J.G., Lackie, J.M., Lawrence, A.J. and Moores, G.R. (1995) *The Dictionary of Cell Biology*, Academic Press, London, 124

**Bork, P. and Koonin, E.V.** (1996) Protein Sequence Motifs. *Curr Opin Struct Biol*, **6**, 366-76.

**Brauer, K.,** Werner, L. and Leibnitz, L. (1982) Perineuronal Nets of Glia. *J Hirnforsch*, 23, 701-8.

**Brauer, K.,** Bruckner, G., Leibnitz, L. and Werner, L. (1984) Structural and Cytochemical Features of Perineuronal Glial Nets in the Rat Brain. *Acta Histochem*, **74**, 53-60.

**Brauer, K.,** Hartig, W., Bigl, V. and Bruckner, G. (1993) Distribution of Parvalbumin-Containing Neurons and Lectin-Binding Perineuronal Nets in the Rat Basal Forebrain. *Brain Res*, **631**, 167-70.

**Bristow, J.,** Tee, M.K., Gitelman, S.E., Mellon, S.H. and Miller, W.L. (1993) Tenascin-X: A Novel Extracellular Matrix Protein Encoded by the Human Xb Gene Overlapping P450c21b. *J Cell Biol,* **122**, 265-78.

**Bruckner, G.,** Seeger, G., Brauer, K., Hartig, W., Kacza, J. and Bigl, V. (1994) Cortical Areas Are Revealed by Distribution Patterns of Proteoglycan Components and Parvalbumin in the Mongolian Gerbil and Rat. *Brain Res*, **658**, 67-86.

**Bruckner, G.,** Hausen, D., Hartig, W., Drlicek, M., Arendt, T. and Brauer, K. (1999) Cortical Areas Abundant in Extracellular Matrix Chondroitin Sulphate Proteoglycans Are Less Affected by Cytoskeletal Changes in Alzheimer's Disease. *Neuroscience*, **92**, 791-805.

**Bruckner, G.,** Brauer, K., Hartig, W., Wolff, J.R., Rickmann, M.J., Derouiche, A., Delpech, B., Girard, N., Oertel, W.H. and Reichenbach, A. (1993) Perineuronal Nets Provide a Polyanionic Glia-Associated Form of Microenvironment Around Certain Neurons in Many Parts of the Rat Brain. *Glia*, **8**, 183-200.

**Brummendorf, T.,** Wolff, J.M., Frank, R. and Rathjen, F.G. (1989) Neural Cell Recognition Molecule F11: Homology with Fibronectin Type III and Immunoglobulin Type C Domains. *Neuron*, **2**, 1351-61.

**Brummendorf, T.,** Hubert, M., Treubert, U., Leuschner, R., Tarnok, A. and Rathjen, F.G. (1993) The Axonal Recognition Molecule F11 Is a Multifunctional Protein: Specific Domains Mediate Interactions with Ng-Cam and Restrictin. *Neuron*, **10**, 711-27.

**Burch, G.H.,** Gong, Y., Liu, W., Dettman, R.W., Curry, C.J., Smith, L., Miller, W.L. and Bristow, J. (1997) Tenascin-X Deficiency Is Associated with Ehlers-Danlos Syndrome. *Nat Genet*, **17**, 104-8.

**Carlson, S.S. and Hockfield, S.** (1996) *Central Nervous System* in *Extracellular Matrix: Molecular Components and Interactions*. Harwood Academic Publishers, Amsterdam, Vol. 1, pp. 1-59.

**Carnemolla, B.,** Leprini, A., Borsi, L., Querze, G., Urbini, S. and Zardi, L. (1996) Human Tenascin-R. Complete Primary Structure, Pre-mRNA Alternative Splicing and Gene Localization on Chromosome 1q23-Q24. *J Biol Chem*, **271**, 8157-60.

**Celio, M.R.** (1986) Parvalbumin in Most Gamma-Aminobutyric Acid-Containing Neurons of the Rat Cerebral Cortex. *Science*, **231**, 995-7.

**Celio, M.R.** (1990) Calbindin D-28k and Parvalbumin in the Rat Nervous System. *Neuroscience*, **35**, 375-475.

**Celio, M.R.** (1993) Perineuronal Nets of Extracellular Matrix around Parvalbumin-Containing Neurons of the Hippocampus. *Hippocampus*, **3**, 55-60.

**Celio, M.R. and Chiquet-Ehrismann, R.** (1993) 'Perineuronal Nets' around Cortical Interneurons Expressing Parvalbumin Are Rich in Tenascin. *Neurosci Lett*, **162**, 137-40.

**Celio, M.R. and Rathjen, F.G.** (1993) Restrictin Occurs in 'Perineuronal Nets' of the Adult Brain. *Soc. Neuroscience. Abstr.*, Vol. 19, p. 689.

**Celio, M.R. and Blümcke, I.** (1994) Perineuronal Nets-a Specialized Form of Extracellular Matrix in the Adult Nervous System. *Brain Research Reviews*, **19**, 128-145.

**Celio, M.R.,** Spreafico, R., De Biasi, S. and Vitellaro-Zuccarello, L. (1998) Perineuronal Nets:Past and Present. *TINC*, **21**, 510-515.

**Celio, M.R.** (1999) Evolution of the Concept of 'Extracellular Matrix' in the Brain. *J Hist Neurosci*, **8**, 186-190.

**Celis, J.E.,** Dejgaard, K., Aagaard Jensen, N., Leffers, H., Madsen, P., Rasmussen, H.H., Haunso, A., Oestergaard Jensen, M. and Kristensen, D.B. (1995) FEBS Laboratory Course. *Basic and Specialized Techniques in Cell Biology*. Department of Medical Biochemistry and Danish Centre for Human Genome Research, University of Aarhus, Denmark, Aarhus, pp. 1-45.

**Chiquet-Ehrismann, R.,** Mackie, E.J., Pearson, C.A. and Sakakura, T. (1986) Tenascin: An Extracellular Matrix Protein Involved in Tissue Interactions During Fetal Development and Oncogenesis. *Cell*, **47**, 131-9.

**Chiquet-Ehrismann, R.,** Hagios, C. and Matsumoto, K. (1994) The Tenascin Gene Family. *Perspect Dev Neurobiol*, **2**, 3-7.

**Chiquet-Ehrismann, R.** (1995) Tenascins, a Growing Family of Extracellular Matrix Proteins. *Experientia*, **51**, 853-62.

**Creighton, T.E.** (1993) *Posttranslational Covalent Modifications of Polypeptide Chains* in *Proteins : Structure and Molecular Properties*. W.H. Freeman and Company, New York, pp. 78-100.

**Daniloff, J.K.,** Crossin, K.L., Pincon-Raymond, M., Murawsky, M., Rieger, F. and Edelman, G.M. (1989) Expression of Cytotactin in the Normal and Regenerating Neuromuscular System. *J Cell Biol*, **108**, 625-35.

**Delpech, A.,** Girard, N. and Delpech, B. (1982) Localization of Hyaluronectin in the Nervous System. *Brain Research*, **245**, 251-257.

**Elefteriou, F.,** Exposito, J.Y., Garrone, R. and Lethias, C. (1999) Cell Adhesion to Tenascin-X Mapping of Cell Adhesion Sites and Identification of Integrin Receptors. *Eur J Biochem*, **263**, 840-8.

**Erickson, H.P. and Inglesias, J.L.** (1984) A Six-Armed Oligomer Isolated from Cell Surface Fibronectin Preparations. *Nature*, **311**, 267-9.

**Erickson, H.P. and Bourdon, M.A.** (1989) Tenascin: An Extracellular Matrix Protein Prominent in Specialized Embryonic Tissues and Tumors. *Annu Rev Cell Biol*, **5**, 71-92.

**Erickson, H.P.** (1993) Tenascin-C, Tenascin-R and Tenascin-X: A Family of Talented Proteins in Search of Functions. *Curr Opin Cell Biol*, **5**, 869-76.

**Evan, G.I.,** Lewis, G.K., Ramsay, G. and Bishop, J.M. (1985) Isolation of Monoclonal Antibodies Specific for Human C-Myc Proto-Oncogene Product. *Mol Cell Biol*, **5**, 3610-6.

**Faissner, A. and Kruse, J.** (1990) J1/Tenascin Is a Repulsive Substrate for Central Nervous System Neurons. *Neuron*, **5**, 627-37.

**Fawcett, J.W.,** Fersht, N., Housden, L., Schachner, M. and Pesheva, P. (1992) Axonal Growth on Astrocytes Is Not Inhibited by Oligodendrocytes. *J Cell Sci*, **103**, 571-9.

**Feliciello, I. and Chinali, G.** (1993) A Modified Alkaline Lysis Method for the Preparation of Highly Purified Plasmid DNA from Escherichia Coli. *Anal Biochem*, **212**, 394-401.

**Ffrench-Constant, C. and Raff, M.C.** (1986) The Oligodendrocyte-Type-2 Astrocyte Cell Lineage Is Specialized for Myelination. *Nature*, **323**, 335-8.

**Fujimaru, Y. and Kosaka, T.** (1996) The Distribution of Two Calcium Binding Proteins, Calbindin D-28k and Parvalbumin, in the Entorhinal Cortex of the Adult Mouse. *Neurosci Res*, **24**, 329-43.

**Fuss, B.,** Wintergerst, E.-S., Bartsch, U. and Schachner, M. (1993) Molecular Characterization and in Situ mRNA Localization of Neural Recognition Molecule J1-160/180 a Molecular Structure Similar to Tenascin. *The Journal of Cell Biology*, **120**, 1237-1249.

**Gennarini, G.,** Cibelli, G., Rougon, G., Mattei, M.G. and Goridis, C. (1989) The Mouse Neuronal Cell Surface Protein F3: A Phosphatidylinositol-Anchored Member of the Immunoglobulin Superfamily Related to Chicken Contactin. *J Cell Biol*, **109**, 775-88.

**Gladson, C.L. and Cheresh, D.A.** (1991) Glioblastoma Expression of Vitronectin and the Alpha V Beta 3 Integrin. Adhesion Mechanism for Transformed Glial Cells. *J Clin Invest*, **88**, 1924-32.

**Grumet, M.,** Hoffman, S., Crossin, K.L. and Edelman, G.M. (1985) Cytotactin, an Extracellular Matrix Protein of Neural and Non-Neural Tissues That Mediates Glia-Neuron Interaction. *Proc Natl Acad Sci U S A*, **82**, 8075-9.

**Guan, K.L. and Dixon, J.E.** (1991) Eukaryotic Proteins Expressed in Escherichia Coli: An Improved Thrombin Cleavage and Purification Procedure of Fusion Proteins with Glutathione S-Transferase. *Anal Biochem*, **192**, 262-7.

**Guentchev, M.,** Groschup, M.H., Kordek, R., Liberski, P.P. and Budka, H. (1998) Severe, Early and Selective Loss of a Subpopulation of GABAergic Inhibitory Neurons in Experimental Transmissible Spongiform Encephalopathies. *Brain Pathol*, **8**, 615-23.

**Gulcher, J.R.,** Nies, D.E., Marton, L.S. and Stefansson, K. (1989) An Alternatively Spliced Region of the Human Hexabrachion Contains a Repeat of Potential N-Glycosylation Sites. *Proc Natl Acad Sci U S A*, **86**, 1588-92.

**Gutowski, N.J.,** Newcombe, J. and Cuzner, M.L. (1999) Tenascin-R and C in Multiple Sclerosis Lesions: Relevance to Extracellular Matrix Remodelling. *Neuropathol Appl Neurobiol*, **25**, 207-14.

**Hagihara, K.,** Miura, R., Kosaki, R., Berglund, E., Ranscht, B. and Yamaguchi, Y. (1999) Immunohistochemical Evidence for the Brevican-Tenascin-R Interaction: Colocalization in Perineuronal Nets Suggests a Physiological Role for the Interaction in the Adult Rat Brain. *J Comp Neurol*, **410**, 256-64.

**Hagios, C.,** Koch, M., Spring, J., Chiquet, M. and Chiquet-Ehrismann, R. (1996) Tenascin-Y: A Protein of Novel Domain Structure Is Secreted by Differentiated Fibroblasts of Muscle Connective Tissue. *J Cell Biol*, **134**, 1499-512.

**Hagios, C.,** Brown-Luedi, M. and Chiquet-Ehrismann, R. (1999) Tenascin-Y, a Component of Distinctive Connective Tissues, Supports Muscle Cell Growth. *Exp Cell Res*, **253**, 607-17.

**Hames, B.D. and Rickwood, D.** (1990) *Gel Electrophoresis of Proteins: A Practical Approach*. IRL Press, Oxford University Press.

**Hartig, W.,** Brauer, K. and Bruckner, G. (1992) Wisteria Floribunda Agglutinin-Labelled Nets Surround Parvalbumin-Containing Neurons. *Neuroreport*, **3**, 869-72.

**Hartig, W.,** Brauer, K., Bigl, V. and Bruckner, G. (1994) Chondroitin Sulfate Proteoglycan-Immunoreactivity of Lectin-Labeled Perineuronal Nets around Parvalbumin-Containing Neurons. *Brain Res*, **635**, 307-11.

**Hartig, W.,** Derouiche, A., Welt, K., Brauer, K., Grosche, J., Mader, M., Reichenbach, A. and Bruckner, G. (1999) Cortical Neurons Immunoreactive for the Potassium Channel Kv3.1b Subunit Are Predominantly Surrounded by Perineuronal Nets Presumed as a Buffering System for Cations. *Brain Res*, **842**, 15-29.

**Haunso, A.,** Celio, M.R., Margolis, R.K. and Menoud, P.A. (1999) Phosphacan Immunoreactivity Is Associated with Perineuronal Nets around Parvalbumin-Expressing Neurones. *Brain Research*, **834**, 219-222.

**Haunso, A.,** Ibrahim, M., Bartsch, U., Letiembre, M. and Celio, M.R. (2000) Morphology of Perineuronale Nets in Tenascin-R and Parvalbumin Single and Double Knockout Mice. *Brain Research*, **864**, 142-145.

**Heimer, L.** (1995) *The Cerebral Cortex and Thalamus* in *The Human Brain and Spinal Cord*. Springer-Verlag, pp. 433-454.

**Hockfield, S. and McKay, R.D.** (1983) A Surface Antigen Expressed by a Subset of Neurons in the Vertebrate Central Nervous System. *Proc Natl Acad Sci U S A*, **80**, 5758-61.

**Husmann, K.,** Faissner, A. and Schachner, M. (1992) Tenascin Promotes Cerebellar Granule Cell Migration and Neurite Outgrowth by Different Domains in the Fibronectin Type Iii Repeats. *J Cell Biol*, **116**, 1475-86.

**Inuzuka, T.,** Fujita, N., Sato, S., Baba, H., Nakano, R., Ishiguro, H. and Miyatake, T. (1991) Expression of the Large Myelin-Associated Glycoprotein Isoform During the Development in the Mouse Peripheral Nervous System. *Brain Res*, **562**, 173-5.

**Invitrogen,** (1997a). *Easy-select Pichia Expression Kit, Version B.* Invitogen BV, Leek.

**Invitrogen,** (1997b) *Xpress System Protein Purification: A Manual of Methods for Purification of Polyhistidine-Containing Recombinant Proteins.* pp 1-10, Invitrogen BV, Leek

**Invitrogen,** (1997c). *pSecTag2 A, B, and C product Specifications, Version A. pp 1-17,* Invitogen BV, Leek.

**Isom, L.L.,** Ragsdale, D.S., De Jongh, K.S., Westenbroek, R.E., Reber, B.F., Scheuer, T. and Catterall, W.A. (1995) Structure and Function of the Beta 2 Subunit of Brain Sodium Channels, a Transmembrane Glycoprotein with a CAM Motif. *Cell*, **83**, 433-42.

**Johansson, S.** (1996) *Non-Collagenous Matrix Proteins* in *Extracellular Matrix: Molecular Components and Interactions*. Harwood Academic Publishers, Amsterdam, Vol. 2, pp. 60-94.

**Jones, F.S.,** Burgoon, M.P., Hoffman, S., Crossin, K.L., Cunningham, B.A. and Edelman, G.M. (1988) A cDNA Clone for Cytotactin Contains Sequences Similar to Epidermal Growth Factor-Like Repeats and Segments of Fibronectin and Fibrinogen. *Proc Natl Acad Sci U S A*, **85**, 2186-90.

**Jones, F.S.,** Hoffman, S., Cunningham, B.A. and Edelman, G.M. (1989) A Detailed Structural Model of Cytotactin: Protein Homologies, Alternative RNA Splicing, and Binding Regions. *Proc Natl Acad Sci U S A*, **86**, 1905-9.

**Kaufman, D.L.,** McGinnis, J.F., Krieger, N.R. and Tobin, A.J. (1986) Brain Glutamate Decarboxylase Cloned in Lambda Gt-11: Fusion Protein Produces Gamma-Aminobutyric Acid. *Science*, **232**, 1138-40.

**Kobayashi, K.,** Emson, P.C., Mountjou, C.Q. (1989) Vicia villosa lectin-positive neurones in human cerebral cortex. Loss of Alzheimer-type dementia. *Brain Research*, **498**, 170-174

**Kosaka, T. and Heizmann, C.W.** (1989) Selective Staining of a Population of Parvalbumin-Containing GABAergic Neurons in the Rat Cerebral Cortex by Lectins with Specific Affinity for Terminal N-Acetylgalactosamine. *Brain Res*, **483**, 158-63.

**Kosaka, T.,** Heizmann, C.W. and Barnstable, C.J. (1989) Monoclonal Antibody Vc1.1 Selectively Stains a Population of GABAergic Neurons Containing the Calcium-Binding Protein Parvalbumin in the Rat Cerebral Cortex. *Exp Brain Res*, **78**, 43-50.

**Kosaka, T.,** Heizmann, C.W. and Fujita, S.C. (1992) Monoclonal Antibody 473 Selectively Stains a Population of GABAergic Neurons Containing the Calcium-Binding Protein Parvalbumin in the Rat Cerebral Cortex. *Exp Brain Res*, **89**, 109-14.

**Kosaka, T.,** Isogai, K., Barnstable, C.J. and Heizmann, C.W. (1990) Monoclonal Antibody HNK-1 Selectively Stains a Subpopulation of GABAergic Neurons Containing the Calcium-Binding Protein Parvalbumin in the Rat Cerebral Cortex. *Exp Brain Res*, **82**, 566-74.

**Kruse, J.,** Keilhauer, G., Faissner, A., Timpl, R. and Schachner, M. (1985) The J1 Glycoprotein-a Novel Nervous System Cell Adhesion Molecule of the L2/HNK-1 Family. *Nature*, **316**, 146-8.

**Laemmli, U.K.** (1970) Cleavage of Structural Proteins During the Assembly of the Head of Bacteriophage T4. *Nature*, **227**, 680-5.

**Lafarga, M.,** Berciano, M.T. and Blanco, M. (1984) The Perineuronal Net in the Fastigial Nucleus of the Rat Cerebellum. A Golgi and Quantitative Study. *Anat Embryol*, **170**, 79-85.

**Lambert, S. and Bennett, V.** (1993) Postmitotic Expression of AnkyrinR and Beta R-Spectrin in Discrete Neuronal Populations of the Rat Brain. *J Neurosci*, **13**, 3725-35.

**Lander, C.,** Zhang, H. and Hockfield, S. (1998) Neurons Produce a Neuronal Cell Surface-Associated Chondroitin Sulfate Proteoglycan. *J Neurosci*, **18**, 174-83.

**Lawrence, E.** (1995) *Henderson's Dictionary of Biological Terms.* Longman Group Limited, Essex, 1-693

**Lochter, A.,** Vaughan, L., Kaplony, A., Prochiantz, A., Schachner, M. and Faissner, A. (1991) J1/Tenascin in Substrate-Bound and Soluble Form Displays Contrary Effects on Neurite Outgrowth. *J Cell Biol*, **113**, 1159-71.

**Lenga R.E**. (1985) The Sigma-Aldrich Library of Chemical Safety Data, *Sigma-Aldrich*. 1.ed

**Lochter, A. and Schachner, M.** (1993) Tenascin and Extracellular Matrix Glycoproteins: From Promotion to Polarization of Neurite Growth in Vitro. *J Neurosci*, **13**, 3986-4000.

**Lochter, A.,** Taylor, J., Fuss, B. and Schachner, M. (1994) The Extracellular Matrix Molecule Janusin Regulates Neuronal Morphology in a Substrate-and Culture Time-Dependent Manner. *Eur J Neurosci*, **6**, 597-606.

**Lodish, H.,** Baltimore, D., Berk, A., Lawrence Zipursky, S., Matsudaira, P. and Darnell, J. (1995) *Multicellularity: Cell-Cell and Cell-Martix Interactions* in *Molecular Cell Biology*. W.H. Freeman and Company, New York, pp. 1123-1200.

**Maeda, N.,** Hamanaka, H., Oohira, A. and Noda, M. (1995) Purification, Characterization and Developmental Expression of a Brain-Specific Chondroitin Sulfate Proteoglycan, 6b4 Proteoglycan/Phosphacan. *Neuroscience*, **67**, 23-35.

**Maleski, M. and Hockfield, S.** (1997) Glial Cells Assemble Hyaluronan-Based Pericellular Matrices in Vitro. *Glia*, **20**, 193-202.

**Margolis, R.K. and Margolis, R.U.** (1993) Nervous Tissue Proteoglycans. *Experientia*, **49**, 429-46.

**Margolis, R.U. and Margolis, R.K.** (1997) Chondroitin Sulfate Proteoglycans as Mediators of Axon Growth and Pathfinding. *Cell Tissue Res*, **290**, 343-8.

**Martini, R.,** Schachner, M. and Faissner, A. (1990) Enhanced Expression of the Extracellular Matrix Molecule J1/Tenascin in the Regenerating Adult Mouse Sciatic Nerve. *J Neurocytol*, **19**, 601-16.

**Matsui, F.,** Nishizuka, M., Yasuda, Y., Aono, S., Watanabe, E. and Oohira, A. (1998) Occurrence of a N-Terminal Proteolytic Fragment of Neurocan, Not a C-Terminal Half, in a Perineuronal Net in the Adult Rat Cerebrum. *Brain Res*, **790**, 45-51.

**Matsumoto, K.,** Ishihara, N., Ando, A., Inoko, H. and Ikemura, T. (1992) Extracellular Matrix Protein Tenascin-Like Gene Found in Human MHC Class III Region. *Immunogenetics*, **36**, 400-3.

**Meyer-Puttlitz, B.,** Junker, E., Margolis, R.U. and Margolis, R.K. (1996) Chondroitin Sulfate Proteoglycans in the Developing Central Nervous System. II. Immunocytochemical Localization of Neurocan and Phosphacan. *J Comp Neurol*, **366**, 44-54.

**Milev, P.,** Friedlander, D.R., Sakurai, T., Karthikeyan, L., Flad, M., Margolis, R.K., Grumet, M. and Margolis, R.U. (1994) Interactions of the Chondroitin Sulfate Proteoglycan Phosphacan, the Extracellular Domain of a Receptor-Type Protein Tyrosine Phosphatase, with Neurons, Glia, and Neural Cell Adhesion Molecules. *J Cell Biol*, **127**, 1703-15.

**Milev, P.,** Maurel, P., Haring, M., Margolis, R.K. and Margolis, R.U. (1996) Tag-1/Axonin-1 Is a High-Affinity Ligand of Neurocan, Phosphacan/Protein-Tyrosine Phosphatase-Zeta/Beta, and N-Cam. *J Biol Chem*, **271**, 15716-23.

**Milev, P.,** Fischer, D., Haring, M., Schulthess, T., Margolis, R.K., Chiquet-Ehrismann, R. and Margolis, R.U. (1997) The Fibrinogen-Like Globe of Tenascin-C Mediates Its Interactions with Neurocan and Phosphacan/Protein-Tyrosine Phosphatase-Zeta/Beta. *J Biol Chem*, **272**, 15501-9.

**Milev, P.,** Chiba, A., Haring, M., Rauvala, H., Schachner, M., Ranscht, B., Margolis, R.K. and Margolis, R.U. (1998) High Affinity Binding and Overlapping Localization of Neurocan and Phosphacan/Protein-Tyrosine Phosphatase-Zeta/Beta with Tenascin-R, Amphoterin, and the Heparin-Binding Growth-Associated Molecule. *J Biol Chem*, **273**, 6998-7005.

**Morganti,** M.C., Taylor, J., Pesheva, P. and Schachner, M. (1990) Oligodendrocyte-Derived J1-160/180 Extracellular Matrix Glycoproteins Are Adhesive or Repulsive Depending on the Partner Cell Type and Time of Interaction. *Exp Neurol*, **109**, 98-110.

**Murakami, T.,** Su, W.D., Ohtsuka, A., Abe, K. and Ninomiya, Y. (1999) Perineuronal Nets of Proteoglycans in the Adult Mouse Brain Are Digested by Collagenase. *Arch Histol Cytol*, **62**, 199-204.

**Naegele, J.R.,** Arimatsu, Y., Schwartz, P. and Barnstable, C.J. (1988) Selective Staining of a Subset of GABAergic Neurons in Cat Visual Cortex by Monoclonal Antibody Vc1.1. *J Neurosci*, **8**, 79-89.

**Naegele, J.R. and Barnstable, C.J.** (1989) Molecular Determinants of GABAergic Local-Circuit Neurons in the Visual Cortex. *Trends Neurosci*, **12**, 28-34.

**Norenberg, U.,** Wille, H., Wolff, J.M., Frank, R. and Rathjen, F.G. (1992) The Chicken Neural Extracellular Matrix Molecule Restrictin: Similarity with EGF-, Fibronectin Type III-, and Fibrinogen-Like Motifs. *Neuron*, **8**, 849-63.

**Norenberg, U.,** Hubert, M., Brummendorf, T., Tarnok, A. and Rathjen, F.G. (1995) Characterization of Functional Domains of the Tenascin-R (Restrictin) Polypeptide: Cell Attachment Site, Binding with F11, and Enhancement of F11-Mediated Neurite Outgrowth by Tenascin-R. *J Cell Biol*, **130**, 473-84.

**Okamoto, M.,** Mori, S., Ichimura, M. and Endo, H. (1994) Chondroitin Sulfate Proteoglycans Protect Cultured Rat's Cortical and Hippocampal Neurons from Delayed Cell Death Induced by Excitatory Amino Acids. *Neurosci Lett*, **172**, 51-4.

**Pesheva, P.,** Spiess, E. and Schachner, M. (1989) J1-160 and J1-180 Are Oligodendrocyte-Secreted Nonpermissive Substrates for Cell Adhesion. *J Cell Biol,* **109**, 1765-78.

**Pesheva, P.,** Gennarini, G., Goridis, C. and Schachner, M. (1993) The F3/11 Cell Adhesion Molecule Mediates the Repulsion of Neurons by the Extracellular Matrix Glycoprotein J1-160/180. *Neuron*, **10**, 69-82.

**Pesheva, P.,** Gloor, S., Schachner, M. and Probstmeier, R. (1997) Tenascin-R Is an Intrinsic Autocrine Factor for Oligodendrocyte Differentiation and Promotes Cell Adhesion by a Sulfatide-Mediated Mechanism [Published Erratum Appears in J Neurosci 1997 Aug 1;17(15):6021]. *J Neurosci*, **17**, 4642-51.

**Pharmacia**. (1993) *Affinity Chromatography: Principles and Methods*. Pharmacia LKB Biotechnology.

**Pharmacia** (1994) *Isoelectric Focusing: Principles and Methods.* Pharmacia LKB Biotechnology

**Pierce**. (1998) *Supersignal: Western Blotting Substrates Handbook*. Pierce Chemical Company.

**Poltorak, M.,** Sadoul, R., Keilhauer, G., Landa, C., Fahrig, T. and Schachner, M. (1987) Myelin-Associated Glycoprotein, a Member of the L2/HNK-1 Family of Neural Cell Adhesion Molecules, Is Involved in Neuron-Oligodendrocyte and Oligodendrocyte-Oligodendrocyte Interaction. *J Cell Biol*, **105**, 1893-9.

**Prieto, A.L.,** Jones, F.S., Cunningham, B.A., Crossin, K.L. and Edelman, G.M. (1990) Localization During Development of Alternatively Spliced Forms of Cytotactin mRNA by in Situ Hybridization. *J Cell Biol*, **111**, 685-98.

**Prieto, A.L.,** Andersson-Fisone, C. and Crossin, K.L. (1992) Characterization of Multiple Adhesive and Counteradhesive Domains in the Extracellular Matrix Protein Cytotactin. *J Cell Biol*, **119**, 663-78.

**Rathjen, F.G.,** Wolff, J.M. and Chiquet-Ehrismann, R. (1991) Restrictin: A Chick Neural Extracellular Matrix Protein Involved in Cell Attachment Co-Purifies with the Cell Recognition Molecule F11. *Development*, **113**, 151-64.

**Rauch, U.,** Gao, P., Janetzko, A., Flaccus, A., Hilgenberg, L., Tekotte, H., Margolis, R.K. and Margolis, R.U. (1991) Isolation and Characterization of Developmentally Regulated Chondroitin Sulfate and Chondroitin/Keratan Sulfate Proteoglycans of Brain Identified with Monoclonal Antibodies. *J Biol Chem*, **266**, 14785-801.

**Revest, J.M.,** Faivre-Sarrailh, C., Schachner, M. and Rougon, G. (1999) Bidirectional Signaling between Neurons and Glial Cells Via the F3 Neuronal Adhesion Molecule. *Adv Exp Med Biol*, **468**, 309-18.

**Rucklidge, G.J.,** Dean, V., Robins, S.P., Mella, O. and Bjerkvig, R. (1989) Immunolocalization of Extracellular Matrix Proteins During Brain Tumor Invasion in Bd Ix Rats. *Cancer Res*, **49**, 5419-23.

**Ruoslahti, E. and Giancotti, F.G.** (1989) Integrins and Tumor Cell Dissemination. *Cancer Cells*, **1**, 119-26.

**Ruoslahti, E. and Yamaguchi, Y.** (1991) Proteoglycans as Modulators of Growth Factor Activities. *Cell*, **64**, 867-9.

**Rutka, J.T.,** Apodaca, G., Stern, R. and Rosenblum, M. (1988) The Extracellular Matrix of the Central and Peripheral Nervous Systems: Structure and Function. *J Neurosurg*, **69**, 155-70.

**Ruoslahti, E.** (1996) Brain Extracellular Matrix. *Glycobiology*, **6**, 489-92.

**Saga, Y.,** Tsukamoto, T., Jing, N., Kusakabe, M. and Sakakura, T. (1991) Murine Tenascin: cDNA Cloning, Structure and Temporal Expression of Isoforms. *Gene*, **104**, 177-85.

**Saga, Y.,** Yagi, T., Ikawa, Y., Sakakura, T. and Aizawa, S. (1992) Mice Develop Normally without Tenascin. *Genes Dev*, **6**, 1821-31.

**Saiki, R.K.,** Gelfand, D.H., Stoffel, S., Scharf, S.J., Higuchi, R., Horn, G.T., Mullis, K.B. and Erlich, H.A. (1988) Primer-Directed Enzymatic Amplification of DNA with a Thermostable DNA Polymerase. *Science*, **239**, 487-91.

**Schachner, M.** (1994) Neural Recognition Molecules in Disease and Regeneration. *Curr Opin Neurobiol*, **4**, 726-34.

**Schachner, M.,** Taylor, J., Bartsch, U. and Pesheva, P. (1994) The Perplexing Multifunctionality of Janusin, a Tenascin-Related Molecule. *Perspect Dev Neurobiol*, **2**, 33-41.

**Schachner, M. and Bartsch, U.** (2000) Multiple Functions of the Myelin-Associated Glycoprotein MAG (Siglec-4a) in Formation and Maintenance of Myelin. *Glia*, **29**, 154-65.

**Schumacher, S.,** Volkmer, H., Buck, F., Otto, A., Tarnok, A., Roth, S. and Rathjen, F.G. (1997) Chicken Acidic Leucine-Rich EGF-Like Domain Containing Brain Protein (CALEB), a Neural Member of the EGF Family of Differentiation Factors, Is Implicated in Neurite Formation. *J Cell Biol*, **136**, 895-906.

**Schwaller, B.,** Dick, J., Dhoot, G., Carroll, S., Vrbova, G., Nicotera, P., Pette, D., Wyss, A., Bluethmann, H., Hunziker, W. and Celio, M.R. (1999) Prolonged Contraction-Relaxation Cycle of Fast-Twitch Muscles in Parvalbumin Knockout Mice. *Am J Physiol*, **276**, C395-403.

**Schweizer, M.,** Streit, W.J. and Muller, C.M. (1993) Postnatal Development and Localization of an N-Acetylgalactosamine Containing Glycoconjugate Associated with Nonpyramidal Neurons in Cat Visual Cortex. *J Comp Neurol*, **329**, 313-27.

**Scopes, R.K.** (1994) *Protein Purification: Principles and Practice*. Springer-Verlag.

**Spring, J.,** Beck, K. and Chiquet-Ehrismann, R. (1989) Two Contrary Functions of Tenascin: Dissection of the Active Sites by Recombinant Tenascin Fragments. *Cell*, **59**, 325-34.

**Srinivasan, J.,** Schachner, M. and Catterall, W.A. (1998) Interaction of Voltage-Gated Sodium Channels with the Extracellular Matrix Molecules Tenascin-C and Tenascin-R. *Proc Natl Acad Sci U S A*, **95**, 15753-7.

**Tandon, P.,** Villa, A., Tetko, I.V., Silveira, D.C., Celio, M.R. and Schwaller, B. (1999) Impairment of the Inhibitory System in Parvalbumin-Knockout Mice Increases Susceptibility Towards Epileptic Seizures. *Soc. Neuroscience. Abstr*,, Miami, Florida.

**Taylor, J.,** Pesheva, P. and Schachner, M. (1993) Influence of Janusin and Tenascin on Growth Cone Behavior in Vitro. *J Neurosci Res*, **35**, 347-62.

**Tucker, R.P.,** Hagios, C. and Chiquet-Ehrismann, R. (1999) Tenascin-Y in the Developing and Adult Avian Nervous System. *Dev Neurosci*, **21**, 126-33.

**Weber, P.,** Montag, D., Schachner, M. and Bernhardt, R.R. (1998) Zebrafish Tenascin-W, a New Member of the Tenascin Family. *J Neurobiol,* **35**, 1-16.

**Weber, P.,** Bartsch, U., Rasband, M.N., Czaniera, R., Lang, Y., Bluethmann, H., Margolis, R.U., Levinson, S.R., Shrager, P., Montag, D. and Schachner, M. (1999) Mice Deficient for Tenascin-R Display Alterations of the Extracellular Matrix and Decreased Axonal Conduction Velocities in the CNS. *J Neurosci*, **19**, 4245-62.

**Wintergerst, E.S.,** Fuss, B. and Bartsch, U. (1993) Localization of Janusin mRNA in the Central Nervous System of the Developing and Adult Mouse. *Eur J Neurosci,* **5**, 299-310.

**Wintergerst, E.S.,** Vogt Weisenhorn, D.M., Rathjen, F.G., Riederer, B.M., Lambert, S. and Celio, M.R. (1996) Temporal and Spatial Appearance of the Membrane Cytoskeleton and Perineuronal Nets in the Rat Neocortex. *Neurosci Lett*, **209**, 173-6.

**Xiao, Z.C.,** Taylor, J., Montag, D., Rougon, G. and Schachner, M. (1996) Distinct Effects of Recombinant Tenascin-R Domains in Neuronal Cell Functions and Identification of the Domain Interacting with the Neuronal Recognition Molecule F3/11. *Eur J Neurosci*, **8**, 766-82.

**Xiao, Z.C.,** Bartsch, U., Margolis, R.K., Rougon, G., Montag, D. and Schachner, M. (1997) Isolation of a Tenascin-R Binding Protein from Mouse Brain Membranes. A Phosphacan-Related Chondroitin Sulfate Proteoglycan. *J Biol Chem*, **272**, 32092-101.

**Xiao, Z.C.,** Revest, J.M., Laeng, P., Rougon, G., Schachner, M. and Montag, D. (1998) Defasciculation of Neurites Is Mediated by Tenascin-R and Its Neuronal Receptor F3/11. *J Neurosci Res*, **52**, 390-404.

**Xiao, Z.C.,** Ragsdale, D.S., Malhotra, J.D., Mattei, L.N., Braun, P.E., Schachner, M. and Isom, L.L. (1999) Tenascin-R Is a Functional Modulator of Sodium Channel Beta Subunits. *J Biol Chem*, **274**, 26511-7.

**Yang, H.,** Xiao, Z.C., Becker, B., Hillenbrand, R., Rougon, G. and Schachner, M. (1999) Role for Myelin-Associated Glycoprotein as a Functional Tenascin-R Receptor. *J Neurosci Res*, **55**, 687-701.

**Yamagata, T.,** Saito, H., Habachi, O. and Suzuki, S. (1968) Purification and properties of bacterial chondroitinases and chondrosylfatases. *J Biol Chem*, **243(7)**, 1523-1535.

**Zamze, S.,** Harvey, D.J., Pesheva, P., Mattu, T.S., Schachner, M., Dwek, R.A. and Wing, D.R. (1999) Glycosylation of a CNS-Specific Extracellular Matrix Glycoprotein, Tenascin-R, is Dominated by O-Linked Sialylated Glycans and "Brain-Type" Neutral N-Glycans. *Glycobiology*, **9**, 823-31.

**Zaremba, S.,** Naegele, J.R., Barnstable, C.J. and Hockfield, S. (1990) Neuronal Subsets Express Multiple High-Molecular-Weight Cell-Surface Glycoconjugates Defined by Monoclonal Antibodies Cat-301 and Vc1.1. *J Neurosci*, **10**, 2985-95.

# 15. Acknowledgements

First, I would like to thank all the people at the Institute for Histology and General Embryology for helping me overcome whatever problems I encountered during the years at this institute.

I am especially grateful to Marco R. Celio (professor and director of the institute) for giving me the opportunity to work in Switzerland and to my thesis supervisor Dr. Pierre-Alain Menoud for valuable help and discussions during the time I worked in his group and for translating the summary in this thesis into French. I would also like to thank my fellow PhD student Maryse Letiembre for sharing my 'ups and downs' for more than three years.

I am also indebted to Drs Tuinhof, Ibrahim and Racay for their helpful comments on and their encouragement during the preparation of this PhD thesis.

A special thank should go to Dr. M, without whom my stay in Switzerland would not have been the same, and to the Friday beer club / lotto syndicate and its members (Merdol, Peter, Rienk and Roland) for all the good times we spent together and for listening to all my problems. You really made the stay in Switzerland an experience !

Last but not least, I would like to thank all the players at BC Fribourg for their kindness towards me and for making my stay in Switzerland a pleasant one.

Anders Haunsø
26.04.2000

# 16. Curriculum Vitae

## Anders Kristian Haunsø

**Date of birth:** 7th March, 1972
**Nationality:** Danish
**Sex:** Male
**Marital status:** Single
**Languages:** Danish, English and some proficiency in German and French
**E-mail:** Anders.Haunsoe@unifr.ch

**Present position and project:**

**February 1997 – August 2000**: PhD student at Institute of Histology and General Embryology and Program in Neuroscience, Faculty of Sciences, University of Fribourg, CH-1705 Fribourg, Switzerland (supervised by: Ass. Prof. Pierre-Alain Menoud)
February 1997 – July 2000, enrolled in the "BENEFRI PhD Programme in Neuroscience" (Bern - Neuchâtel - Fribourg).
**Home pages:** http://www.unifr.ch/histologie/homepage/welcome.html
http://www.unibe.ch/benefri/
**Project:** Biochemical and immunohistochemical characterisation of the role of tenascin-R in perineuronal nets of extracellular matrix around cortical interneurones

**Previous position:**

**September 1995 – January 1997**: MSc student at Department of Medical Biochemistry and Danish Centre for Human Genome Research, Faculty of Health Sciences, University of Aarhus, Build. 170, Ole Worms Allé. DK-8000 Aarhus C, Denmark (supervised by Profs. Julio E. Celis and Brian F. Clark)
**Home pages**: http://www.au.dk/en/sun/medbiokm/index.html
http://biobase.dk/cgi-bin/celis
**Projects:** Identification of – and generation of monoclonal antibodies against – biomarkers of urinary bladder cancer progression

**September 1994 – August 1995**: BSc student at Department of Medical Biochemistry and Danish Centre for Human Genome Research, Faculty of Health Sciences, University of Aarhus, Denmark (supervised by Prof. Julio E. Celis).

**Research interests:**

Brain extracellular matrix
Receptor biology
Neuropharmacology
Signal transduction
Cortical GABAergic interneurones

**Memberships:**

The Danish Society for Molecular Biology and Biochemistry.
Société Suisse de Biologie Cellulaire Moléculaire et Génétique

**Techniques:**

Recombinant DNA technology & molecular biology:

PCR, cDNA cloning, DNA & RNA purification, DNA sequencing, non-radioactive *in situ* hybrizidation, Northern blotting, transformation of bacteria, transfection of yeast and mammalian cells, prokaryotic, yeast (*P. pastoris*) and mammalian protein expression systems, construction and screening of plasmid cDNA libraries.

Biochemistry & protein chemistry:

SDS-PAGE & 2D-PAGE, Western / immunoblotting, immuno-precipitation, ELISA, recombinant protein purification, protein purification from crude extracts, 1st dimension IPG Immobiline DryStrips.

Cell biology:

Generation of monoclonal antibodies, general procedures for cell & tissue culture, preparation of primary cell cultures, generation of transient and stable transfected cell lines.

Immunohistochemistry:

Combining single, double and triple antibody labelling, fluorescence microscopy, confocal microscopy (MRC 1024), cryostat & vibratome sectioning.

**Courses and exams under the 'BENEFRI PhD programme in Neuroscience':**

BENEFRI postgraduate course in Neuroscience, spring 2000 *"The Hypothalamus : Integrated behavioral, Autonomic, and Endocrine control"*: University of Fribourg, Switzerland. **Organiser**: Profs. C.B. Saper and M.R. Celio

BENEFRI postgraduate exam in neuroanatomy, neurohistology & neuroembryology, January 2000. **Examiners**: Profs. J.-M. Burgunder and M.R. Celio

BENEFRI postgraduate course in Neuroscience, spring 1999 *"Motor Control: Physiology, Molecular Biology and Clinics"*: University of Bern, Switzerland. **Organiser**: Assoc. prof. L. Streit.

BENEFRI postgraduate exam in neurophysiology & neurobiochemstry, March 1998. **Examiners**: Prof. E. Rouiller and assoc. prof. L. Streit.

BENEFRI postgraduate course in Neuroscience, spring 1998 *"Motor Cortical Areas"*: University of Fribourg, Switzerland. **Organiser**: Prof. E. Rouiller.

BENEFRI postgraduate course in Neuroscience, spring 1997 *"Memory and Memory Disorders"*: University of Bern, Switzerland; **Organiser**: Prof. J.-M. Burgunder.

**Other postgraduate courses:**

Academic Writing for Graduate Students, autumn 1997 - spring 1998 *"A course for Nonnative Speakers of English*": English Language Institute, University of Fribourg, Switzerland. **Organisor**: Ass. Prof. Anthony L. Clark.

3e Cycle Roman en Sciences Biologiques, June 1997 *"Practical course in Rapid Purification of Proteins"*. Laboratory for Vegetable Biochemistry, University of Neuchâtel, Switzerland. **Organiser**: Prof. P. Schürmann.

**Educational background:**

**PhD in Neuroscience**, 24th of July 2000: Institute of Histology and General Embryology and Program in Neuroscience, Faculty of Sciences, University of Fribourg, Switzerland; **Examiners**: PD Dr. sc. nat. ETH M. Chiquet, Dr. Z.-C. Xiao and Prof. M.R. Celio.
Title of PhD thesis: *"Tenascin-R and perineuronal nets of extracellular matrix"*

**Cand. Scient. (MSc) in chemistry and biotechnology**, 30st of January 1997: Department of Biostructural Chemistry, Institute of Chemistry, Faculty of Science, University of Aarhus, Denmark; **Examiners**: Profs. J. Zeuthen, J.E. Celis and B.F. Clark.
Title of MSc thesis: *"Preparation and Characterisation of a Monoclonal Antibody against a Biomarker in Bladder Cancer"*

**BSc in chemistry and biotechnology**, September 1991 – August 1995: Department of Biostructural Chemistry, Institute of Chemistry, Faculty of Science, University of Aarhus, Denmark.
Title of MSc work: *"Preparation and Characterisation of a Monoclonal Antibody against BIP/GRP78"*

**Other qualifications (Gymnasium, Denmark)**

**A Levels:** Chemistry, physics, mathematics

**Teaching experiences:**

Instructor and co-examiner in histology for first and second year medical students, 1997 - present: Institute of Histology and General Embryology, Faculty of Sciences, University of Fribourg, Switzerland; **Head**: Prof. M.R. Celio.

Instructor in biochemistry for dental students, 1995 & 1996: School of Dentistry, Faculty of Health Sciences, University of Aarhus, Denmark; **Head**: Assoc. prof. U. Kragh-Hansen.

Instructor at the FEBS Laboratory Course, 1995 & 1996:*"Basic and Specialized Techniques in Cell Biology*": Institute of Medical Biochemistry and Danish Centre for Human Genome Research, Faculty of Health Sciences, University of Aarhus, Denmark; **Organiser**: Prof. J.E. Celis.

**Bibliography:**

Publications:

**Haunsø A.**, Ibrahim M., Bartsch U., Letiembre M., Celio M.R., Menoud P.-A. "*Morphology of perineuronal nets in tenascin-r and parvalbumin single and double knockout mice*" **Brain Research, 2000, 864 (1)**: 142-145.

**Haunsø A.**, Celio M.R., Margolis R.K., Menoud P.-A. "*Phosphacan immunoreactivity is associated with perineuronal nets around parvalbumin-expressing neurones*" **Brain Research, 1999, 834**: 219-222.

Celis J.E., Gromov P., Østergaard M., Madsen P., Honore B., Dejgaard K.,Olsen E., Vorum H., Kristensen D.B., Gromov I., **Haunsø A**., Van Damme J., Puype M., Vandekerckhove J., Rasmussen H.H *"Human 2-D PAGE database for proteome analysis in health and disease: http://biobase.dk/cgi-bin/celis*." **FEBS Letters, 1996, 398 (2-3)**: 129-134.

Celis J.E., Rasmussen H.H., Gromov P., Olsen E., Madsen P., Leffers H., Honore B., Dejgaard K., Vorum H., Kristensen D.B., Østergaard M., **Haunsø A**., Jensen N.A., Celis A., Basse B., Lauridsen J.B., Ratz G. P., Andersen A.H., Walbum E., Kjærgaard I., Andersen I., Puype M., Damme J. van, Vandekerckhove J. *"The human keratinocyte two-dimensional gel protein database (update 1995): Mapping components of signal transduction pathways*" **Electrophoresis, 1995, 16:** 2177-2240.

Presentations:

June 2000: *"Tenascin-R and Perineuronal Nets of Extracellular Matrix"*; Structural Biochemistry Group, Institute of Cell and Molecular Biology, The University of Edinburgh, Michael Swann Building, Mayfield Road, Edinburgh EH9 3JR, Scotland, United Kingdom. Oral presentation.

October 1999: *"Morphology of Perineuronal Nets in Tenascin-R and Parvalbumin Single and Double Knockout Mice"*; Society for Neuroscience: 29th Annual Meeting, Miami, USA, Poster presentation (# 511.20).

October 1998: *"The Brain Extracellular Matrix"*; Societe Suisse d'Anatomie, d'Histologie et d'Embryologie: 60ème Assemblee Annuelle, Fribourg, Switzerland, Oral communication.

October 1998: *"La Matrice Extracellulaire"*; Societe Suisse d'Anatomie, d'Histologie et d'Embryologie: 60ème Assemblee Annuelle, Fribourg, Switzerland, Poster presentation.

ELSEVIER

Brain Research 834 (1999) 219–222

BRAIN RESEARCH

www.elsevier.com/locate/bres

Short communication

# Phosphacan immunoreactivity is associated with perineuronal nets around parvalbumin-expressing neurones

Anders Haunsø [a], Marco R. Celio [a], Renée K. Margolis [b], Pierre-Alain Menoud [a,*]

[a] *Institute of Histology and General Embryology and Program in Neuroscience, University of Fribourg, CH-1705 Fribourg, Switzerland*
[b] *Department of Pharmacology, State University of New York, Health Science Center, Brooklyn, NY 11203, USA*

Accepted 4 May 1999

**Abstract**

A special feature of the extracellular matrix in adult brains of various species is the concentration of certain components around different sub-populations of neurones, giving rise to net-like structures termed perineuronal nets. Recently, some of these components have been identified but the function of these nets has yet to be resolved. Using immunofluorescence microscopy, we report here that phosphacan, a chondroitin sulphate proteoglycan, is an additional component of *Wisteria floribunda* labelled perineuronal nets surrounding parvalbumin-expressing neurones in rat cerebral cortex. Glycoproteins such as tenascin-C and -R have been identified in perineuronal nets and the present detection of phosphacan immunoreactivity in the same entity is of potential physiological importance because of their previously described interactions. 

*Keywords:* Chondroitin sulphate proteoglycan; Extracellular matrix; Parvalbumin; Perineuronal net; Phosphacan; Rat cerebral cortex; WFA

It is generally recognised that brain extracellular matrix (B-ECM) plays an important role in the development and maintenance of the central nervous system. B-ECM, which mainly consists of hyaluronan, glycoproteins and proteoglycans can influence the nervous system by binding growth factors and cell receptors, and by modulating cell adhesion and signalling (for review, see Ref. [19]). A large part of potential signalling molecules in the B-ECM belongs to the chondroitin sulphate proteoglycan family (CSPGs), whose members tend to have distinct distribution patterns in the brain [10,18]. Phosphacan (reviewed in Ref. [12]), comprising the extracellular region of the receptor protein tyrosine phosphatase ζ/β (RPTP ζ/β), belongs to this family of CSPGs. Phosphacan is synthesised by astrocytes [17] and its localisation, carbohydrate and sulphate compositions are developmentally regulated in the nervous tissue [14]. In embryonic and early postnatal rat brain, phosphacan immunoreactivity is distributed in the neuropil of the cerebral cortex and in the adult rat brain is localised mainly around multipolar non-pyramidal neurones [11]. CSPGs have been shown to be present in the perineuronal net [5] surrounding GABAergic interneurones expressing the calcium-binding protein parvalbumin (PV) [8] (for an overview of PV distribution in the brain, see Ref. [4]). In this report, we show that phosphacan immunoreactivity is present in the perineuronal net surrounding PV-positive GABAergic interneurones in the adult rat cerebral cortex.

Eight adult Wistar rats of either sex weighing ~300 g were euthanised with carbon dioxide and perfused via the left ventricle with 150 ml of 4% (w/v) paraformaldehyde in PBS (0.147 M NaCl, 2.68 mM KCl, 1.76 mM $KH_2PO_4$ and 10.14 mM $Na_2HPO_4$; pH = 7.4). Brains were removed and placed for a further 1 h in 4% paraformaldehyde, then transferred for an additional 1 h in PBS and subsequently incubated overnight at 4°C in 18% (w/v) sucrose in PBS. Brains were frozen and cut, using a cryostat, into 40 μm thick horizontal sections. Prior to applying the primary antibodies the sections were washed in PBS for 5 min, post-fixed for 1 min in 4% paraformaldehyde and subsequently washed again in PBS for 2 min. Double-immunolabelling was performed by incubating the sections with a rabbit polyclonal anti-phosphacan antibody [17] (dilution 1:1000) and either with the biotinylated lectin *Wisteria floribunda* agglutinin (WFA, Sigma) at a

* Corresponding author. Fax: +41-26-300-9732; E-mail: pierre-alain.menoud@unifr.ch

0006-8993/99/$ - see front matter 
PII: S0006-8993(99)01596-6

concentration of 20 μg/ml or with a mouse monoclonal anti-PV antibody (PV235, Swant) diluted 1:1000. Free-floating sections were incubated overnight at 4°C in PBS containing 10% (v/v) bovine serum. Sections were rinsed three times 10 min in PBS. All the following incubations were carried out at room temperature in PBS containing 10% (v/v) bovine serum and all washes for three times 10 min in PBS. Sections incubated with the anti-PV antibody were revealed with an anti-mouse Cy3™-conjugated antibody (Jackson Laboratories). Sections incubated with biotinylated WFA were revealed by a Cy2™-conjugated streptavidin (Jackson Laboratories). The anti-phosphacan antibody incubation was carried out as a two step reaction by first applying a goat anti-rabbit IgG antibody (Jackson Laboratories), followed by washes and subsequent incubated with a donkey anti-goat Cy2™-conjugated antibody (Amersham). The goat anti-rabbit antibody, the Cy2™- and Cy3™-conjugated antibodies and the Cy2™-conjugated streptavidin were all applied at dilutions of 1:100 for 2 h at room temperature. After extensive washes, sections were air dried on slides for 2 h at room temperature, rehydrated in double distilled water, dried for 30 min and subsequently mounted in SlowFade™ (Molecular Probes), coverslipped and sealed using clear nail varnish. Controls were carried out in the absence of the primary antibodies or the lectin. Slides were visualised under a Zeiss Axiophot fluorescence microscope, photographed using a Spot camera™ (Diagnostic instruments), imported into Adobe Photoshop 3.0.5 where minor changes in brightness and contrast were performed and photographic plates were printed on a Kodak DS 8650 PS Color printer.

Detailed analysis of phosphacan immunoreactivity in the adult rat cerebral cortex revealed a pericellular staining resembling perineuronal net-like structures, ensheathing the cell-body and major dendrites of non-pyramidal neurones. Neurones surrounded by phosphacan immunoreactivity were found in all layers of the cortex, except layer I, and were mainly distributed in layers II, IV and VI. The immunofluorescence intensity varied from a strong staining in the deeper layers revealing both the contours of the cell body and dendrites, to an almost indistinct staining of the perimeter of a subclass of neurones in layer II. Moreover, a difference in the density and intensity of positive neurones was also observed depending upon the region of the cerebral cortex, but this was not further studied. In double-staining experiments using both anti-phosphacan and anti-PV antibodies, it was shown that all phosphacan immunoreactive neurones in the cerebral cortex were also PV-positive (Fig. 1A,B). Very few PV-positive neurones were found without a phosphacan net (Fig. 1C,D), but the variation in intensity of the phosphacan immunoreactivity made it difficult to distinguish negative from weakly stained cells. When sections were incubated concomitantly with WFA, a marker for the perineuronal

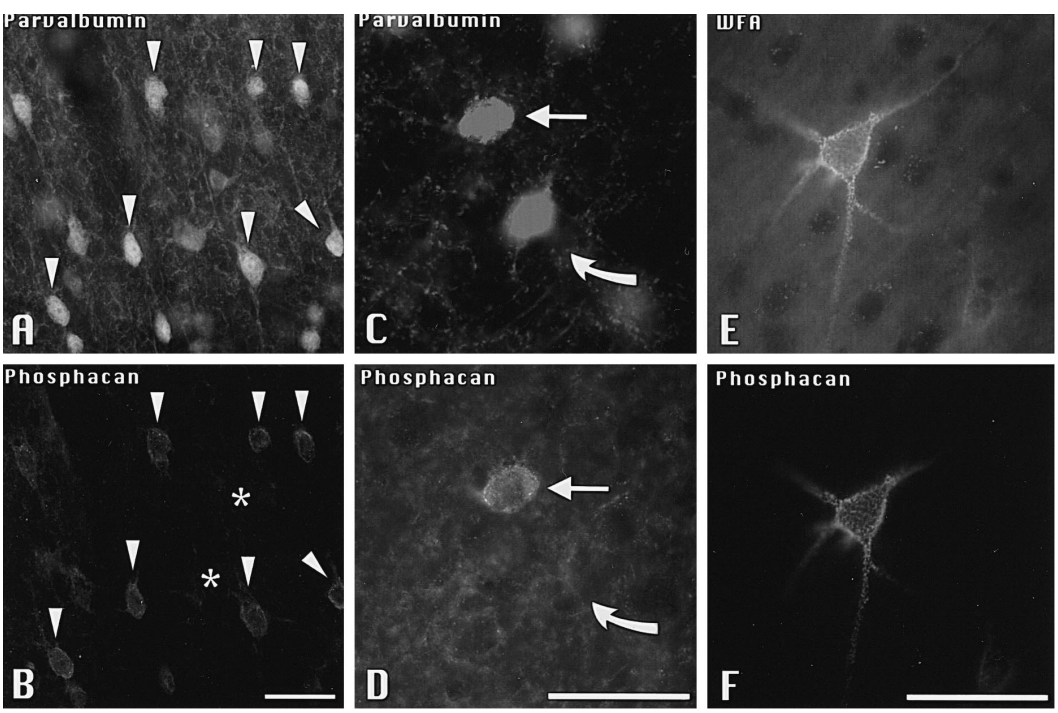


Fig. 1. Co-localisation of phosphacan immunoreactivity within perineuronal nets around parvalbumin expressing neurones in the cerebral cortex of adult rats. A and B show a double stained section incubated with anti-PV (A) and anti-phosphacan (B) antibodies. Some of the double stained cells in A and B are marked with arrow heads whereas the asterisks in B denote the position of faintly stained neurones in A that are out of focus. C and D depict a double stained section illustrating the lack of phosphacan immunoreactivity (curved arrow in D) around a PV-expressing neurone (C, curved arrow). E and F show a double stained section incubated respectively with WFA (E) and the anti-phosphacan antibody (F). Scale bars = 50 μm.

net, and anti-phosphacan, we observed that phosphacan immunoreactivity was localised around the same sub-population of neurones as the perineuronal net (Fig. 1E,F). In addition, there was a correlation between the intensity of the phosphacan immunoreactivity and that of WFA in the deeper cortical layers, but not in layer II where the phosphacan immunoreactivity was generally weak. Similar results were obtained when the monoclonal anti-phosphacan antibody 3F8 [18] was applied (not shown).

The amount of extracellular material detected in the brain is relatively low [19] when compared to the ECM of many other tissues. Moreover, many if not all of the ECM components in the brain have restricted regional distributions and in addition some also tend to accumulate around specific sub-populations of neurones giving rise to net-like structures termed perineuronal nets (for review, see Refs. [5,7]). ECM compounds such as hyaluronan [1], neurocan [13], tenascin-C [6] and tenascin-R [5] are seen to accumulate around PV-expressing GABAergic interneurones [9] comprising a proportion of the neurones surrounded by perineuronal nets. The distribution of PV-expressing neurones in the cerebral cortex [4] and their co-localisation with WFA labelled perineuronal nets is well established in the literature [2,3,9]. Moreover, it has also been shown that CSPGs constitute part of the perineuronal nets around PV-positive neurones [8]. Furthermore, using the monoclonal anti-phosphacan antibody 6B4, Maeda et al. [11] have detected phosphacan immunoreactivity around certain multipolar non-pyramidal neurones in the adult rat cerebral cortex. In this paper, we expand on these results by showing that phosphacan is one of the CSPGs in perineuronal nets and that it surrounds only PV-positive neurones in the cortex. The few PV-positive neurones we found not to be surrounded by phosphacan immunoreactivity were localised in the cortical regions where the intensity of the phosphacan immunoreactivity was generally weak. This made it difficult to determine if phosphacan immunoreactivity truly was absent around the PV-positive neurones or if the immunoreactivity was lower than could be detected. In the deeper layers of the cortex, where the intensity of the phosphacan immunoreactivity appeared to be strong, there was a perfect correlation between neurones surrounded by WFA and those surrounded by phosphacan immunoreactivity. However, certain regions of the cortex had a low phosphacan immunoreactivity even though no apparent difference could be observed in the WFA staining. Here we suggest that the proportion between phosphacan and other CSPGs within perineuronal nets varies depending on region and layer of the cortex. The appearance of phosphacan immunoreactivity in WFA labelled perineuronal nets was not surprising as the former contains *N*-acetylgalactosamine carbohydrates (GalNAc) [11] which are recognised by WFA. Moreover, phosphacan is also known to bind to certain glycoproteins found in perineuronal nets such as tenascin-C [16] and tenascin-R [15]. Therefore, the co-localisation of all three compounds in perineuronal nets suggests a potential physiological relevance for their interactions.

Perineuronal nets are thus not only heterogeneous in composition [5,7] but the proportion of their components vary depending upon the localisation within the cerebral cortex. Such regional differences in the composition of the ECM may reflect subdivisions of functionally defined areas. So far, the functions and the exact composition of perineuronal nets are still far from being determined [5] but the identification of phosphacan in this structure adds a further component to this special form of extracellular matrix and may enable us to better understand its role.

## Acknowledgements

This project was supported by the Desirée and Nils Yde Foundation and by Novartis. We are grateful to Dr. Merdol Ibrahim for his help, valuable advice and comments on this manuscript.

## References

[1] A. Bignami, R. Asher, G. Perides, Co-localization of hyaluronic acid and chondroitin sulfate proteoglycan in rat cerebral cortex, Brain Res. 579 (1992) 173–177.
[2] K. Brauer, W. Hartig, V. Bigl, G. Bruckner, Distribution of parvalbumin-containing neurons and lectin-binding perineuronal nets in the rat basal forebrain, Brain Res. 631 (1993) 167–170.
[3] G. Bruckner, G. Seeger, K. Brauer, W. Hartig, J. Kacza, V. Bigl, Cortical areas are revealed by distribution patterns of proteoglycan components and parvalbumin in the Mongolian gerbil and rat, Brain Res. 658 (1994) 67–86.
[4] M.R. Celio, Calbindin D-28k and parvalbumin in the rat nervous system, Neuroscience 35 (1990) 375–475.
[5] M.R. Celio, I. Blumcke, Perineuronal nets — a specialized form of extracellular matrix in the adult nervous system, Brain Res. Rev. 19 (1994) 128–145.
[6] M.R. Celio, R. Chiquet-Ehrismann, 'Perineuronal nets' around cortical interneurons expressing parvalbumin are rich in tenascin, Neurosci. Lett. 162 (1993) 137–140.
[7] M.R. Celio, R. Spreafico, S. De Biasi, L. Vitellaro-Zuccarello, Perineuronal nets: past and present, TINC 21 (1998) 510–515.
[8] W. Hartig, K. Brauer, V. Bigl, G. Bruckner, Chondroitin sulfate proteoglycan-immunoreactivity of lectin-labeled perineuronal nets around parvalbumin-containing neurons, Brain Res. 635 (1994) 307–311.
[9] W. Hartig, K. Brauer, G. Bruckner, *Wisteria floribunda* agglutinin-labelled nets surround parvalbumin-containing neurons, NeuroReport 3 (1992) 869–872.
[10] C. Lander, H. Zhang, S. Hockfield, Neurons produce a neuronal cell surface-associated chondroitin sulfate proteoglycan, J. Neurosci. 18 (1998) 174–183.
[11] N. Maeda, H. Hamanaka, A. Oohira, M. Noda, Purification, characterization and developmental expression of a brain-specific chondroitin sulfate proteoglycan, 6B4 proteoglycan/phosphacan, Neuroscience 67 (1995) 23–35.
[12] R.U. Margolis, R.K. Margolis, Chondroitin sulfate proteoglycans as mediators of axon growth and pathfinding, Cell Tissue Res. 290 (1997) 343–348.
[13] F. Matsui, M. Nishizuka, Y. Yasuda, S. Aono, E. Watanabe, A. Oohira, Occurrence of a N-terminal proteolytic fragment of neuro-

can, not a C-terminal half, in a perineuronal net in the adult rat cerebrum, Brain Res. 790 (1998) 45–51.
[14] B. Meyer-Puttlitz, E. Junker, R.U. Margolis, R.K. Margolis, Chondroitin sulfate proteoglycans in the developing central nervous system: II. Immunocytochemical localization of neurocan and phosphacan, J. Comp. Neurol. 366 (1996) 44–54.
[15] P. Milev, A. Chiba, M. Haring, H. Rauvala, M. Schachner, B. Ranscht, R.K. Margolis, R.U. Margolis, High affinity binding and overlapping localization of neurocan and phosphacan/protein-tyrosine phosphatase-zeta/beta with tenascin-R, amphoterin, and the heparin-binding growth-associated molecule, J. Biol. Chem. 273 (1998) 6998–7005.
[16] P. Milev, D. Fischer, M. Haring, T. Schulthess, R.K. Margolis, R. Chiquet-Ehrismann, R.U. Margolis, The fibrinogen-like globe of tenascin-C mediates its interactions with neurocan and phosphacan/protein-tyrosine phosphatase-zeta/beta, J. Biol. Chem. 272 (1997) 15501–15509.
[17] P. Milev, D.R. Friedlander, T. Sakurai, L. Karthikeyan, M. Flad, R.K. Margolis, M. Grumet, R.U. Margolis, Interactions of the chondroitin sulfate proteoglycan phosphacan, the extracellular domain of a receptor-type protein tyrosine phosphatase, with neurons, glia, and neural cell adhesion molecules, J. Cell Biol. 127 (1994) 1703–1715.
[18] U. Rauch, P. Gao, A. Janetzko, A. Flaccus, L. Hilgenberg, H. Tekotte, R.K. Margolis, R.U. Margolis, Isolation and characterization of developmentally regulated chondroitin sulfate and chondroitin/keratan sulfate proteoglycans of brain identified with monoclonal antibodies, J. Biol. Chem. 266 (1991) 14785–14801.
[19] E. Ruoslahti, Brain extracellular matrix, Glycobiology 6 (1996) 489–492.

ELSEVIER

Brain Research 864 (2000) 142–145

BRAIN RESEARCH

www.elsevier.com/locate/bres

Short communication

# Morphology of perineuronal nets in tenascin-R and parvalbumin single and double knockout mice

Anders Haunsø[a], Merdol Ibrahim[a], Udo Bartsch[b], Maryse Letiembre[a], Marco R. Celio[a], Pierre-Alain Menoud[a,*]

[a]*Institute of Histology and General Embryology and Program in Neuroscience, University of Fribourg, CH-1705 Fribourg, Switzerland*
[b]*Zentrum für Molekulare Neurobiologie, Universität Hamburg, D-20246 Hamburg, Germany*

Accepted 15 February 2000

**Abstract**

Recently identified chondroitin sulphate proteoglycans in perineuronal nets include neurocan and phosphacan. However, the function and assembly of these components has yet to be resolved. In this study we show morphological alteration in *Wisteria floribunda* labelled nets around cortical interneurones both in tenascin-R knockout and tenascin-R/parvalbumin double knockout mice. This alteration reflects the loss of phosphacan and neurocan from cortical nets in mice deficient in tenascin-R. No effect on the membrane related cytoskeleton, as revealed by ankyrin$_R$, was observed in any of the mice. These results on mice lacking tenascin-R substantiate previously reported in vitro interactions between tenascin-R and phosphacan and neurocan. 

*Themes:* Cellular and molecular biology

*Topics:* Membrane composition and cell-surface macromolecules

*Keywords:* Ankyrin; Chondroitin sulphate proteoglycan; Extracellular matrix; Neurocan; Perineuronal net; Phosphacan; WFA

A special feature of the brain extracellular matrix (ECM) [18] is the aggregation of certain components around specific sub-populations of neurones giving rise to net-like structures termed perineuronal nets of extracellular matrix (PNEMs) [6]. PNEMs are well characterised around cortical GABAergic parvalbumin immunoreactive (PV-IR) interneurones [8] and are composed of hyaluronan, tenascin-C [4], -R [3] and defined chondroitin sulphate proteoglycans (CSPGs) such as brevican [7], neurocan [13] and phosphacan [9]. However, neither function [8] nor process of assembly of PNEMs has yet been determined [6]. In vitro studies have shown binding between tenascin-R (TN-R) and members of the CSPG family [7,14] suggesting its involvement in the assembly and structure of PNEMs. In addition, the intracellular organisation of the ankyrin$_R$ membrane-related cytoskeleton (MRC) may also be involved in the formation of the lattice-like structure of PNEMs, by controlling the position of integral membrane proteins [21] involved in forming the nets. In this report we show that TN-R is essential for attracting and/or retaining neurocan and phosphacan in cortical PNEMs as no pericellular staining was observed for these CSPGs when TN-R was lacking.

Mice lacking either TN-R [20] or PV [19] were used and double knockout mice for both TN-R and PV were generated by cross-breeding TN-R and PV single knockout mice. The genotype of TN-R, PV and PV/TN-R deficient mice were determined by Southern blotting as previously described [19,20]. In total twelve adult mice ~30 g, comprising three of each genotype — wild type (WT), PV knockout (KO), TN-R KO and PV/TN-R double KO — of either sex, were used in these experiments. Animals were sacrificed, brains dissected out and processed for immunohistochemistry as previously described [9]. Biotinylated *Wisteria floribunda* agglutinin (WFA, Sigma) immunoreactivity (IR) was detected by applying the lectin at a concentration of 20 μg/ml and TN-R-IR by applying a 1:500 dilution of mouse anti-tenascin-R antibody (restrictin

*Corresponding author. Tel.: +41-26-300-8509; fax: +41-26-300-9732.

*E-mail address:* pierre-alain.menoud@unifr.ch (P.-A. Menoud)

0006-8993/00/$ – see front matter 
PII: S0006-8993(00)02173-9

23–14). Double-immunolabelling was performed by incubating sections with a mouse monoclonal anti-PV antibody (PV235, Swant) diluted 1:500 together with rabbit polyclonal antibodies against either phosphacan [15], neurocan [16] or ankyrin$_R$ [10], all diluted 1:1000. Sections incubated with the anti-PV antibody were visualised with a fluorescein isothiocyanate-conjugated (FITC, 1:200) anti-mouse antibody (Molecular Probes) and biotinylated WFA was visualised by Texas Red-conjugated streptavidine (Vector, 1:200). Detection of all rabbit polyclonal antibodies or the monoclonal TN-R antibody was carried out as two step reactions by first applying biotinylated goat anti-rabbit IgG antibodies (Vector, 1:200) or biotinylated horse anti-mouse IgG antibody (Vector, 1:200), respectively, followed by washes and subsequent incubation with Texas Red-conjugated streptavidine(1:200). Controls were carried out in the absence of primary antibodies or the lectin. Slides were analysed with a Bio-Rad 1024, argon/krypton confocal laser scanning fluorescence microscope (LSCM, Bio-Rad Microsciences Division Ltd). Both green and blue-lines of laser excitation were used and detected at 522 nm for FITC and 680 nm for Texas Red-labelled structures. Using ×60 oil immersion objective and real-time zoom feature of the confocal program, captured optical sections of 0.2-μm thickness were superimposed and images transferred to Adobe Photoshop™ software where photographic plates were prepared and printed using a Kodak dye sublimation printer (DS 8650 PS)

In both WT and TN-R KO animals cortical PV-IR neurones had a normal pattern of distribution and normal pericellular staining was observed in WT and PV KO animals (not shown). Confocal analysis of individual WFA-labelled PNEMs revealed a lattice-like staining around cell soma and dendritic aborisations in both WT and PV KO animals (Fig. 1A,B). However, in both TN-R KO and PV/TN-R KO animals WFA-labelled PNEMs around the cell soma showed punctuated immunolabelling (Fig. 1C,D). Labelling along dendrites was also markedly

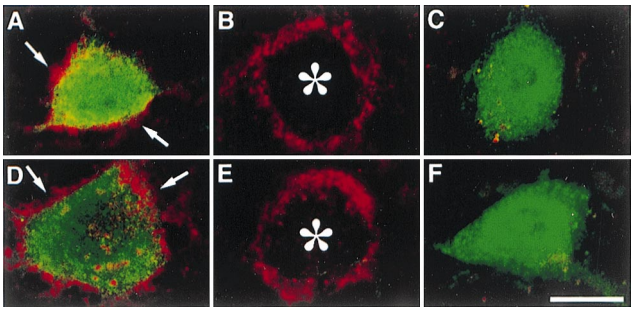


Fig. 2. Double confocal images of neurocan (A–C) and phosphacan (D–F) immunoreactivity around cortical interneurones. (A) Neurocan-IR (red, arrows) around a PV-labelled neurone (green) in WT. (B) Neurocan-IR (red) surrounding PV-negative (asterisk) neurone in PV KO. (C) PV-labelled neurone (green) lacking neurocan-IR around cell soma in TN-R KO. (D) Phosphacan-IR (red, arrows) around PV-labelled neurone (green) in WT. (E) Phosphacan-IR (red) surrounding PV-negative (asterisk) neurone in PV KO. (F) PV-labelled neurone (green) lacking phosphacan-IR around cell soma in TN-R KO. Scale bar=20 μm.

reduced or absent (Fig. 1C,D). Despite this, no apparent change in the overall distribution or density of cells with WFA-labelled nets was observed in any of the animals, as also shown by Weber et al. [20]. In WT and PV KO animals, double-immunofluorescence labelling using neurocan or phosphacan combined with PV-IR revealed a normal net-like staining pattern around cortical interneurones (Fig. 2A,B,D,E). In TN-R deficient mice we observed a massively reduced and more diffusely distributed cortical neurocan-IR in mutant mice when compared to wild-type animals (Fig. 2C), whereas no pericellular phosphacan-IR (Fig. 2F) could be detected in any tenascin-R deficient mice. The ankyrin$_R$-IR MRC (characteristic for cortical PV-IR interneurones [21]) showed no morphological differences in any of the mice studied, even in neurones lacking PV or those showing altered neurocan and phosphacan PNEMs (Fig. 3).

Many if not all ECM components in the brain show a

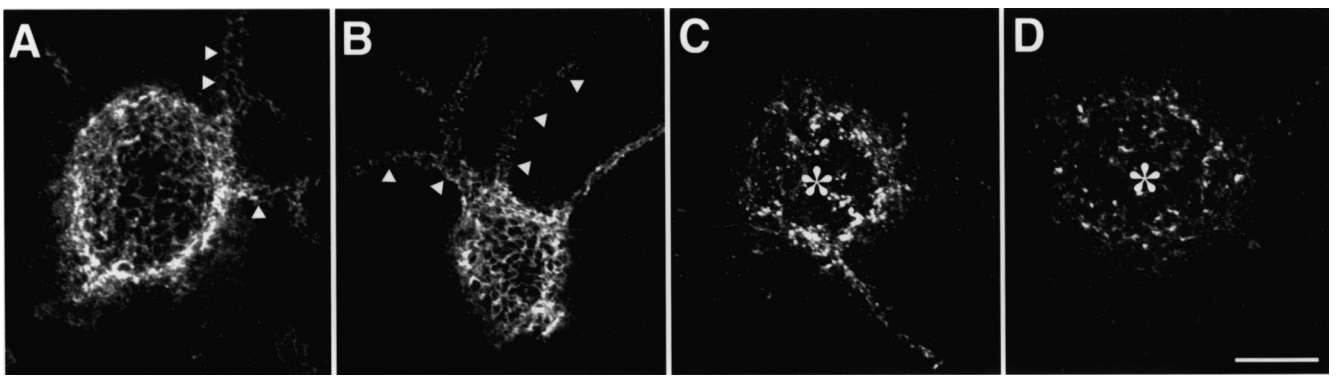


Fig. 1. Confocal images of WFA-labelled perineuronal nets in the cerebral cortex of WT (A), PV KO (B), TN-R KO (C) and PV/TN-R double KO (D). In both WT (A) and PV KO (B) mice the nets have a normal lattice-like morphology around soma and extend along dendritic aborisations (arrow heads). Nets were punctuated and disrupted around soma (asterisk) in TN-R KO (C) and to a similar extent in PV/TN-R double KO (D) mice. Labelling of nets along dendrites was generally absent in both genotypes. Scale bar=20 μm.

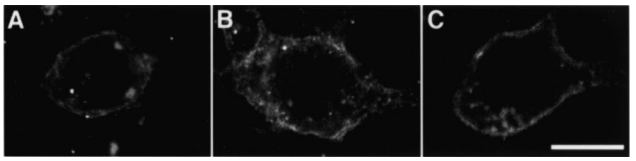


Fig. 3. Confocal images of ankyrin$_R$ membrane-related cytoskeleton immunoreactivity in WT (A), PV KO (B) and TN-R KO (C) mice. Ankyrin$_R$-IR showed normal pattern of distribution and morphology in cortical neurones of all genotypes. Scale bar=20 μm.

restricted regional distribution [11,17] with some accumulating around specific sub-populations of neurones giving rise to net-like structures termed PNEMs (for review, see Ref. [3,6]). Recently, interactions between TN-R and defined CSPGs such as brevican [2], phosphacan [14], neurocan [14] and versican [1] have been shown in vitro. Furthermore, IR for brevican, phosphacan and neurocan together with TN-R [3] has also been associated with PNEMs [7,9,13], conferring physiological importance to their previously described interactions in vitro. In this paper we report for the first time that the removal of a defined PNEM molecule can alter the distribution and levels of other specific components in perineuronal nets. We report that TN-R is needed for the correct assembly of PNEMs and when absent, CSPGs such as phosphacan and neurocan are no longer present, or in extremely low amounts, in cortical PNEMs, leading to a marked alteration in their appearance. The lectin WFA, used in this investigation, recognises N-acetylgalactosamine carbohydrates [12] on both phosphacan and neurocan. The observed alteration in the WFA-labelled nets in mice lacking tenascin-R (as also reported by Weber et al. [20]) therefore reflects a significant reduction of the two investigated components and perhaps other CSPGs. It is noteworthy that in areas such as the cerebellum, olfactory bulb and spinal cord some neurocan-IR remained in tenascin-R deficient animals, but this was not investigated further. In contrast phosphacan-IR nets were not detected anywhere else in the CNS in these mice. This indicates that TN-R is not involved in determining which neurones form PNEMs but may be involved in attracting and/or retaining phosphacan and neurocan in cortical PNEMs. The MRC may be a prerequisite for the organisation of PNEMs and may be involved in defining the area of synaptic contacts by keeping in register the overlaying PNEM [21,5]. The results presented here indicate that the MRC is more likely to be involved in determining the position of integral membrane proteins, rather than retaining the lattice-like structure of the PNEM. Evidence for this comes from the fact that the MRCs remain constant even though PNEMs have morphologically degenerated into a punctuated structure.

The lack of both PV and the alteration in morphology of PNEMs seemed not to have affected the distribution of individual cortical interneurones. It has been proposed that perineuronal nets are required for fast-spiking behaviour of GABAergic interneurones [8]. Modification of PNEMs could therefore influence the fast-spiking properties of these neurones or the distribution of synapses contacting their cell body, since the lattice-like structure of PNEMs defines the area of synaptic contacts [3]. Together with a changed calcium homeostasis this could modulate the inhibitory output from these GABAergic interneurones in mice lacking both TN-R and PV.

## Acknowledgements

We are grateful to Dr M. Schachner for providing the tenascin-R knockout, Dr B. Schwaller for providing the parvalbumin knockout mice, and to Dr R.K. Margolis for the kind gift of antibodies against phosphacan and neurocan. This project was supported by the Desirée and Nils Yde Foundation and by Novartis.

## References

[1] A. Aspberg, C. Binkert, E. Ruoslahti, The versican C-type lectin domain recognizes the adhesion protein tenascin-R, Proc. Natl. Acad. Sci. USA 92 (1995) 10590–10594.
[2] A. Aspberg, R. Miura, S. Bourdoulous, M. Shimonaka, D. Heinegard, M. Schachner, E. Ruoslahti, Y. Yamaguchi, The C-type lectin domains of lecticans, a family of aggregating chondroitin sulfate proteoglycans, bind tenascin-R by protein–protein interactions independent of carbohydrate moiety, Proc. Natl. Acad. Sci. USA 94 (1997) 10116–10121.
[3] M.R. Celio, I. Blumcke, Perineuronal nets: a specialized form of extracellular matrix in the adult nervous system, Brain Res. Rev. 19 (1994) 128–145.
[4] M.R. Celio, R. Chiquet-Ehrismann, 'Perineuronal nets' around cortical interneurons expressing parvalbumin are rich in tenascin, Neurosci. Lett. 162 (1993) 137–140.
[5] M.R. Celio, F.G. Rathjen, Restrictin occurs in 'perineuronal nets' of the adult brain, Soc. Neurosci. Abstr. 19 (1993) 689.
[6] M.R. Celio, R. Spreafico, S. De Blasi, L. Vitellaro-Zuccarello, Perineuronal nets: past and present, Trends Neurosci. 21 (1998) 510–515.
[7] K. Hagihara, R. Miura, R. Kosaki, E. Berglund, B. Ranscht, Y. Yamaguchi, Immunohistochemical evidence for the brevican–tenascin-R interaction: colocalization in perineuronal nets suggests a physiological role for the interaction in the adult rat brain, J. Comp. Neurol. 410 (1999) 256–264.
[8] W. Hartig, A. Derouiche, K. Welt, K. Brauer, J. Grosche, M. Mäder, A. Reichenbach, G. Brückner, Cortical neurons immunoreactive for the potassium channel Kv3.1b subunit are predominantly surrounded by perineuronal nets presumed as a buffering system for cations, Brain Res. 842 (1999) 15–29.
[9] A. Haunso, M.R. Celio, R.K. Margolis, P.A. Menoud, Phosphacan immunoreactivity is associated with perineuronal nets around parvalbumin-expressing neurones, Brain Res. 834 (1999) 219–222.
[10] S. Lambert, V. Bennett, Postmitotic expression of ankyrinR and beta R-spectrin in discrete neuronal populations of the rat brain, J. Neurosci. 13 (1993) 3725–3735.
[11] C. Lander, H. Zhang, S. Hockfield, Neurons produce a neuronal cell surface-associated chondroitin sulfate proteoglycan, J. Neurosci. 18 (1998) 174–183.

[12] N. Maeda, H. Hamanaka, A. Oohira, M. Noda, Purification, characterization and developmental expression of a brain-specific chondroitin sulfate proteoglycan, 6B4 proteoglycan/phosphacan, Neuroscience 67 (1995) 23–35.
[13] F. Matsui, M. Nishizuka, Y. Yasuda, S. Aono, E. Watanabe, A. Oohira, Occurrence of a N-terminal proteolytic fragment of neurocan, not a C-terminal half, in a perineuronal net in the adult rat cerebrum, Brain Res. 790 (1998) 45–51.
[14] P. Milev, A. Chiba, M. Haring, H. Rauvala, M. Schachner, B. Ranscht, R.K. Margolis, R.U. Margolis, High affinity binding and overlapping localization of neurocan and phosphacan/protein-tyrosine phosphatase-zeta/beta with tenascin-R, amphoterin, and the heparin-binding growth-associated molecule, J. Biol. Chem. 273 (1998) 6998–7005.
[15] P. Milev, D.R. Friedlander, T. Sakurai, L. Karthikeyan, M. Flad, R.K. Margolis, M. Grumet, R.U. Margolis, Interactions of the chondroitin sulfate proteoglycan phosphacan, the extracellular domain of a receptor-type protein tyrosine phosphatase, with neurons, glia, and neural cell adhesion molecules, J. Cell. Biol. 127 (1994) 1703–1715.
[16] P. Milev, P. Maurel, M. Haring, R.K. Margolis, R.U. Margolis, TAG-1/axonin-1 is a high-affinity ligand of neurocan, phosphacan/protein-tyrosine phosphatase-zeta/beta, and N-CAM, J. Biol. Chem. 271 (1996) 15716–15723.
[17] U. Rauch, P. Gao, A. Janetzko, A. Flaccus, L. Hilgenberg, H. Tekotte, R.K. Margolis, R.U. Margolis, Isolation and characterization of developmentally regulated chondroitin sulfate and chondroitin/keratan sulfate proteoglycans of brain identified with monoclonal antibodies, J. Biol. Chem. 266 (1991) 14785–14801.
[18] E. Ruoslahti, Brain extracellular matrix, Glycobiology 6 (1996) 489–492.
[19] B. Schwaller, J. Dick, G. Dhoot, S. Carroll, G. Vrbova, P. Nicotera, D. Pette, A. Wyss, H. Bluethmann, W. Hunziker, M.R. Celio, Prolonged contraction–relaxation cycle of fast-twitch muscles in parvalbumin knockout mice, Am. J. Physiol. 276 (1999) C395–403.
[20] P. Weber, U. Bartsch, M.N. Rasband, R. Czaniera, Y. Lang, H. Bluethmann, R.U. Margolis, S.R. Levinson, P. Shrager, D. Montag, M. Schachner, Mice deficient for tenascin-R display alterations of the extracellular matrix and decreased axonal conduction velocities in the CNS, J. Neurosci. 19 (1999) 4245–4262.
[21] E.S. Wintergerst, D.M. Vogt Weisenhorn, F.G. Rathjen, B.M. Riederer, S. Lambert, M.R. Celio, Temporal and spatial appearance of the membrane cytoskeleton and perineuronal nets in the rat neocortex, Neurosci. Lett. 209 (1996) 173–176.